



**Habilitation à diriger des recherches
PRÉSENTÉE À L'UNIVERSITÉ D'ORSAY**

par

Radu IGNAT

Discipline : **Mathématiques**

**Singularités des champs de vecteurs à divergence
nulle et à valeurs dans S^1 ou S^2 . Applications en
micromagnétisme.**

Soutenue le 12 décembre 2011

après avis de:

François ALOUGES

Luigi AMBROSIO

Benoît PERTHAME

devant le jury composé de:

François ALOUGES

Yann BRENIER

Patrick GERARD

Felix OTTO

Benoît PERTHAME

Sylvia SERFATY

Contents

Remerciements	5
Introduction	7
Liste de publications	13
1 Divergence-free unit-length vector fields	15
1.1 Entropies	16
1.2 The space $W_{div}^{1/p,p}(\Omega, S^1)$. Vortices.	18
1.2.1 Regularity results	19
1.2.2 Density results	21
1.3 The <i>BV</i> case. Line energies.	22
1.3.1 Motivation	23
1.3.2 Lower semicontinuity	25
1.3.3 Cost functions	27
1.3.4 Existence of minimizers for relaxed line-energies	29
1.3.5 Viscosity solution	30
1.4 Generalized entropies	32
1.4.1 Compactness	32
1.4.2 Entropies for S^2 -valued vector fields	33
1.4.3 A zigzag pattern	38
2 Singular patterns in thin-film micromagnetics	43
2.1 Micromagnetics	43
2.1.1 The general three-dimensional model	43
2.1.2 A reduced thin-film model	45
2.2 Néel wall	51
2.3 360° Néel wall and vortex energy	56
2.4 Landau state	60
2.5 Boundary vortices	65
2.6 Bloch line	69
2.7 Cross-over from symmetric to asymmetric walls	70

Remerciements

Je remercie très chaleureusement François Alouges, Luigi Ambrosio et Benoît Perthame d'avoir accepté de rapporter ce mémoire, ainsi que Yann Brenier, Patrick Gérard, Felix Otto et Sylvia Serfaty pour m'avoir fait l'honneur et le plaisir de participer à mon jury. L'originalité et la variété de leurs travaux sont pour moi un exemple.

Un grand merci à mes collègues mathématiciens avec qui j'ai eu la chance de discuter et travailler. Tout d'abord, je souhaite exprimer ma profonde reconnaissance à ceux qui ont encadré mes premiers pas dans la recherche. Benoît Perthame qui a dirigé mon mémoire de maîtrise en me donnant le goût des équations de Hamilton-Jacobi, étude dont je me suis beaucoup servi ces dernières années. Haïm Brezis pour son enthousiasme, son exigence mathématique et la confiance qu'il m'a accordée dès le début de ma thèse. Felix Otto, pour son soutien, sa bienveillance et sa grande disponibilité, pour les recherches passionnantes menées en sa compagnie lors des nombreuses visites (et le PostDoc) à Bonn et Leipzig ; une partie des travaux présentés ici sont les fruits de nos discussions.

Je tiens à remercier mes collaborateurs Raphaël Côte, Juan Dávila, Lukas Döring, Hans Knüpfer, Matthias Kurzke, Robert Jerrard, Benoît Merlet, Vincent Millot, Evelyne Miot, Roger Moser, Luc Nguyen, Felix Otto, Arkady Poliakovsky, Valeriy Slastikov et Arghir Zarnescu. Travailler avec eux est une source d'enrichissement et de plaisir pour moi.

Je voudrais adresser mes vifs remerciements au laboratoire de Mathématiques d'Orsay, en particulier, à l'équipe AN-EDP pour les excellentes conditions de travail et l'accueil très chaleureux dès mon arrivée en 2007. Je suis très reconnaissant à nos directeurs, Patrick Gérard et Bertrand Maury, d'avoir créé un environnement aussi stimulant que convivial. Un grand merci à François Alouges pour sa gentillesse et son attention à mon égard, pour les nombreuses discussions sur le micromagnétisme et notre ANR Micro-MANIP. Je pense aussi à Nicolas Burq, mon cher co-organisateur du séminaire et à ses actes de "mécénat", à Frédéric Lagoutière, pour son amitié qui m'est si chère, à Evelyne Miot, avec qui le "destin mathématique" m'a mené à partager le même bureau ... Et la liste est longue car elle contient au moins tous les membres de l'équipe AN-EDP: je les remercie pour le dynamisme et la vie qu'ils y apportent.

Je suis aussi très reconnaissant à mes collègues à l'étranger pour les nombreuses invitations, pour les discussions enrichissantes et l'hospitalité reçue dans leurs laboratoires et instituts. Je tiens à témoigner du soutien financier dont j'ai pu bénéficier : à Orsay et dans les universités visitées, dans les projets ANR Micro-MANIP et AMAM, le laboratoire LEA CNRS franco-roumain "Mathématiques et Modélisation" et le laboratoire franco-japonais LIA ReaDiLab.

Un grand merci à mes amis pour leur présence constante et dévouée.

Les derniers mots iront à mes parents et à ma soeur qui m'ont soutenu et encouragé sans cesse tout au long de ces années. Je leur dédie ce mémoire.

Introduction

Ce mémoire porte sur une partie de mes travaux effectués depuis mon arrivée à l'Université Paris-Sud 11 en 2007. Il comporte deux parties:

- Une première partie concerne l'étude des champs de vecteurs $2D$ ou $3D$ à divergence nulle et à valeurs dans S^1 ou S^2 . Le but consiste à analyser la rigidité de ces champs de vecteurs par la structure de leurs singularités, ainsi qu'à caractériser les énergies concentrées sur les singularités de co-dimension un en utilisant le concept d'entropie. Il s'agit d'un sujet à la frontière de plusieurs domaines: l'analyse fonctionnelle, les lois de conservation scalaires, le calcul des variations, les EDP elliptiques et la théorie géométrique de la mesure. Les résultats présentés dans ce chapitre font l'objet des travaux suivants [37, 33, 40, 41, 42].

- Une deuxième partie porte sur l'analyse des structures singulières de l'aimantation en micromagnétisme. Ces phénomènes de singularités correspondent à des couches limites (parois unidimensionnelles ou microstructures $2D$ ou $3D$) ou bien à des défauts topologiques de type vortex (placés à l'intérieur ou au bord de l'échantillon magnétique). Il s'agit des travaux suivants [27, 28, 35, 36, 38, 39, 44] qui utilisent des outils de plusieurs domaines: la modélisation mathématique, la physique des solides, le calcul des variations, les EDP elliptiques, la théorie géométrique de la mesure, la théorie d'interpolation, la théorie des bifurcations et les systèmes dynamiques.

Il y a un lien étroit entre les deux chapitres: le fil conducteur est donné par la structure des champs de vecteurs à divergence nulle et de longueur un. D'un côté, la problématique traitée dans le premier chapitre est souvent inspirée par des questions liées au micromagnétisme. D'un autre côté, l'analyse asymptotique portée sur l'aimantation dans le deuxième chapitre est décrite au niveau mésoscopique par des champs $3D$ de vecteurs m à divergence nulle et à valeurs dans S^2 . Selon le régime asymptotique ou l'ansatz utilisé, le champ vectoriel m peut être invariant dans une direction de sorte que la contrainte de divergence joue seulement sur deux variables. De plus, certaines contraintes du régime asymptotique imposent une restriction des valeurs de m à S^1 . Ceci justifie l'étude faite dans la première partie concernant les champs de vecteurs à divergence nulle et à valeurs dans S^1 ou S^2 .

Ce mémoire s'inscrit d'un côté dans la continuité (au sens large) des sujets abordés en thèse de doctorat (2003-2006) sous la direction de Haïm Brezis: l'étude des fonctions à valeurs dans S^1 (le problème du relèvement optimal pour des fonctions BV et l'étude de leurs singularités topologiques), ainsi que l'analyse des singularités présentes dans quelques problèmes variationnels: l'étude asymptotique des vortex dans les condensats de Bose-Einstein en rotation et l'optimalité des parois de Néel dans les films ferromagnétiques minces. D'un autre côté, de nouveaux sujets sont abordés ainsi que de nouvelles techniques qui permettent d'approfondir la compréhension des

défauts pour des champs de vecteurs portant une certaine rigidité et les applications en micro-magnétisme.

Présentation du Chapitre 1¹. Nous commençons par étudier les champs de vecteurs $m : \Omega \rightarrow S^1$ à divergence nulle pour des domaines planaires $\Omega \subset \mathbf{R}^2$. Ceci revient à analyser la rigidité de l'équation eikonale $2D$, qui se transpose sous la forme d'une loi de conservation scalaire. Cependant, l'objet fondamental utilisé dans ce chapitre est constitué par les entropies $\Phi \in C^\infty(S^1, \mathbf{R}^2)$.

1. La première partie du chapitre (Section 1.1) est consacrée à l'étude de la notion d'entropie associée à m . Elle correspond à la paire (entropie, flux d'entropie) des lois de conservation scalaires habituelles, mais définie sur S^1 qui est le contexte géométrique adapté à nos champs de vecteurs. La propriété essentielle d'une entropie Φ consiste à générer une production d'entropie $\nabla \cdot [\Phi(m)]$ nulle pour tout champ de vecteurs régulier $m \in C_{div}^\infty(\Omega, S^1)$. De manière équivalente, cette propriété correspond à l'interprétation géométrique suivante: la dérivée angulaire de Φ en $z \in S^1$ est orthogonale à z . C'est pourquoi les entropies sont déterminées par leur composante normale $\Phi(z) \cdot z$ selon la décomposition de Φ dans le repère (z, z^\perp) ; cette correspondance biunivoque fournit une méthode de construction des entropies dont nous nous servirons par la suite. Comme l'on s'y attend, la production d'entropie est une mesure concentrée sur des lignes de sauts (les "chocs") de m pour des champs de vecteurs $m \in BV_{div}(\Omega, S^1)$.
2. Dans la Section 1.2, nous montrons des résultats de régularité et densité pour les champs de vecteurs $m \in W_{div}^{1/p,p}(\Omega, S^1)$. Ici l'hypothèse de régularité $W^{1/p,p}$ est critique afin d'éviter les lignes de singularités. Dans ce cas, nous nous attendons à la formation des singularités de type vortex. Effectivement, nous démontrons que m est localement Lipschitz en dehors d'un nombre localement fini de points vortex si $p \in [1, 2]$. Ce résultat repose sur le concept d'entropie introduit auparavant. D'abord, la production d'entropie d'un tel champ de vecteurs est nulle pour toute entropie $\Phi \in C^\infty(S^1, \mathbf{R}^2)$. De plus, cette propriété s'étend à des entropies non lisses qui est transcrite sous la formulation cinétique suivante: pour toute caractéristique $\chi(\cdot, \xi)$ associée à m (au sens faible) dans la direction $\xi \in S^1$, on a $\xi \cdot \nabla \chi(\cdot, \xi) = 0$ dans $\mathcal{D}'(\Omega)$. La régularité Lipschitz est optimale et la géométrie du domaine Ω influence le nombre de singularités vortex d'un champ de vecteurs m . Le second objectif est d'établir des résultats de densité dans le cas des domaines Lipschitz Ω . Premièrement, tout champ de vecteurs $m \in W_{div}^{1/p,p}(\Omega, S^1)$ (où $p \in [1, 2]$) peut être approché dans la topologie $W_{loc}^{1,q}$ (pour $q \in [1, 2)$) par des champs de vecteurs m_k réguliers sauf en un nombre fini de points. Deuxièmement, on cherche à approcher m par des champs de vecteurs partout réguliers $m_k \in C^\infty(\Omega, S^1)$ (pas nécessairement à divergence nulle) dans une topologie plus faible. En effet, une configuration "vortex" (par exemple, $x^\perp/|x|$) ne peut pas être approchée dans la topologie L^1 (forte) par des champs de vecteurs $m_k \in C_{div}^\infty(\Omega, S^1)$. Par contre, le résultat d'approximation dans L^1 est vrai si on relaxe la condition de divergence nulle pour la suite régularisante dans la topologie $\dot{H}^{-1/2}$, i.e., $(\nabla \cdot m_k)1_\Omega \rightarrow 0$ dans $\dot{H}^{-1/2}(\mathbf{R}^2)$.
3. La Section 1.3 porte sur les champs de vecteurs $m \in BV_{div}(\Omega, S^1)$ qui présentent des singularités lignes. Le but consiste à étudier les "énergies de lignes", i.e., les fonctionnelles

¹Les références aux résultats cités sont données dans le texte du chapitre.

d'énergie concentrées sur les lignes de saut $J(m)$ de m :

$$\mathcal{I}_f(m) := \int_{J(m)} f(|m^+ - m^-|) d\mathcal{H}^1.$$

Remarquons que la densité d'énergie dépend seulement de la taille du saut $|m^+ - m^-|$ via une *fonction coût* $f : [0, 2] \rightarrow \mathbf{R}_+$. Nous nous proposons de caractériser les fonctions coût f qui engendrent une énergie de lignes \mathcal{I}_f semi-continue inférieure (s.c.i.) par rapport à la topologie L^1 . Cette caractérisation utilise les entropies. Plus précisément, nous associons à chaque sous-ensemble S d'entropies une fonction coût c_S qui représente la production d'entropie maximale engendrée par S :

$$c_S(t) = \sup_{\Phi \in S} \{[\Phi(z^+) - \Phi(z^-)] \cdot \nu : |z^+ - z^-| = t, (z^+ - z^-) \cdot \nu = 0, z^-, z^+, \nu \in S^1\},$$

pour tout $t \in [0, 2]$. Nous démontrons que les fonctions coût c_S correspondent bien à des énergies de lignes s.c.i. si l'ensemble S est symétrique et equivariant par les rotations $SO(2)$. Cette propriété nous permet de construire une grande famille de fonctions coût appropriées, en particulier, certaines fonctions puissance $t \mapsto t^p$ pour $p \in [1, 3]$. Ensuite, nous traitons le problème de minimisation de \mathcal{I}_f sous la condition aux limites $m \cdot n = 0$ au bord de $\partial\Omega$. L'existence des minimiseurs de la fonctionnelle relaxée $\overline{\mathcal{I}}_f$ dans L^1 est montrée par un résultat de compacité relatif aux sous-ensembles de niveau de $\overline{\mathcal{I}}_f$. Sous l'hypothèse plus restrictive $m = n^\perp$ sur $\partial\Omega$, nous étudions les situations où la solution de viscosité $m_* = \nabla^\perp \text{dist}(x, \partial\Omega)$ est un minimiseur de \mathcal{I}_f selon des critères de convexité du domaine Ω et du type de fonction coût f .

4. Le but de la Section 1.4 est de généraliser la notion d'entropie afin d'étudier la Γ -convergence des fonctionnelles de perturbation singulière G_ε (lorsque $\varepsilon \rightarrow 0$):

$$G_\varepsilon(m_\varepsilon) = \varepsilon \int_{\Omega} |\nabla m_\varepsilon|^2 + \frac{1}{\varepsilon} \int_{\Omega} g(|1 - |m_\varepsilon|^2|),$$

définie pour $m_\varepsilon \in H_{div}^1(\Omega, \mathbf{R}^2)$ et pour un potentiel $g : \mathbf{R}_+ \rightarrow \mathbf{R}_+$ (ou bien, $m_\varepsilon \in H_{div}^1(\Omega, S^2)$ et l'énergie G_ε pénalise $g(m_{3,\varepsilon}^2)$). En effet, nous nous attendons à ce que m_ε converge dans L^1 vers un champ $m_0 \in L_{div}^\infty(\Omega, S^1)$ et à ce que G_ε soit asymptotiquement concentrée sur une énergie de ligne \mathcal{I}_f ; la dépendance entre f et g est en général établie par une analyse asymptotique $1D$. Afin de montrer la compacité de G_ε , les entropies sont prolongées à des applications $\Phi : \mathbf{R}^2 \rightarrow \mathbf{R}^2$ en gardant la dérivée angulaire $\frac{\partial}{\partial\theta}\Phi(z)$ orthogonale à $z \in \mathbf{R}^2 \setminus \{0\}$. Ces applications Φ sont adaptées aux champs m_ε de G_ε puisque la contrainte de module 1 est relaxée. La propriété essentielle de ces entropies généralisées consiste à générer une production d'entropie $\nabla \cdot [\Phi(m_\varepsilon)]$ asymptotiquement contrôlée (en mesure) par l'énergie $G_\varepsilon(m_\varepsilon)$. D'un côté, cette caractéristique permet d'exclure à la limite les oscillations des configurations m_ε d'énergie uniformément bornée, donc de conclure à leur compacité dans L^1 . D'un autre côté, elle fournit la structure des configurations limites m_0 qui présentent des lignes de saut (même si en général $m_0 \notin BV_{div}(\Omega, S^1)$). Malheureusement, ces entropies ne conduisent pas en général à des bornes inférieures optimales pour G_ε . A cette fin, nous étudions une autre classe d'entropies généralisées $\Phi : S^2 \rightarrow \mathbf{R}^2$ adaptées aux champs de vecteurs m_ε à valeurs dans S^2 . Nous montrons que l'énergie de ligne \mathcal{I}_f est la borne inférieure

optimale de G_ε dans certains cas de potentiel g (linéaire ou quadratique) où les couches limites de G_ε sont unidimensionnelles. Nous traitons aussi un cas d'énergie G_ε modifiée (qui pénalise $g(m_{2,\varepsilon}^2)$ au lieu de $g(m_{3,\varepsilon}^2)$) où la méthode d'entropie permet de montrer la Γ -convergence même si les couches limites comportent une microstructure $2D$ en forme de zigzag.

Présentation du Chapitre 2². Le micromagnétisme est un principe variationnel multi-échelle non convexe et non local dont l'objet principal est donné par l'aimantation correspondant aux minimiseurs (locaux) de l'énergie micromagnétique. Dans certains régimes asymptotiques, l'aimantation est caractérisée au niveau mésoscopique par un champ de vecteurs $3D$ à divergence nulle et à valeurs dans S^2 . C'est pourquoi le chapitre présente un lien étroit avec le chapitre précédent, le but consistant à caractériser la formation des singularités pour l'aimantation. Notre stratégie utilise deux approches. Une première dont l'objectif est d'identifier l'échelle de l'énergie minimale, ainsi que la structure de l'aimantation qui réalise ce minimum; une deuxième approche qui consiste à identifier des modèles plus simples, valides dans des régimes asymptotiques appropriés, qui facilitent la compréhension du comportement de l'aimantation.

1. Nous commençons dans la Section 2.1 par introduire le contexte général du micromagnétisme, une théorie largement étudiée de nos jours qui modélise les matériaux ferromagnétiques. Dans cette théorie, les matériaux sont décrits par une distribution d'un champ de vecteurs, appelé *aimantation*, dont les états stables comportent de vastes régions uniformément magnétisées séparées par des couches limites, les *parois*, où l'aimantation varie très vite. Plusieurs types de paroi sont prédits par les expériences physiques: *paroi de Néel et Bloch (symétrique)*, *paroi de Néel et Bloch asymétrique*, ou des défauts de type vortex (*ligne de Bloch*), vortex au bord, ou bien des défauts de type mixte paroi-vortex (par exemple, *paroi "en noeud de cravate"*). Nous nous proposons d'analyser qualitativement et quantitativement ces singularités dans les films ferromagnétiques minces. A cette fin, nous identifions des régimes asymptotiques qui correspondent à une certaine ordre de l'énergie des défauts de l'aimantation; le choix de l'échelle d'énergie minimale détermine les contraintes du modèle réduit (imposées par les défauts d'énergie supérieure), ainsi que les parois d'énergie inférieure qui seront négligées. Avec ces choix, l'approche mathématique est basée sur l'analyse asymptotique, le but étant d'établir des bornes inférieures et supérieures appropriées de l'énergie (dans l'esprit de la Γ -convergence).
2. Dans la Section 2.2, nous décrivons la paroi de Néel qui est la couche limite prédominante dans les films très minces. Elle est caractérisée par une rotation unidimensionnelle dans S^1 qui connecte deux directions d'angle $-\theta$ et θ de l'aimantation. C'est un objet à deux échelles: un petit coeur où l'aimantation varie rapidement et deux queues à décroissance logarithmique. Nous décrivons trois modèles où les parois de Néel apparaissent et correspondent à des mécanismes différents de confinement des queues de Néel. Pour chaque modèle, nous démontrons le comportement asymptotique de ces parois par un résultat de Γ -convergence. Puisque le coût énergétique de cette paroi est quartique en θ , la méthode d'entropie n'est pas adaptée à cette étude. La difficulté est portée par le terme non local qui contribue au premier ordre de l'énergie de la paroi. Dans cette étude, les techniques utilisées sont basées sur un

²Les références aux résultats cités sont données dans le texte du chapitre.

argument de dualité et des inégalités d'interpolation de type Gagliardo-Nirenberg avec un taux logarithmique.

3. Le but de la Section 2.3 consiste à étudier la structure particulière d'un défaut vortex induit par une paroi de Néel d'angle 360° . En fait, une telle paroi de Néel comporte une rotation complète de l'aimantation autour d'un mur mésoscopique, portant un degré topologique non nul. Les parois de Néel à 360° sont caractérisées par l'angle α entre la direction mésoscopique de l'aimantation et la direction normale du mur. Nous montrons que l'angle α contribue au terme d'énergie principal d'une paroi de Néel de 360° . En effet, la structure interne d'une telle paroi consiste en deux transitions à charge magnétique nulle: une première paroi de Néel d'angle $2\theta = 2(\pi - \alpha)$ et une deuxième transition d'angle 2α . Ensuite, nous analysons le comportement asymptotique d'un vortex dans une section circulaire B^2 d'un film mince: le choix du régime asymptotique est donné par l'ordre suivant de l'énergie des défauts

$$E(\text{vortex au bord}) \ll E(\text{paroi de Néel}) \ll E(\text{ligne de Bloch}),$$

avec l'échelle d'énergie minimale imposée au niveau de la paroi de Néel. Au niveau microscopique, cette structure de l'aimantation correspond à un champ de vecteurs dans $H^1(B^2, S^1)$ créée par une paroi de Néel de 360° (d'angle initial $\alpha = 0$) autour d'un rayon du disque B^2 . La particularité de ce vortex est de porter un degré total nul, qui le différencie des autres structures de vortex, e.g., ligne de Bloch ou les vortex de type Ginzburg-Landau de degré topologique non nul. Ceci présente un lien étroit avec la Section 1.2 du Chapitre 1, ce modèle fournissant la topologie optimale $H^{-1/2}$ d'un des résultats d'approximation pour les champs de vecteurs à valeurs dans S^1 et à divergence nulle.

4. Nous étudions dans la Section 2.4 la structure optimale de l'aimantation, appelée *état de Landau*, qui correspond au minimiseur global de l'énergie micromagnétique. Ici, le régime asymptotique est choisi de sorte que la ligne de Bloch soit énergétiquement plus chère que la paroi de Néel et les vortex au bord soient fortement pénalisés, l'échelle d'énergie étant choisie au niveau de la ligne de Bloch. Par rapport à la section précédente, l'aimantation prend ses valeurs dans S^2 car on s'attend à la formation de défauts vortex à degré non nul pour l'état de Landau. Effectivement, nous montrons qu'asymptotiquement l'énergie de l'état de Landau est portée par des lignes de Néel et un défaut vortex intérieur (ligne de Bloch) ou bien deux défauts vortex au bord. De plus, nous prouvons la compacité des aimantations d'énergie proche de l'état de Landau, la difficulté consistant à garder la contrainte $|m| = 1$ à la limite. Ceci constitue une justification rigoureuse de la prédiction physique: les aimantations mésoscopiques dans les films minces correspondent à des champs de vecteurs $2D$ de module un et à divergence nulle; en effet, asymptotiquement l'état de Landau représente la solution de viscosité analysée dans la Section 1.3 du Chapitre 1. Les techniques utilisées reposent d'abord sur un argument d'approximation des champs de vecteurs à valeurs S^2 par des champs de vecteurs à valeurs S^1 en dehors d'une petite région créée par les défauts topologiques. La localisation des vortex est basée sur des techniques topologiques développées pour les énergies de type Ginzburg-Landau.
5. La Section 2.5 concerne le comportement asymptotique des vortex au bord ainsi que leurs énergie d'interaction. Le régime asymptotique correspond à un film mince où l'énergie de la

ligne de Bloch est prépondérante par rapport à l'énergie des vortex au bord et la paroi de Néel n'est pas confinée (donc, elle sera négligée); l'échelle de l'énergie minimale est choisie au niveau du coût des vortex au bord. L'objet fondamental réside dans la notion de "jacobien au bord" qui détecte les défauts vortex. La concentration de l'énergie autour des vortex au bord est démontrée par un résultat de type Γ -convergence comme pour les énergies de type Ginzburg-Landau; la différence ici consiste à avoir la mesure de vorticit  concentr e au bord. Nous d terminons aussi l' nergie renormalis e qui repr sente l'interaction entre les vortex au bord et qui gouverne la position optimale de ces d fauts. La difficult  majeure consiste   estimer la partie non locale de l' nergie g n r e par l' quation de Maxwell stationnaire afin de d tecter les termes exactes correspondant aux d fauts topologiques.

6. Dans la Section 2.6, nous analysons un  chantillon sph rique ferromagn tique o  l'effet de l'anisotropie et le champ magn tique induit la formation d'une ligne de Bloch. Ceci revient   un probl me similaire aux mod les 3D de type Ginzburg-Landau pour la supraconductivit  o  les lignes de vortex sont g n r es par des conditions de Dirichlet au bord portant des d fauts topologiques. Le but est de d terminer le comportement asymptotique de l' nergie micromagn tique port e par la ligne de Bloch.
7. Dans la derni re section, nous nous int ressons au r gime critique de film mince o  une bifurcation se produit entre les couches limites sym triques et asym triques. Il s'agit de comprendre la d pendance de l' nergie micromagn tique de l'angle θ de la transition de l'aimantation, ainsi que de d crire les propri t s qualitatives de la couche limite optimale. Nous d montrons la pr diction physique suivante: pour un petit angle de transition θ , la couche limite optimale est port e par la paroi de N el (sym trique) pr sent e dans la Section 2.2, donc son  nergie r sident dans les queues de N el   d croissance logarithmique. Ensuite, il existe un angle critique θ^* o  une brisure de sym trie se produit: une paroi asym trique tente   se former au coeur de la transition. En effet, pour des angles $\theta > \theta^*$, la couche limite optimale pr sente un coeur o  l'aimantation est   charge magn tique nulle (paroi asym trique d'angle θ_{in}) et en dehors du coeur, elle pr serve les queues de la paroi sym trique (unidimensionnelle, d'angle $\theta - \theta_{in}$). Nous montrons cette s paration de l' nergie entre la partie asym trique et la partie sym trique de la couche limite dans l'esprit de la Γ -convergence au niveau des minimiseurs. Afin de trouver l'angle critique θ^* de la bifurcation, nous r alisons un d veloppement asymptotique de l' nergie de la paroi asym trique   l'ordre θ^4 qui correspond au co t  nerg tique de la paroi sym trique. Ceci revient    tudier l' nergie de Dirichlet pour des champs de vecteurs   divergence nulle et   valeurs dans S^2 soumis   une transition d'angle θ_{in} . En fonction de θ_{in} , une deuxi me brisure de sym trie et un changement de degr  topologique se produisent, de sorte que nous distinguons la paroi de N el asym trique pour des angles petits θ_{in} , respectivement la paroi de Bloch asym trique pour θ_{in} grand.

Liste de publications *

Articles publiés ou à paraître.

- * (avec R. Moser), *A zigzag pattern in micromagnetics*, J. Math. Pures Appl., à paraître.
- * *Gradient vector fields with values into S^1* , C. R. Math. Acad. Sci. Paris **349** (2011), 883-887.
- * (avec B. Merlet) *Entropy method for line-energies*, Calc. Var. Partial Differential Equations, à paraître.
- * (avec F. Otto) *A compactness result for the Landau state in thin-film micromagnetics*, Ann. Inst. H. Poincaré Anal. Non Linéaire **28** (2011), 247-282.
- * (avec B. Merlet) *Lower bound for the energy of Bloch walls in micromagnetics*, Arch. Ration. Mech. Anal. **199** (2011), 369-406.
- * (avec H. Knuepfer) *Vortex energy and 360° Néel walls in thin films micromagnetics*, Comm. Pure Appl. Math. **63** (2010), 1677-1724.
- * *A Γ -convergence result for Néel walls in micromagnetics*, Calc. Var. Partial Differential Equations **36** (2009), 285-316.
- (avec F. Otto) *A compactness result in thin-film micromagnetics and the optimality of the Néel wall*, J. Eur. Math. Soc. (JEMS) **10** (2008), 909-956.
- * *A survey of some new results in ferromagnetic thin films*, Séminaire d'Équations aux Dérivées Partielles (Ecole Polytechnique) 2007–2008, Exp. No. VI, 19 pp.
- *Pohozaev type identities for an elliptic equation*, CRM Proceedings and Lecture Notes **44** (2008), 75-88.
- (avec A. Poliakovsky) *On the relation between minimizers of a Γ -limit energy and optimal lifting in BV-space*, Commun. Contemp. Math. **9** (2007), 447-472.
- (avec V. Millot) *Energy expansion and vortex location for a two dimensional rotating Bose-Einstein condensate*, Rev. Math. Phys. **18** (2006), 119-162.
- (avec V. Millot) *The critical velocity for vortex existence in a two dimensional rotating Bose-Einstein condensate*, J. Funct. Anal. **233** (2006), 260-306.

*Les articles précédés d'une astérisque sont inclus au dossier scientifique de ce mémoire.

- (avec V. Millot) *Vortices in a 2d rotating Bose-Einstein condensate*, C. R. Math. Acad. Sci. Paris **340** (2005), 571-576.
- *The space $BV(S^2, S^1)$: minimal connection and optimal lifting*, Ann. Inst. H. Poincaré Anal. Non Linéaire **22** (2005), 283-302.
- *Optimal lifting for $BV(S^1, S^1)$ functions*, Calc. Var. Partial Differential Equations **23** (2005), 83-96.
- *On an open problem about how to recognize constant functions*, Houston J. Math. **31** (2005), 285-304.
- (avec J. Dávila) *Lifting of BV functions with values in S^1* , C. R. Math. Acad. Sci. Paris **337** (2003), 159-164.
- *Équations de Hamilton Jacobi et Contrôle Optimal*, Proceedings of the International Conference on Nonlinear Operators, Differential Equations and Applications (Cluj-Napoca, 2001). Semin. Fixed Point Theory Cluj-Napoca **3** (2002), 239-248.
- *Sur les Conjectures de Markus-Yamabe et de la Jacobienne*, Séminaire de la Théorie de la Meilleure Approximation, Convexité et Optimisation, Ed. Srma (2000), 125-141.
- *About an interesting sequence*, Octogon **1** (2000), 173-180.
- *A generalization of convex and midconvex functions*, Analysis, Functional equations, Approximation and Convexity, Proceedings of the Conference Held in Honor of Professor Elena Popoviciu on the Occasion of her 75th Birthday, Ed. Carpatica (1999), 89-93.

Livre

Singularities in some variational problems, VDM Verlag Dr. Müller, Saarbrücken, 2010, 260pp.

Prépublications

- * *Two-dimensional unit-length vector fields of vanishing divergence*, prépublication.
- * (avec L. Döring et F. Otto) *Asymmetric domain walls of small angle in micromagnetics*, prépublication.
- * (avec L. Döring et F. Otto) *Cross-over from symmetric to asymmetric transition layers in micromagnetics*, prépublication.
- (avec L. Nguyen, V. Slastikov et A. Zarnescu) *On the uniqueness and instability of the radially symmetric solution in the Landau - de Gennes model for liquid crystals*, prépublication.
- * (avec M. Kurzke) *An effective model for boundary vortices in thin-film micromagnetics*, en préparation.

Chapter 1

Divergence-free unit-length vector fields and Entropies

Let $\Omega \subset \mathbf{R}^2$ be an open bounded set. We will focus on measurable vector fields $m : \Omega \rightarrow \mathbf{R}^2$ that satisfy

$$|m| = 1 \text{ a.e. in } \Omega \quad \text{and} \quad \nabla \cdot m = 0 \quad \text{in } \mathcal{D}'(\Omega). \quad (1.1)$$

One can equivalently consider measurable vector fields $v : \Omega \rightarrow \mathbf{R}^2$ such that

$$|v| = 1 \text{ a.e. in } \Omega \quad \text{and} \quad \nabla \times v = 0 \quad \text{in } \mathcal{D}'(\Omega). \quad (1.2)$$

(The passage from (1.1) to (1.2) is done via $v = m^\perp = (-m_2, m_1)$. The notation m comes from micromagnetics and stands for the magnetization.) Locally, m (resp. v) can be written in terms of a stream function ψ , i.e., $m = \nabla^\perp \psi$ (resp. $v = -\nabla \psi$) so that we get to the eikonal equation through ψ :

$$|\nabla \psi| = 1. \quad (1.3)$$

Typically, one can construct such vector fields by considering stream functions of the form $\psi = \text{dist}(\cdot, K)$ for some closed set $K \subset \mathbf{R}^2$; these vector fields are called Landau states in micromagnetic jargon (see Figure 1.1). However, not every stream function can be written as a distance function

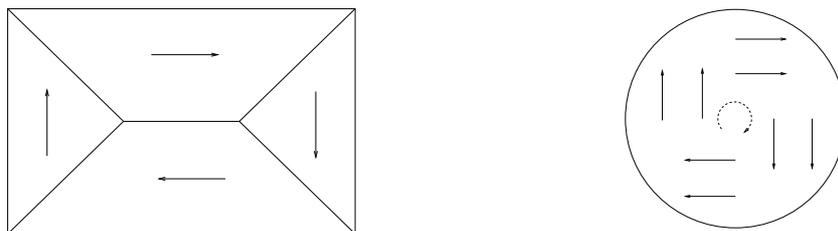
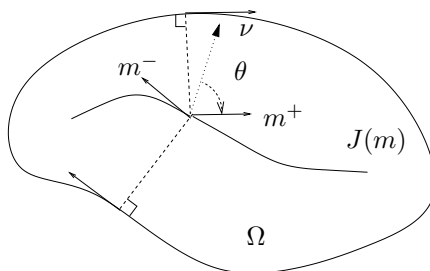


Figure 1.1: Landau states in a rectangle and a disc.

(up to a sign ± 1 and an additive constant); for example, if $\psi(x) = \max\{\text{dist}(x, P_1), \text{dist}(x, P_2)\}$ for two different points $P_1, P_2 \in \mathbf{R}^2$, then (1.3) holds even if ψ is not a distance function.

We denote

$$C_{div}^\infty(\Omega, S^1) = \{m \in C^\infty(\Omega, \mathbf{R}^2) : m \text{ satisfies (1.1)}\}.$$

Figure 1.2: Configuration m in $BV_{div}(\Omega, S^1)$.

Idem, $W_{div}^{s,p}(\Omega, S^1)$ stands for Sobolev spaces of order $s > 0$ and $p \geq 1$ of divergence-free unit-length vector fields, as well as $BV_{div}(\Omega, S^1)$ for vector fields of bounded total variation. For a vector field $m \in BV_{div}(\Omega, S^1)$, we denote the jump set of m by $J(m)$ which is a \mathcal{H}^1 -rectifiable set oriented by a unit vector field $\nu : J(m) \rightarrow S^1$ and $m^\pm : J(m) \rightarrow S^1$ stand for the traces of m on $J(m)$ with respect to ν . Notice that the divergence-free hypothesis on m ensures that the normal component $m \cdot \nu$ is continuous across the jump set $J(m)$. So, for \mathcal{H}^1 -almost every $x \in J(m)$, we can characterize the jump of m by a so called "wall angle" $\theta(x)$ such that $m^\pm(x) = \cos \theta(x) \nu(x) \pm \sin \theta(x) \nu^\perp(x)$ (see Figure 1.2).

1.1 Entropies

In the study of vector fields (1.1), the main tool we use in the following is the concept of entropies coming from scalar conservation laws. The starting point consists in regarding the structure (1.1) of our vector fields as a scalar conservation law. Indeed, writing $m = (u, h(u))$ for the flux $h(u) = \pm \sqrt{1 - u^2}$, the vanishing divergence condition in m turns into

$$\partial_t u + \partial_s h(u) = 0, \quad (1.4)$$

where $(t, s) := (x_1, x_2)$ correspond to (time, space) variables. Let us recall some definitions from the theory of scalar conservation laws. Since the flux h is nonlinear, there is in general no smooth solution of the Cauchy problem associated to (1.4). Therefore, the solutions of (1.4) are to be understood in the sense of distributions and in general, there are infinitely many weak solutions for the Cauchy problem. The concept of entropy solution has been formulated in order to have uniqueness (see Kruřkov [50]). To introduce this notion, the pair (entropy, entropy-flux) is defined as a couple of scalar functions (η, q) such that $\frac{dq}{ds} = \frac{dh}{ds} \frac{d\eta}{ds}$ which entails that every smooth solution u of (1.4) has vanishing entropy production, i.e.,

$$\partial_t[\eta(u)] + \partial_s[q(u)] = 0.$$

A solution u of (1.4) (in the sense of distributions) is called entropy solution if for every convex entropy η , the entropy production $\partial_t[\eta(u)] + \partial_s[q(u)] \leq 0$ is a nonpositive measure. Moreover, such solutions u have the property that for every pair (η, q) , the entropy production is a (signed) measure that concentrates on lines (corresponding to "shocks" of u). It suggests the interest of using "global" quantities (η, q) to detect "local" line-singularities of u . This idea has been used when dealing with reduced models in micromagnetics by Jin-Kohn [48], Aviles-Giga [6],

DeSimone-Kohn-Müller-Otto [25], Ambrosio-DeLellis-Mantegazza [2], Alouges-Riviere-Serfaty [1], Ignat-Merlet [41, 40], Ignat-Moser [42].

In the sequel we will always use the following notion of entropy introduced in [25] (see also [48], [19], [40]). It corresponds to the pair (entropy, entropy-flux) from the scalar conservation laws, but here the pair is defined in terms of the couple $(u, h(u))$ and not only on u .

Definition 1 (DKMO [25]) *We will say that $\Phi \in C^\infty(S^1, \mathbf{R}^2)$ is an entropy if*

$$\frac{d}{d\theta}\Phi(z) \cdot z = 0, \quad \text{for every } z = e^{i\theta} = (\cos \theta, \sin \theta) \in S^1. \quad (1.5)$$

Here, $\frac{d}{d\theta}\Phi(z) := \frac{d}{d\theta}[\Phi(e^{i\theta})]$ stands for the angular derivative of Φ . The set of all entropies is denoted by *ENT*.

We will often use a second characterization of entropies that provides a way to construct entropies:

Proposition 1 (DKMO [25]) *Let $\Phi \in C^\infty(S^1, \mathbf{R}^2)$. Then $\Phi \in ENT$ if and only if there exists a (unique) 2π -periodic $\varphi \in C^\infty(\mathbf{R})$ such that for every $z = e^{i\theta} \in S^1$,*

$$\Phi(z) = \varphi(\theta)z + \frac{d\varphi}{d\theta}(\theta)z^\perp. \quad (1.6)$$

In this case,

$$\frac{d}{d\theta}\Phi(z) = \lambda(\theta)z^\perp, \quad (1.7)$$

where $\lambda \in C^\infty(\mathbf{R})$ is the 2π -periodic function defined by $\lambda = -\Lambda\varphi := \varphi + \frac{d^2}{d\theta^2}\varphi$ in \mathbf{R} .

Remark 1 There exists a unique extension of $\Lambda : C^\infty(S^1 \approx \mathbf{R}/2\pi\mathbb{Z}) \rightarrow C^\infty(S^1)$ as a linear nonbounded operator $\Lambda : L^2(S^1) \rightarrow L^2(S^1)$ with the domain $D(\Lambda) = H^2(S^1)$. Moreover, the kernel of Λ is given by $\ker \Lambda = \mathbf{R}\sin \oplus \mathbf{R}\cos$, the spectrum of Λ is $\sigma(\Lambda) = \{k^2 - 1 : k \in \mathbb{N}^*\}$ and the range of Λ is $R(\Lambda) = (\ker \Lambda)^\perp$. Consequently, for every $\lambda \in (\ker \Lambda)^\perp$, there exists a unique $\varphi \in L^2(S^1)/(\ker \Lambda)$ such that $-\Lambda\varphi = \lambda$ and the corresponding entropy Φ given by (1.6) is uniquely defined by λ up to a constant.

This notion is coherent with the property that a smooth vector field m satisfying (1.1) induces vanishing entropy production $\nabla \cdot [\Phi(m)] = 0$. In fact, it is equivalent¹ to Definition 1 as stated in the following property:

Proposition 2 (Ignat [33]) *Let $\Phi \in C^\infty(S^1, \mathbf{R}^2)$. Then Φ is an entropy if and only if for every $m \in W_{div}^{1/p,p}(\Omega, S^1)$, $p \in [1, 2]$ (in particular, for every $m \in C_{div}^\infty(\Omega, S^1)$), the following identity holds:*

$$\nabla \cdot [\Phi(m)] = 0 \quad \text{in } \mathcal{D}'(\Omega). \quad (1.8)$$

As we explain later, the assumption $m \in W^{1/p,p}$ is a critical regularity to avoid line-singularities. We conjecture that the above Proposition should hold also for $p > 2$. However, for $m \in BV_{div}(\Omega, S^1)$, the *entropy production*

$$\mu_\Phi(m) := \nabla \cdot [\Phi(m)]$$

is a measure supported on the jump set of m .

¹In fact, (1.5) can be deduced from (1.8) by choosing m to be an appropriate vortex configuration (see [40]).

Proposition 3 (Ignat-Merlet [40]) *Let $\Phi \in ENT$ be an entropy and $m \in BV_{div}(\Omega, S^1)$. Then we have*

$$\mu_\Phi(m) = \{\Phi(m^+) - \Phi(m^-)\} \cdot \nu \mathcal{H}^1 \llcorner J(m), \quad (1.9)$$

where $J(m)$ is the \mathcal{H}^1 -rectifiable jump set of m oriented by ν and m^\pm are the traces of m on $J(m)$.

Observe that for the orientation $\nu = e^{i\beta}$ ($\beta \in \mathbf{R}$) and traces $m^\pm = e^{i(\beta \pm \theta)}$ with $\theta \in [-\pi, \pi)$ be the "wall angle" of the jump of m at some point $x \in J(m)$, the entropy production density can be written as a convolution formula via (1.7):

$$[\Phi(m^+) - \Phi(m^-)] \cdot \nu = (\lambda \star \sin_\theta)(\beta), \quad \beta \in \mathbf{R}, \quad (1.10)$$

where

$$\sin_\theta(\beta) = \begin{cases} \operatorname{sgn}(\theta) \sin \beta & \text{for } |\beta| \leq |\theta|, \\ 0 & \text{for } |\beta| > |\theta|. \end{cases}$$

Remark 2 The proof of Propositions 2 and 3 strongly relies on the structure of lifting of vector fields $m \in BV(\Omega, S^1)$ (resp. $m \in W^{1/p,p}(\Omega, S^1)$) and an appropriate chain rule. More precisely, if $m \in BV(\Omega, S^1)$, then there exists a lifting $\Theta \in BV(\Omega, \mathbf{R})$ such that $m = e^{i\Theta}$ a.e. in Ω (see e.g. [29], [12], [17], [34]). While if $m \in W^{1/p,p}(\Omega, S^1)$ with $p \geq 1$, then one can find a lifting $\Theta = \Theta_1 + \Theta_2$ of m with $\Theta_1 \in W^{1/p,p}$, $\Theta_2 \in SBV$ and $e^{i\Theta_2} \in W^{1/p,p} \cap W^{1,1}$ (see [11], [57], [56]). Recall that $SBV(\Omega, \mathbf{R}^d)$ is the subspace of vector fields $m \in BV(\Omega, \mathbf{R}^d)$ whose differential Dm has vanishing Cantor part $D^c m$ (i.e., $D^c m \equiv 0$ as a measure in Ω).

As shown in [40], these properties can be extended for nonsmooth entropies. Moreover, there is a special class of BV entropies that play an important role in the following: for each $\xi \in S^1$, we call "elementary entropies" the maps $\Phi^\xi : S^1 \rightarrow \mathbf{R}^2$ given by

$$\Phi^\xi(z) := \begin{cases} \xi & \text{for } z \cdot \xi > 0, \\ 0 & \text{for } z \cdot \xi \leq 0. \end{cases} \quad (1.11)$$

Although Φ^ξ is not a smooth entropy (in fact, Φ^ξ has a jump at the points $\pm \xi^\perp \in S^1$), the equality (1.5) trivially holds in $\mathcal{D}'(S^1)$. Moreover, as shown in [25], there exists a sequence of smooth entropies $\{\Phi_k\} \subset ENT$ such that $\{\Phi_k\}$ is uniformly bounded and $\lim_k \Phi_k(z) = \Phi^\xi(z)$ for every $z \in S^1$ (this approximation result follows via (1.6)).

1.2 The space $W_{div}^{1/p,p}(\Omega, S^1)$. Vortices. ²

The aim of this section consists in the study of vector fields (1.1) of critical regularity $m \in W^{1/p,p}$ that insures avoidance of line-singularities. In this case, we expect that such vector fields m present vortex singular points. The main feature of these vector fields resides in a kinetic formulation. It comes via Propositions 2 and 3 when writing the entropy production for the "elementary entropies" $\Phi^\xi = \xi \tilde{\chi}$ (see (1.11)). We succeed to prove the following kinetic formulation for $W_{div}^{1/p,p}(\Omega, S^1)$ with $p \in [1, 2]$ and we conjecture that it still holds for $p > 2$.

²All the results appearing in this section are part of the articles of the author [37, 33]. Therefore, we don't specify in the following these references for each result.

Proposition 4 (Kinetic formulation) *Let $m \in W_{div}^{1/p,p}(\Omega, S^1)$ with $p \in [1, 2]$. For every direction $\xi \in S^1$, we define $\chi(\cdot, \xi) : \Omega \rightarrow \{0, 1\}$ (resp. $\tilde{\chi}(\cdot, \xi) : S^1 \rightarrow \{0, 1\}$) by*

$$\chi(x, \xi) = \tilde{\chi}(m(x), \xi) = \begin{cases} 1 & \text{for } m(x) \cdot \xi > 0, \\ 0 & \text{for } m(x) \cdot \xi \leq 0. \end{cases}$$

Then the following kinetic equation holds for every $\xi \in S^1$:

$$\xi \cdot \nabla \chi(\cdot, \xi) = 0 \quad \text{in } \mathcal{D}'(\Omega). \quad (1.12)$$

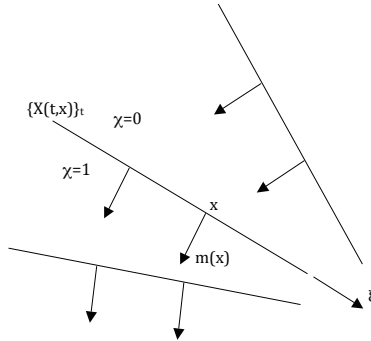


Figure 1.3: Characteristics of m .

Here, χ corresponds to the concept of characteristic of a weak solution m satisfying (1.1). Indeed, if m is smooth around a point $x \in \Omega$, then the characteristic of m at x (by means of the eikonal equation (1.3) with $m = \nabla^\perp \psi$ around x) is given by $\dot{X}(t, x) = m^\perp(X(t, x))$ with the initial condition $X(0, x) = x$; then the orbit $\{X(t, x)\}_t$ is a straight line (i.e., $X(t, x) = x + tm^\perp(x)$ for t in some interval around 0) along which m is perpendicular and constant. Therefore, in the direction $\xi := m^\perp(x)$, either $\nabla \chi(\cdot, \xi)$ locally vanishes (if m is constant in a neighborhood of x), or it concentrates on $\{X(t, x)\}_t$ and is oriented by ξ^\perp (see Figure 1.3). The knowledge of $\chi(\cdot, \xi)$ in every direction $\xi \in S^1$ determines completely the vector field m due to the straightforward formula

$$m(x) = \frac{1}{2} \int_{S^1} \xi \chi(x, \xi) d\xi \quad \text{for a.e. } x \in \Omega. \quad (1.13)$$

Remark 3 Classical kinetic averaging lemma (see e.g. Golse-Lions-Perthame-Sentis [31]) shows that a measurable vector-field $m : \Omega \rightarrow S^1$ satisfying (1.12) belongs to $H_{loc}^{1/2}$ (due to (1.13)). This property can be read as the inverse of Proposition 4 for the case $m \in H^{1/2}(\Omega, S^1)$.

1.2.1 Regularity results

The first goal is to prove the following regularity result:

Theorem 1 *If $m \in W_{div}^{1/p,p}(\Omega, S^1)$ with $p \in [1, 2]$ then m is locally Lipschitz continuous inside Ω except at a locally finite number of singular points. Moreover, every singular point P of m*

corresponds to a vortex singularity of degree 1 of m , i.e., there exists a sign $\alpha = \pm 1$ such that

$$m(x) = \alpha \frac{(x-P)^\perp}{|x-P|} \quad \text{for every } x \neq P \text{ in any convex neighborhood of } P \text{ in } \Omega.$$

In particular, if $m \in H_{div}^1(\Omega, S^1)$ then m is locally Lipschitz.

Remark 4 The above result was proved by Jabin-Otto-Perthame [45] in the particular case of zero-energy states of a line-energy Ginzburg-Landau model. More precisely, for $\varepsilon > 0$, one defines the functional $E_\varepsilon : H^1(\Omega, \mathbf{R}^2) \rightarrow \mathbf{R}_+$ by

$$E_\varepsilon(m_\varepsilon) = \varepsilon \int_\Omega |\nabla m_\varepsilon|^2 dx + \frac{1}{\varepsilon} \int_\Omega (1 - |m_\varepsilon|^2)^2 dx + \frac{1}{\varepsilon} \|\nabla \cdot m_\varepsilon\|_{H^{-1}(\Omega)}^2, \quad m_\varepsilon \in H^1(\Omega, \mathbf{R}^2)$$

(we refer to [2, 6, 48, 25, 46, 66, 45] for the analysis of this model). A vector field $m : \Omega \rightarrow \mathbf{R}^2$ is called zero-energy state if there exists a family $\{m_\varepsilon \in H^1(\Omega, \mathbf{R}^2)\}_{\varepsilon \rightarrow 0}$ satisfying

$$m_\varepsilon \rightarrow m \quad \text{in } L^1(\Omega) \quad \text{and} \quad E_\varepsilon(m_\varepsilon) \rightarrow 0 \quad \text{as } \varepsilon \rightarrow 0.$$

Then m satisfies (1.1). Moreover, it is proved in [45] that a zero-energy state satisfies the kinetic formulation (1.12) and furthermore, m shares the structure in Theorem 1. Therefore, the proof of Theorem 1 strongly relies on [45] and Proposition 4 (via Proposition 2).

As consequence of Theorem 1, one has for $p \in [1, 2]$:

$$\{m \in W_{loc}^{1/p,p}(\Omega, \mathbf{R}^2) : m \text{ satisfies (1.1)}\} = \{m \in H_{loc}^{1/2}(\Omega, \mathbf{R}^2) : m \text{ satisfies (1.1)}\}.$$

Let us now discuss the optimality of the result in Theorem 1: Firstly, observe that Lipschitz regularity cannot be improved.

Proposition 5 *There exist Lipschitz vector fields $m : \Omega \rightarrow \mathbf{R}^2$ that satisfy (1.1) and are not C^1 in Ω .*

In general, a vector field $m \in W_{div}^{1/p,p}(\Omega, S^1)$ with $p \in [1, 2]$ (without interior vortex singularities) is only locally Lipschitz, and not necessary globally Lipschitz in Ω . This is the case of a "boundary vortex" vector field, e.g., $m(x) = \frac{(x-P)^\perp}{|x-P|}$ for every $x \in \Omega$ where P is some point on $\partial\Omega$. If the domain Ω has a cusp in $P \in \partial\Omega$, the "boundary vortex" vector field could belong even to $H^1(\Omega, \mathbf{R}^2)$; moreover, there even exist convex domains Ω and $m \in H_{div}^1(\Omega, S^1)$ such that m is not globally Lipschitz in Ω .

The geometry of Ω influences the number of vortex singularities of $W_{div}^{1/p,p}$ -vector fields satisfying (1.1). For example, if Ω is convex, then every vector field $m \in W_{div}^{1/p,p}(\Omega, S^1)$ with $p \in [1, 2]$ is either a "vortex" vector field (i.e., $m(x) = \pm \frac{(x-P)^\perp}{|x-P|}$ for every $x \in \Omega$ where P is some point in Ω), or locally Lipschitz (i.e. no interior vortex); therefore, convex domains do not allow for more than one interior vortex. However, we prove that there are nonconvex domains where configurations with arbitrary number of vortices do exist.

Proposition 6 *There exist an open simply-connected nonconvex piecewise Lipschitz domain Ω and a vector field $m \in W_{div}^{1,q}(\Omega, S^1)$ for every $q \in [1, 2)$ that has infinitely many vortices $\{P_1, P_2, \dots\}$.*

Observe that $W_{loc}^{1,q}(\Omega, S^1) \subset W_{loc}^{1/p,p}(\Omega, S^1)$ for $q > 1$ and $p \geq 1$, and the embedding fails for $q = 1$. Also notice that configurations with infinitely many (interior) vortices can occur only in a non-Lipschitz domain Ω ; indeed, if $\partial\Omega$ is Lipschitz, then a configuration $m \in W_{div}^{1/p,p}(\Omega, S^1)$ with $p \in [1, 2]$ has only a finite number of interior vortex singularities.

We address the following open problem:

Open Problem 1 *Does Theorem 1 hold in the case $m \in W_{div}^{1/p,p}(\Omega, S^1)$ with $p > 2$?*

A positive answer is equivalent to proving Proposition 2 for $m \in W_{div}^{1/p,p}(\Omega, S^1)$ with $p > 2$ which would yield the kinetic formulation (1.12) for such m . However, standard chain rule does not allow to conclude that for $p > 2$. A natural question concerns higher dimensions $d \geq 3$ in the same context of the eikonal equation. We mention that the above technics seem to be typical for the two-dimensional case and do not adapt to the case $d \geq 3$. Indeed, if $d = 3$, the system of scalar conservation laws associated to (1.3) admits only the trivial entropies. Moreover, the regularity result in Theorem 1 is based on a certain order relation between the characteristics of m . Obviously, such an order relation does not exist in higher dimensions. We conjecture the following for dimension $d = 3$:

Open Problem 2 *Let $\Omega \subset \mathbf{R}^3$ be a bounded open set and $v \in H^1(\Omega, S^2)$ be a gradient field, i.e., $v = \nabla\psi$ with (1.3). Is it true that v is locally Lipschitz continuous inside Ω except at a locally finite number of vortex singularities of v and $v(x) = \alpha \frac{(x-P)}{|x-P|}$ in any convex neighborhood of a vortex point P in Ω with a sign $\alpha = \pm 1$?*

1.2.2 Density results

The second goal of the section is to present approximation results for the class of vector fields $W_{div}^{1/p,p}(\Omega, S^1)$ with $p \in [1, 2]$: our subsets are formed either by divergence-free vector fields that are smooth except at a finite number of points and the approximation result holds in the $W^{1/p,p}$ -topology, or by everywhere smooth S^1 -valued vector fields (not necessarily divergence-free) and the approximation result holds in a weaker topology. We start by extending Bethuel-Zheng's density result (see [8]) for $W^{1,1}(\Omega, S^1)$ vector fields, respectively Riviere's density result (see [65]) for $H^{1/2}(\Omega, S^1)$ vector fields to the case of divergence-free vector fields:

Theorem 2 *Let Ω be a Lipschitz bounded simply-connected domain and $m \in W_{div}^{1/p,p}(\Omega, S^1)$ with $p \in [1, 2]$. Then m has a finite number $N \geq 0$ of vortices $\{P_1, \dots, P_N\}$ and m can be approximated in $W_{loc}^{1,q}(\Omega)$ (for any $q \in [1, 2)$) by divergence-free vector fields $m_k \in C^\infty(\Omega \setminus \{P_1, \dots, P_N\}, S^1)$ that are smooth except at the N vortex points of m . In particular, if $m \in H_{div}^1(\Omega, S^1)$, the sequence $\{m_k\}$ can be chosen to be smooth everywhere in Ω and the approximation result holds in $H_{loc}^1(\Omega)$.*

In various applications (see e.g. Remark 5 below), we need to approximate vector fields m (with the structure given in Theorem 1) by $H^1(\Omega, S^1)$ vector fields. But $H^1(\Omega, S^1)$ -vector fields cannot allow for vortices. Therefore, an approximation result by everywhere smooth S^1 -valued vector fields is needed in some weaker topology than in Theorem 2. What is the optimal weak topology where such a density result holds? The following result shows that L^1 -topology is too strong for having density of smooth vector fields of vanishing divergence and values in S^1 .

Proposition 7 *Let $m : B^2 \rightarrow S^1$ be the vortex configuration $m(x) = \frac{x^\perp}{|x|}$ in the unit disc B^2 . Then there exists no sequence of vector fields $m_k \in C_{div}^\infty(\Omega, S^1)$ such that $m_k \rightarrow m$ a.e. in B^2 as $k \rightarrow \infty$.*

We now generalize this property: the density result still fails if we relax the divergence-free constraint on the approximated smooth vector fields, but we impose this restriction in the limit in L^1 -topology (or H^{-s} weak topology for some $s \in [0, \frac{1}{2})$).

Proposition 8 *Let $m : B^2 \rightarrow S^1$ be the vortex configuration $m(x) = \frac{x^\perp}{|x|}$ in B^2 . Then there exists no sequence of vector fields $m_k \in C^\infty(\Omega, S^1)$ such that $m_k \rightarrow m$ a.e. in B^2 as $k \rightarrow \infty$ and one of the following two conditions holds:*

- a) $\nabla \cdot m_k \rightarrow 0$ in $L^1(B^2)$;
- b) $\nabla \cdot m_k \rightarrow 0$ weakly in $H^{-s}(B^2)$ for some $s \in [0, \frac{1}{2})$.

Finally, we prove an approximation result in L^1 -topology by smooth vector fields with values in S^1 (not necessary divergence-free), but the divergence-free constraint holds in the limit in the $H^{-1/2}$ topology. This topology is optimal (due Proposition 8 b)).

Theorem 3 *Let Ω be a Lipschitz bounded simply-connected domain and $m \in W_{div}^{1/p,p}(\Omega, S^1)$ with $p \in [1, 2]$. Then there exists a sequence of vector fields $m_k \in C^\infty(\Omega, S^1)$ such that $m_k \rightarrow m$ a.e. in Ω and $(\nabla \cdot m_k)\mathbf{1}_\Omega \rightarrow 0$ in $\dot{H}^{-1/2}(\mathbf{R}^2)$ as $k \rightarrow \infty$.*

Remark 5 The motivation of Theorem 3 comes from thin-film micromagnetics. The following 2D energy (see [22]) is considered as an approximation of the 3D micromagnetic model in a thin-film regime: for $\varepsilon > 0$, one defines the functional $\tilde{E}_\varepsilon : H^1(\Omega, S^1) \rightarrow \mathbf{R}_+$ by

$$\tilde{E}_\varepsilon(m_\varepsilon) = \varepsilon \int_\Omega |\nabla m_\varepsilon|^2 dx + \|(\nabla \cdot m_\varepsilon)\mathbf{1}_\Omega\|_{\dot{H}^{-1/2}(\mathbf{R}^2)}^2, \quad m_\varepsilon \in H^1(\Omega, S^1).$$

This model was analyzed in [20], [43], [38]. In particular, it is proved in [38] that a vortex configuration $m(x) = \frac{x^\perp}{|x|}$ in B^2 is a zero-energy state, i.e., there exists a family $\{m_\varepsilon\} \subset H^1(B^2, S^1)$ such that $m_\varepsilon \rightarrow m$ a.e. in B^2 and $\tilde{E}_\varepsilon(m_\varepsilon) \rightarrow 0$ as $\varepsilon \rightarrow 0$. The role of Theorem 3 is to generalize this approximation result for every vector field $m \in W^{1/p,p}$ (with $p \in [1, 2]$) satisfying (1.1).

1.3 The BV case. Line energies. ³

The topic of this section concerns vector fields m satisfying (1.1) that present line-singularities. The context is the following: Let $\Omega \subset \mathbf{R}^2$ be a bounded domain with piecewise Lipschitz boundary that is oriented by the outer unit normal vector n . We start by addressing the following conjecture concerning the regularity of vector fields $m \in BV_{div}(\Omega, S^1)$: the measure Dm doesn't concentrate on sets of Hausdorff dimension $d \in (1, 2)$.

³All the results appearing in this section are part of the article Ignat-Merlet [40]. Therefore, we don't specify in the following this reference for each result.

Open Problem 3 *Is it true that every $m \in BV_{div}(\Omega, S^1)$ satisfies $m \in SBV$?*

This question is related with a recent work of Bianchini-DeLellis-Robyr [9]: they show that the viscosity solution ψ of a Hamilton-Jacobi equation $H(\nabla\psi) = 0$ in Ω (with a uniformly convex hamiltonian H) satisfies $\nabla\psi \in SBV$. Open Problem 3 asks whether for the particular case of the eikonal equation (1.3), the result in [9] still holds when replacing the assumption of viscosity solution with the hypothesis of a general solution ψ of (1.3) with $\nabla\psi \in BV$.

In the following, we focus on line-energies, i.e., energy functionals that concentrate on the jump set of $m \in BV_{div}(\Omega, S^1)$:

$$\mathcal{I}_f(m) := \int_{J(m)} f(|m^+ - m^-|) d\mathcal{H}^1.$$

We only consider energy densities that depend on the jump size $|m^+ - m^-|$ via a *cost function* $f : [0, 2] \rightarrow \mathbf{R}_+$ which satisfies $f(0) = 0$ and is assumed to be *lower semicontinuous*. Notice that if $\theta(x)$ is the "wall angle" of the jump of m at $x \in J(m)$, then $|m^+(x) - m^-(x)| = 2|\sin \theta(x)|$. Since m is of vanishing divergence, the trace of the normal component $m \cdot n$ is well defined on $\partial\Omega$ and we will consider the minimization problem in the subset

$$\mathcal{S}_0(\Omega) = \{m \in BV_{div}(\Omega, S^1) : m \cdot n = 0 \text{ on } \partial\Omega\}$$

(see Figure 1.2).

Our problem can be equivalently interpreted in terms of the stream function $\psi : \Omega \rightarrow \mathbf{R}$ associated to $m = \nabla^\perp \psi \in \mathcal{S}_0(\Omega)$. Then the above variational principle turns in analyzing the following energy functional

$$\int_{J(\nabla\psi)} f(|(\nabla\psi)^+ - (\nabla\psi)^-|) d\mathcal{H}^1 \quad (1.14)$$

over the set of solutions of the Dirichlet problem associated to the eikonal equation

$$|\nabla\psi| = 1 \text{ in } \Omega \quad \text{and} \quad \psi = 0 \text{ on } \partial\Omega.$$

The method of characteristics shows that for a simply-connected bounded domain there is no smooth solution of the eikonal equation $|\nabla\psi| = 1$ in Ω satisfying the constraint $\psi = 0$ on $\partial\Omega$. Typical singularities are jump discontinuities of $\nabla\psi$ (equivalently of m) through line-singularities or vortices.

1.3.1 Motivation

Line-energy functionals \mathcal{I}_f appear as natural candidates for the asymptotic energy of family of singularly perturbed functionals $\{G_\varepsilon\}_{\varepsilon \downarrow 0}$,

$$G_\varepsilon(m_\varepsilon) = \varepsilon \int_\Omega |\nabla m_\varepsilon|^2 + \frac{1}{\varepsilon} \int_\Omega g(|1 - |m_\varepsilon|^2|), \quad (1.15)$$

defined for $m_\varepsilon \in H^1(\Omega, \mathbf{R}^2)$ satisfying the constraints $\nabla \cdot m_\varepsilon = 0$ in Ω . One can eventually impose a boundary condition $m_\varepsilon \cdot n = 0$ on $\partial\Omega$. Here, $\varepsilon > 0$ is a small parameter and $g : \mathbf{R}_+ \rightarrow \mathbf{R}_+$ is some lower semicontinuous function such that $g(0) = 0$ and $g(t) > 0$ for $t > 0$. Variational models (1.15) arise in several physical applications such as smectic liquid crystals, film blisters or convective pattern formation (see e.g. [4], [62], [48], [41]).

Observe that the vector fields m_ε in (1.15) are not S^1 -valued but their distance to S^1 is penalized by the second term of G_ε . As ε tends to 0, we expect that families $\{m_\varepsilon\}$ of uniformly bounded energies (1.15) will converge (up to extraction and in a certain topology, see below) to some limit m_0 satisfying (1.1).

A natural question arises: if \mathcal{I}_f is indeed the asymptotic energy of $\{G_\varepsilon\}$ as $\varepsilon \rightarrow 0$, what is the relation between the energy density f and the function g ? The ansatz consists in reducing the 2D variational problem to a 1D asymptotic analysis: Assume that m_0 is of bounded variation and satisfies (1.1), i.e., $m_0 \in BV_{div}(\Omega, S^1)$. We also assume that at level $\varepsilon > 0$ the energy $G_\varepsilon(m_\varepsilon)$ concentrates on 1D transition layers of length scale ε through the line-singularities of m_0 . With the above notation, let x_0 be a jump point of m_0 , θ_0 be the "wall angle" defining the jump $m_0^\pm(x_0)$ and ν_0 be the orientation of the jump set at x_0 (see Figure 1.4). At level $\varepsilon > 0$, a 1D transition layer in the direction ν_0 has the form

$$m_\varepsilon(x_0 + t\nu_0) = \cos \theta_0 \nu_0 + u(t/\varepsilon) \nu_0^\perp,$$

where $u : \mathbf{R} \rightarrow \mathbf{R}$ is the rescaled profile of the tangential component of the layer satisfying $u(s) \xrightarrow{\pm s \uparrow \infty} \pm \sin \theta_0$. (Observe that a divergence-free 1D transition layer has a constant normal component.) Using this ansatz, we obtain that the limit energy is given by \mathcal{I}_f with the cost

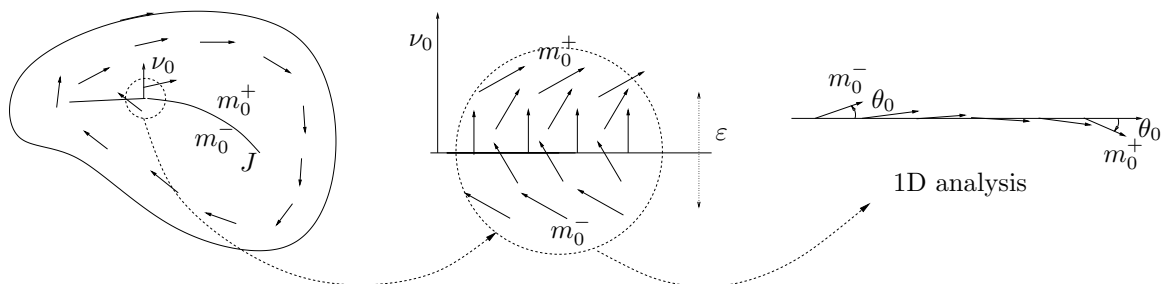


Figure 1.4: 1D ansatz : A line-singularity of a limit configuration m_0 (left picture) is regularized by a smooth 1D transition layer at the level $\varepsilon > 0$ connecting two limit states m_0^\pm (middle picture). The full transition occurs in the normal direction ν_0 as represented in the right picture.

function computed as follows:

$$\begin{aligned} f(|2 \sin \theta_0|) &= \min \left\{ \int_{\mathbf{R}} \left(\left| \frac{du}{ds}(s) \right|^2 + g(|\sin^2 \theta_0 - u^2(s)|) \right) ds : u : \mathbf{R} \rightarrow \mathbf{R}, u \xrightarrow{\pm s \uparrow \infty} \pm \sin \theta_0 \right\} \\ &= 4 \int_0^{\sin \theta_0} \sqrt{g(\sin^2 \theta_0 - u^2)} du, \quad \theta_0 \in [0, \frac{\pi}{2}], \end{aligned} \quad (1.16)$$

which yields the connection between f and g . In particular, every power function $f(t) = t^p$ corresponds to $g(t) = ct^{p-1}$ in (1.16) where the constant $c = c(p)$ depends only on p .

For $g(t) = t^2$, the above ansatz is known to be relevant. The corresponding functional (1.15) has been introduced by Aviles and Giga [4] and we will explain in Section 1.4 why \mathcal{I}_f with $f(t) = t^3/3$ (given by (1.16)) is indeed the asymptotic energy of $\{G_\varepsilon\}$ (in the sense of Γ -convergence in the strong L^1 -topology). However, let us stress that for a general function g , the above 1D ansatz may be wrong. Indeed, in some cases, it is possible to decrease strictly the energy by substituting

2D mesoscopic structures for 1D transition layers. In these cases, the 1D asymptotic energy \mathcal{I}_f (with f given by (1.16)) does not match the 2D Γ -limit energy of (1.15). Such counterexamples are obtained with non lower semicontinuous functionals \mathcal{I}_f (see Definition 2 below). Indeed, a Γ -limit functional over a metric space (which is the space L^1 in our case) must be lower semicontinuous with respect to the induced topology. A first counterexample is given in [2]: it is shown that power functions $f(t) = t^p$ lead to non lower semicontinuous functional \mathcal{I}_f for $p > 3$. A second counterexample is described in [1]: the cost function $f_{ARS}(2 \sin \theta) = \sin \theta - \theta \cos \theta$ for $0 \leq \theta \leq \pi/2$ (stemmed from the energy of 1D transition layers associated to a particular asymptotics of the micromagnetic energy). It turns out that $\mathcal{I}_{f_{ARS}}$ is not lower semicontinuous. In both cases it is possible to build a 2D mesoscopic structure with length-scale $\eta \ll 1$ between two limit states m^- and m^+ with an energetic cost strictly smaller than the cost of a direct 1D jump. An example of such 2D structure is described in [1] (see Figure 1.5) and stands for the cross-tie wall pattern in micromagnetics.

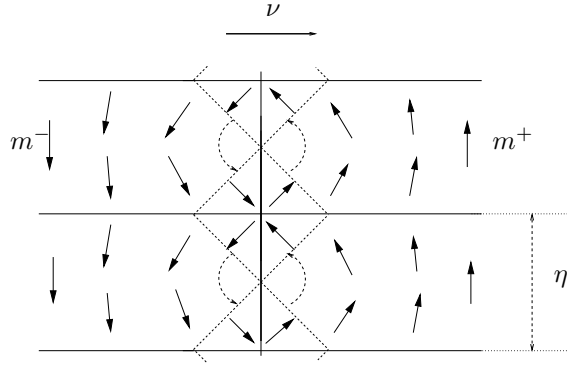


Figure 1.5: A cross tie wall. As $\eta \downarrow 0$, the 2D microstructure tends to a jump configuration (m^-, m^+) in direction ν and has less energy than the initial cost $f_{ARS}(2)$ corresponding to the 1D jump m^\pm of angle $\theta = 90^\circ$.

1.3.2 Lower semicontinuity

As explained above, lower semicontinuity implies the optimality of the 1D structure, i.e. it is not possible to decrease the energy of a (direct) jump by constructing 2D mesoscopic structures. So it is important to characterize cost functions f such that the line-energy \mathcal{I}_f is lower semicontinuous in a relevant functional space. In general, the weak BV -topology is too strong for this aim; due to applications (see Section 1.4), it is natural to weaken the regularity by using the topology of L^1 . Of course, in order for the constraint $|m_0| = 1$ to be stable under convergence, we need to use the strong L^1 -topology. Then, let us extend the functional \mathcal{I}_f in $L^1(\Omega, \mathbf{R}^2)$ by $+\infty$, i.e.,

$$\mathcal{I}_f(m) = +\infty \quad \text{if} \quad m \in L^1(\Omega, \mathbf{R}^2) \setminus BV_{div}(\Omega, S^1),$$

and let us introduce the relaxed functional $\overline{\mathcal{I}}_f$, i.e., the lower semicontinuous envelope of \mathcal{I}_f with respect to the strong L^1 -topology: $\overline{\mathcal{I}}_f : L^1(\Omega, \mathbf{R}^2) \rightarrow \mathbf{R} \cup \{+\infty\}$ is defined as

$$\overline{\mathcal{I}}_f(m) = \inf \left\{ \liminf_{k \rightarrow \infty} \mathcal{I}_f(m_k) : m_k \rightarrow m \text{ strongly in } L^1 \right\}, \quad \forall m \in L^1(\Omega, \mathbf{R}^2).$$

Obviously, $\overline{\mathcal{I}_f} \leq \mathcal{I}_f$ and all configurations of finite relaxed energy $\overline{\mathcal{I}_f}(m) < +\infty$ belong to

$$\mathcal{L}(\Omega) = \{m \in L^1(\Omega, \mathbf{R}^2) : |m| = 1 \text{ and } \nabla \cdot m = 0 \text{ in } \Omega\}$$

which is a closed set in L^1 . Recall that the normal component of $m \in \mathcal{L}(\Omega)$ at the boundary $\partial\Omega$ is well defined. In particular,

$$\mathcal{L}_0(\Omega) = \{m \in \mathcal{L}(\Omega) : m \cdot n = 0 \text{ on } \partial\Omega\} \quad (1.17)$$

is a closed subset of $\mathcal{L}(\Omega)$.

Definition 2 We say that the line-energy $\mathcal{I}_f : L^1(\Omega, \mathbf{R}^2) \rightarrow \mathbf{R} \cup \{+\infty\}$ is lower semicontinuous (l.s.c.) if $\mathcal{I}_f(m) = \overline{\mathcal{I}_f}(m)$ for every $m \in BV_{div}(\Omega, S^1)$.

Remark 6 The above definition is weaker than asking for \mathcal{I}_f to be lower semicontinuous in L^1 (i.e. $\mathcal{I}_f = \overline{\mathcal{I}_f}$ in $L^1(\Omega, \mathbf{R}^2)$). Indeed, for the Aviles-Giga model with cubic jump costs, it is proved in [2] that $\mathcal{I}_{t \rightarrow t^3}(m) = \overline{\mathcal{I}_{t \rightarrow t^3}}(m)$ for every $m \in BV_{div}(\Omega, S^1)$ (so, $\mathcal{I}_{t \rightarrow t^3}$ is lower semicontinuous after Definition 2), but one can construct a limit configuration $m_0 \in L^1 \setminus BV$ with finite relaxed energy $\overline{\mathcal{I}_{t \rightarrow t^3}}(m_0) < +\infty = \mathcal{I}_{t \rightarrow t^3}(m_0)$. The crucial point in the construction of m_0 relies on the cubic cost of small jumps of m_0 in $\mathcal{I}_{t \rightarrow t^3}$ that cannot control the linear cost of the jump part of Dm_0 . Therefore, finite limit energy configurations m_0 do not belong in general to BV ; however, m_0 always shares the structure of BV functions, in particular, an equivalent notion of jump set can be defined for m_0 (see [19]).

A first result states the following necessary condition: in order for the line-energy functional \mathcal{I}_f to be lower semicontinuous, the cost function f should be also lower semicontinuous.

Proposition 9 Let $f : [0, 2] \rightarrow \mathbf{R}_+$ be a measurable function. If \mathcal{I}_f is lower semicontinuous, then f is lower semicontinuous on $[0, 2]$.

Recall that Aviles and Giga [6] proved that $\mathcal{I}_{t \rightarrow t^3}$ is lower semicontinuous and afterwards, Ambrosio, De Lellis and Mantegazza [2] established that \mathcal{I}_f is not lower semicontinuous for power cost functions $f(t) = t^p$ with $p > 3$. We address the following question raised in [2].

Conjecture 1 \mathcal{I}_f is lower semicontinuous for power cost functions $f(t) = t^p$ if $1 \leq p < 3$.

First of all, we give a partial positive answer to this question: the behavior as a power function t^p for $1 \leq p \leq 3$ at the origin $t = 0$ is natural for appropriate cost function.

Theorem 4 For every $p \in [1, 3]$, there exists an appropriate cost function $f : [0, 2] \rightarrow \mathbf{R}_+$ such that $f(t) = t^p$ for $t \in [0, \sqrt{2}]$ and \mathcal{I}_f is lower semicontinuous.

We mention that our method doesn't work for $p < 1$, therefore we don't know if the condition $p \geq 1$ is a necessary condition in Conjecture 1.

Next, we will establish a positive answer to Conjecture 1 for $p = 2$. Our interest for this case has a physical motivation, associated with the study of the energetic behavior of Bloch walls in micromagnetics as we will explain in Section 1.4.

Theorem 5 *If $f(t) = t^2$, then \mathcal{I}_f is lower semicontinuous.*

In fact the quadratic cost function stated in Theorem 5 is a particular case of a large family of cost functions that we will introduce via entropies in Section 1.3.3 and which induce lower semicontinuous line-energies.

1.3.3 Cost functions

The concept of entropies introduced in Section 1.1 reveals to be fundamental for cost functions f leading to l.s.c. functionals \mathcal{I}_f . More precisely, we will associate an appropriate cost function to every subset of entropies $S \subset ENT$:

Definition 3 *For a subset $S \subset ENT$, we define the cost function $c_S : [0, 2] \rightarrow \mathbf{R}_+$ by*

$$c_S(t) := \sup \{ [\Phi(z^+) - \Phi(z^-)] \cdot \nu : \Phi \in S, (z^-, z^+, \nu) \in \mathcal{T}, |z^+ - z^-| = t \},$$

where \mathcal{T} defines the set of admissible jump discontinuities:

$$\mathcal{T} := \{ (z^-, z^+, \nu) \in (S^1)^3 : (z^+ - z^-) \cdot \nu = 0 \}.$$

Remark 7 The set \mathcal{T} is motivated by the structure of jump discontinuities of divergence-free vector fields $m \in BV_{div}(\Omega, S^1)$. Indeed, one has $(m^+ - m^-) \cdot \nu = 0$ \mathcal{H}^1 -a.e. on the jump set $J(m)$ oriented by the normal ν with the traces $m^\pm \in L^\infty(J(m), S^1)$. The cost function c_S is nonnegative since one can switch from ν to $-\nu$ so that $[\Phi(z^+) - \Phi(z^-)] \cdot \nu \geq 0$.

Observe that these cost functions depend only on the jump size. To be consistent with this isotropic property, we will impose the following geometric constraints on our sets of entropies.

Definition 4 *A subset $S \subset ENT$ is symmetric if $S = -S$ and it is said to be equivariant if $R^{-1}SR = S$ for every rotation $R \in SO(2)$. For any subset of entropies $S \subset ENT$, we will denote by*

$$\langle S \rangle := \{ \pm R^{-1}\Phi R : \Phi \in S, R \in SO(2) \},$$

the smallest symmetric and equivariant subset of entropies which contains S .

In terms of the bijective correspondence $\varphi \mapsto \Phi$ given by (1.6), the notion of equivariance of S is equivalent to having the set $\{ \varphi \in C_{per}^\infty(\mathbf{R}) : \Phi \in S \}$ invariant by translations. For proving that \mathcal{I}_{c_S} is lower semicontinuous for nonempty symmetric equivariant subsets $S \subset ENT$, we introduce the following functionals (inspired by (1.9)) which generalize Theorem 2.1 in [6].

Definition 5 *Let $S \subset ENT$. We define $\mathcal{E}_S : L^1(\Omega, \mathbf{R}^2) \rightarrow \bar{\mathbf{R}}$ by*

$$\mathcal{E}_S(m) := \sup \left\{ \sum_{i=1}^n \langle \mu_{\Phi_i}(m), \alpha_i \rangle : n \geq 0, (\Phi_i, \alpha_i) \in S \times C_c^\infty(\Omega, \mathbf{R}_+), \sum_{i=1}^n \alpha_i \leq 1 \right\} \text{ if } m \in \mathcal{L}(\Omega);$$

otherwise, we set $\mathcal{E}_S(m) = +\infty$ for $m \in L^1(\Omega, \mathbf{R}^2) \setminus \mathcal{L}(\Omega)$.

As a supremum of continuous functionals over L^1 , this new energy \mathcal{E}_S is lower semicontinuous with respect to the strong L^1 topology. In the above definition we use a partition of unity to localize the entropy production. In particular, in the neighborhood of a jump discontinuity $x \in J(m)$ of $m \in BV_{div}(\Omega, S^1)$, we can choose a sequence of entropies maximizing the local entropy production as in the definition of $c_S(|m^+(x) - m^-(x)|)$. Using this property, we prove that \mathcal{E}_S coincides with \mathcal{I}_{c_S} on $BV_{div}(\Omega, S^1)$:

Theorem 6 *Let $S \subset ENT$ be nonempty, symmetric and equivariant. For every $m \in BV_{div}(\Omega, S^1)$, we have*

$$\mathcal{E}_S(m) = \mathcal{I}_{c_S}(m) = \overline{\mathcal{I}_{c_S}}(m).$$

In particular, \mathcal{I}_{c_S} is lower semicontinuous and $\mathcal{E}_S \leq \overline{\mathcal{I}_{c_S}}$ in $L^1(\Omega, \mathbf{R}^2)$.

We deduce that the class of cost functions in Definition 3 leads to lower semicontinuous line-energy functionals. Finally, for proving Theorems 4 and 5 we will construct a subset $S \subset ENT$ so that $f = c_S$. Let us give some examples. The simplest case is given by sets $S = \langle \Phi \rangle$ generated by a single entropy $\Phi \in ENT$. If $\lambda(\theta) = \frac{d}{d\theta} \Phi(z) \cdot z^\perp$ (as in (1.7)), then the combination of (1.10) and Definition 3 leads to

$$c_{\langle \Phi \rangle}(2 \sin \beta) = \sup_{x \in [0, 2\pi]} |\lambda \star \sin_\beta|(x), \quad \beta \in [0, \pi/2]. \quad (1.18)$$

We obtained a criteria depending on λ that computes the supremum in (1.18): if λ is an odd π -periodic function and its restriction to $(0, \pi/2)$ is convex and even with respect to $\frac{\pi}{4}$, then the supremum in (1.18) is achieved at $x = 0$ so that

$$c_{\langle \Phi \rangle}(2 \sin \beta) = -2 \int_0^\beta \lambda(\theta) \sin(\theta) d\theta.$$

In particular, this criteria leads to the cost functions mentioned in Examples 1 and 2 below, corresponding to the Aviles-Giga and "cross-tie wall" models.

Example 1 (Aviles-Giga cost function) There exists a subset $S_1 = \langle \{\Phi_1\} \rangle \subset ENT$ generated by one entropy $\Phi_1(z) = \frac{4}{3}(z_2^3, z_1^3)$ for $z \in S^1$ (i.e., $\lambda_1(\theta) = -6 \sin(2\theta)$ in (1.7)) such that $c_{S_1}(t) = t^3/3$ for $t \in [0, 2]$.

Example 2 ("Cross-tie wall" cost function) There exists a subset $S_2 = \langle \{\Phi_2\} \rangle \subset ENT$ generated by one entropy $\Phi_2 \in C^{1,1}(S^1, \mathbf{R}^2)$ (i.e., λ_2 in (1.7) is a π -periodic odd function given by $\lambda_2(\theta) = |\theta - \frac{\pi}{4}| - \frac{\pi}{4}$ on $(0, \pi/2)$) such that

$$c_{S_2}(2 \sin \theta) = \begin{cases} \sin \theta - \theta \cos \theta & \text{if } 0 \leq \theta \leq \pi/4, \\ \sqrt{2} - \left(\frac{\pi}{2} - \theta\right) \cos \theta - \sin \theta & \text{if } \pi/4 < \theta \leq \pi/2. \end{cases}$$

For these examples, the corresponding entropies have been introduced in [48] and [1] respectively. Obviously, not all appropriate cost functions can be associated to subsets of entropies generated by only one entropy. For example, if $c_S(t) = t^2$ for every $t \in [0, 2]$, we are compelled to construct a subset S generated by an infinite family of entropies.

Conjecture 2 Is it true that every lower semicontinuous line-energy \mathcal{I}_f has the form \mathcal{I}_{c_S} for some subset of entropies $S \subset ENT$?

Remark 8 One can address problem (1.14) for higher dimensions $N \geq 3$. In this case, DeLellis proved in [18] that the power function $f(t) = t^3$ (in the Aviles-Giga model) does not lead anymore to a lower semicontinuous hypersurface-energy as in the two-dimensional case. The microscopic structure breaking the one-dimensional ansatz considered in [18] can be adapted to other power functions $f(t) = t^p$. Also we highlight the fact that our approach for treating lower semicontinuous line-energies via entropy method cannot be extended to hypersurface-energy functionals if $N \geq 3$. Indeed, for $N = 3$, standard computations show that the only entropies associated to the system of conservation laws generated by

$$v : \Omega \subset \mathbf{R}^3 \rightarrow \mathbf{R}^3, \quad |v| = 1 \quad \text{and} \quad \nabla \times v = 0 \quad \text{in } \Omega$$

are the trivial entropies.

1.3.4 Existence of minimizers for relaxed line-energies

Now we deal with a second issue: the existence of minimizers of the relaxed energy functional $\overline{\mathcal{I}}_f$ under certain boundary conditions. (Without imposed boundary conditions, the problem is trivial, $\overline{\mathcal{I}}_f$ has vanishing minimal value and every constant unit vector field is a minimizer.) We impose the following boundary condition $m \cdot n = 0$ on $\partial\Omega$ to our configurations m , so we are looking for minimizers in $\mathcal{L}_0(\Omega)$ (see (1.17)). Suppose that the cost function f is equal to c_S for some subset $S \subset ENT$. Then the relative compactness in L^1 of the sublevel sets of $\overline{\mathcal{I}}_f$ would imply the existence of minimizers of the relaxed functional $\overline{\mathcal{I}}_f$ in $\mathcal{L}_0(\Omega)$. For that, one should be able to rule out oscillations for configurations of uniformly bounded energy. It turns out that this statement holds true if the symmetric and equivariant set,

$$S_f := \{ \Phi \in ENT : [\Phi(z^+) - \Phi(z^-)] \cdot \nu \leq f(|z^+ - z^-|), \forall (z^-, z^+, \nu) \in \mathcal{T} \},$$

composed of the admissible entropies associated with f , is large enough. More precisely, we will obtain compactness if

$$t^3 \lesssim f(t) \quad \text{in} \quad [0, 2] \tag{1.19}$$

(see Theorem 7 below) which means in fact that up to multiplicative constants, S_f coincides with ENT , i.e., $\mathbf{R}S_f = ENT$.

Remark 9 Note that $c_{S_f} \leq f$ in $[0, 2]$ and S_f is the maximal subset of ENT such that this inequality holds.

Theorem 7 *Let f be a cost function such that $\inf_{t \in (0, 2]} \frac{f(t)}{t^3} > 0$ and $c_{S_f} = f$. Then $\overline{\mathcal{I}}_f$ (respectively, \mathcal{E}_{S_f}) admits at least one minimizer over $\mathcal{L}_0(\Omega)$.*

It means that a minimizer $m \in \mathcal{L}_0(\Omega)$ of $\overline{\mathcal{I}}_f$ can be written as a limit of a sequence $\{m_k\}$ in $\mathcal{S}_0(\Omega)$ such that $\overline{\mathcal{I}}_f(m) = \lim_k \mathcal{I}_f(m_k)$. However, we do not know whether these minimizers m belong to $\mathcal{S}_0(\Omega)$, in other words, we do not know if \mathcal{I}_f admits a minimizer over $\mathcal{S}_0(\Omega)$.

Remark 10 The existence result in Theorem 7 is still valid if we replace $\mathcal{L}_0(\Omega)$ by any closed subset of $\mathcal{L}(\Omega)$. But this does not cover the case of general Dirichlet boundary conditions. However, the following strategy can be adopted for Dirichlet boundary condition $m = u_{bd}$ on $\partial\Omega$. If we can extend $u_{bd} : \partial\Omega \rightarrow S^1$ as a divergence-free vector field $u \in BV(O, S^1)$ for some smooth open set $O \supset \bar{\Omega}$, then the argument in Theorem 7 shows the existence of minimizers of the functional $F(m) := \mathcal{I}_f(m; O) - \mathcal{I}_f(u; O \setminus \bar{\Omega})$ in the closed set

$$\{m \in \mathcal{L}(O) : m \equiv u \text{ a.e. in } O \setminus \bar{\Omega}\}.$$

Observe that finite energy configurations $F(m) < \infty$ satisfy $m \in BV(O, S^1)$, $m \cdot n = u_{bd} \cdot n$ \mathcal{H}^1 -a.e. on $\partial\Omega$ (since m is of vanishing divergence) and the jump of the tangential component $[m \cdot n^\perp]$ on $\partial\Omega$ is penalized through $F(m)$ by the boundary term:

$$\int_{\partial\Omega} f(|m^+ - m^-|) d\mathcal{H}^1,$$

where m^\pm denote the inner and outer traces of m on $\partial\Omega$ with respect to n (here, $m^+ = u_{bd}$ on $\partial\Omega$). The minimizing problem does not depend on the extended domain O or on the extension vector field u .

1.3.5 Viscosity solution

We are also interested in the minimization problem under the more restrictive boundary condition $m = n^\perp$ on $\partial\Omega$. This condition makes sense for $m \in BV$ and defines a new subset of $\mathcal{S}_0(\Omega)$:

$$\mathcal{S}_\perp(\Omega) := \{m \in \mathcal{S}_0(\Omega) : m = n^\perp \text{ on } \partial\Omega\}.$$

For configurations in this set, no change of orientation is allowed along the boundary. The motivation comes from micromagnetics where the boundary vortices are strongly penalized in certain asymptotic regimes (see Section 2.1.2).

The natural question in this context is whether the minimizer of \mathcal{I}_f over $\mathcal{S}_\perp(\Omega)$ exists and is associated to the viscosity solution of the Dirichlet problem for the eikonal equation, i.e., letting ψ_* be the distance function to the boundary

$$\psi_* = \text{dist}(x, \partial\Omega),$$

we will always denote the corresponding map in $\mathcal{S}_\perp(\Omega)$ by

$$m_* = \nabla^\perp \psi_*.$$

We will still call m_* the *viscosity solution* on Ω (or Landau state in micromagnetic jargon). In relation with (1.14), this amounts to considering stream functions ψ satisfying $m = \nabla^\perp \psi \in BV(\Omega, S^1)$ and the boundary conditions $\psi = 0$ and $\frac{\partial \psi}{\partial n} = -1$ \mathcal{H}^1 -a.e on $\partial\Omega$.

In [48], Jin and Kohn suggested that when the domain Ω is convex, the viscosity solution minimizes \mathcal{I}_f in $\mathcal{S}_\perp(\Omega)$ for $f(t) = t^p$, $1 \leq p \leq 3$. The result is proved for $p = 3$ when Ω is an ellipse in [48]. For $p = 1$ and if Ω a convex polygon, it is proved in [5] that m_* minimizes \mathcal{I}_f over the set $\{m \in \mathcal{S}_\perp(\Omega) : \nabla m \text{ is piecewise constant}\}$. We first give a positive answer in the case of a stadium domain Ω and general appropriate cost functions:

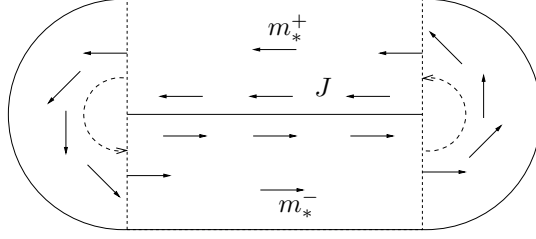


Figure 1.6: Stadium shaped domain and the corresponding viscosity solution.

Theorem 8 *Let $S \subset ENT$ be nonempty, symmetric and equivariant. We consider the stadium-shaped domain Ω (see Figure 1.6)*

$$\Omega = (-L, L) \times (-1, 1) \cup B((-L, 0), 1) \cup B((L, 0), 1),$$

for some $L \geq 0$. Then the viscosity solution m_* minimizes \mathcal{I}_{c_S} over $\mathcal{S}_\perp(\Omega)$.

We also prove positive results for some other special domains non necessarily convex (in particular, ellipse and union of two discs) and some special appropriate cost functions.

For nonconvex domains, it is proved in [5] that for power cost functions $f(t) = t^p$ with $p \leq 4/3$, there exists a nonconvex polygonal domain Ω such that m_* does not minimize \mathcal{I}_f over $\mathcal{S}_\perp(\Omega)$. Moreover, the same counterexamples indicate that for every power cost function with $p > 0$, m_* does not minimize \mathcal{I}_f in $\mathcal{S}_0(\Omega)$. In [48], the authors exhibit a nonconvex Lipschitz domain (a union of two intersecting discs) such that m_* is not a minimizer of \mathcal{I}_f in $\mathcal{S}_\perp(\Omega)$ for every $f(t) = t^p$ with $p \neq 3$; in the case $f(t) = t^3$, m_* is a minimizer of \mathcal{I}_f , but it is not unique. It was conjectured in [48] that for some other nonconvex domains, m_* is not a minimizer of $\mathcal{I}_{t \rightarrow t^3}$. In the following, we prove this conjecture. In fact, we show a more general fact: there exists a nonconvex domain such that for any fixed positive cost function f , the viscosity solution is not optimal in $\mathcal{S}_\perp(\Omega)$.

Theorem 9 *There exists a nonconvex piecewise Lipschitz domain Ω such that the viscosity solution is not a minimizer of \mathcal{I}_f over $\mathcal{S}_\perp(\Omega)$ for every lower semicontinuous function $f : [0, 2] \rightarrow \mathbf{R}_+$ such that $\int_{\sqrt{2}}^2 f(t) dt > 0$.*

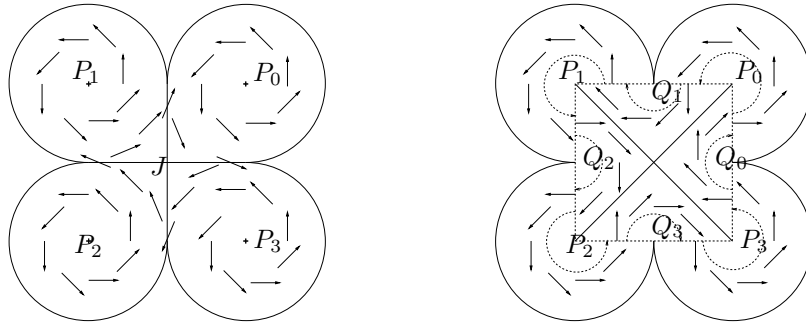


Figure 1.7: The configuration \tilde{m} (left) is given by "vortex" vector fields centered at P_k , $k = 1 \dots 4$. It has less energy \mathcal{I}_f than the viscosity solution m_* (right).

The above domain Ω (a union of four discs and a square) is non smooth, but universal for every positive cost function f . Moreover, by slightly modifying the boundary of Ω , we can show that the result is not restricted to nonsmooth domains. However, the modified smooth domain is no longer universal with respect to the cost function.

Theorem 10 *For every bounded lower semicontinuous function $f : [0, 2] \rightarrow \mathbf{R}_+$ such that $\int_{\sqrt{2}}^2 f(t) dt > 0$, there exists a nonconvex $C^{1,1}$ domain Ω such that the viscosity solution is not a minimizer of \mathcal{I}_f over $\mathcal{S}_\perp(\Omega)$.*

1.4 Generalized entropies

In the previous section we characterized lower-semicontinuous line-energies \mathcal{I}_f . For such a line-energy, one may wonder whether \mathcal{I}_f is indeed the Γ -limit of functionals (1.15) (or of some perturbation functional of (1.15)). If this is the case, how entropies can be used in proving the Γ -convergence program (in order to have compactness and lower bounds)?

1.4.1 Compactness

We focus here on the first step in the method of Γ -convergence, i.e. the compactness issue for functionals G_ε in (1.15):

Claim 1 Any family $\{m_\varepsilon\}_{\varepsilon \downarrow 0} \subset H_{div}^1(\Omega, \mathbf{R}^2)$ of uniformly bounded energy $G_\varepsilon(m_\varepsilon) \leq C$ is relatively compact in $L^1(\Omega)$ and any limit configuration m_0 satisfies (1.1).

We will assume here the following hypothesis:

$$g(t) \geq Ct^2, \quad \text{for every } t \geq 0, \quad (1.20)$$

where $C > 0$ denotes a generic constant. This assumption is motivated by the following. We want that the energy G_ε asymptotically concentrates on line-energies \mathcal{I}_f as $\varepsilon \rightarrow 0$; as discussed in the previous section (see (1.19)), the lower semicontinuity of \mathcal{I}_f is related to the condition $f(t) \geq Ct^3$ (so that $\mathbf{R}S_f = ENT$) and in this case, the 1D ansatz (1.16) suggests (1.20).

Under the assumption (1.20), the compactness issue reduces to the case $g(t) = t^2$ in (1.15), known as the Aviles-Giga model. It is in fact a Ginzburg-Landau model for gradient fields and appears either in solid mechanics, liquid crystals or in micromagnetics (see [13, 32]). It gave rise to a series of articles [48, 6, 2, 25, 16, 64] that justify that \mathcal{I}_f with $f(t) = t^3/3$ (given by (1.16)) is indeed the asymptotic energy of $\{G_\varepsilon\}$ in the sense of Γ -convergence under the strong L^1 -topology.

In particular, Claim 1 was proved by Ambrosio, De Lellis and Mantegazza [2] and DeSimone, Kohn, Müller and Otto [25]. The entropy method comes out to be fruitful in this matter, too. We explain here the ideas in [25]. Since the vector fields m_ε are no longer of values in S^1 , the strategy used in [25] consists in firstly extending the notion of entropies to maps defined in the whole space \mathbf{R}^2 :

Definition 6 (DKMO [25]) *We will say that $\Phi \in C^\infty(\mathbf{R}^2, \mathbf{R}^2)$ is a DKMO-entropy if*

$$\Phi(0) = 0, \quad D\Phi(0) = 0 \quad \text{and} \quad (1.5) \quad \text{holds for all } z \in \mathbf{R}^2.$$

Let us discuss some properties of this extension: First of all, any entropy $\Phi \in ENT$ can be extended at a *DKMO*-entropy by considering

$$\tilde{\Phi}(z) := \rho(|z|)\Phi\left(\frac{z}{|z|}\right) \quad \text{for every } z \in \mathbf{R}^2 \setminus \{0\} \quad (1.21)$$

where $\rho \in C_c^\infty(\mathbf{R}_+)$. A second property concerns the entropy production: For every *DKMO*-entropy Φ , there exist $\Psi \in C_0^\infty(\mathbf{R}^2, \mathbf{R}^2)$ and $\alpha \in C_0^\infty(\mathbf{R}^2, \mathbf{R})$ such that

$$D\Phi(z) = -2\Psi(z) \otimes z + \alpha(z)Id \quad \text{for every } z \in \mathbf{R}^2;$$

consequently, for every $m \in H^1(\Omega, \mathbf{R}^2)$, the entropy production is given by:

$$\nabla \cdot \{\Phi(m)\} - \alpha(m)\nabla \cdot m = \Psi(m) \cdot \nabla(1 - |m|^2) \quad \text{a.e. in } \Omega \quad (1.22)$$

(see [25]).

The main feature of *DKMO*-entropies with respect to Claim 1 is the following: For every *DKMO*-entropies Φ , the family of entropy productions $\{\nabla \cdot \Phi(m_\varepsilon)\}_{\varepsilon \downarrow 0}$ is asymptotically bounded as measure for every family $\{m_\varepsilon\}_{\varepsilon \downarrow 0} \subset H_{div}^1(\Omega, \mathbf{R}^2)$ of uniformly bounded energy. In fact, integration of (1.22) yields (due to (1.20)):

$$\limsup_{\varepsilon \rightarrow 0} \left| \int_{\Omega} \nabla \cdot \{\Phi(m_\varepsilon)\} \zeta \right| \leq C_\Phi \|\zeta\|_\infty \limsup_{\varepsilon \rightarrow 0} G_\varepsilon(m_\varepsilon), \quad \text{for every } \zeta \in C_c^\infty(\Omega), \quad (1.23)$$

where $C_\Phi = 2\|\nabla\Psi\|_\infty$.

On the one hand, this property yields Claim 1 by a nice combination of the theory of Young measures and the div-curl lemma of Murat and Tartar (see e.g. [71, 60]) applied to families $\{\Phi(m_\varepsilon) \wedge \tilde{\Phi}(m_\varepsilon)\}_{\varepsilon \downarrow 0}$ where $\Phi, \tilde{\Phi} \in C^\infty(\mathbf{R}^2, \mathbf{R}^2)$ are two arbitrary *DKMO*-entropies (see in [25]).

On the other hand, the entropy method also yields the structure of the limiting configurations m_0 (that obviously satisfy (1.1)). First, observe that (1.23) implies that the entropy production $\nabla \cdot \Phi(m_0)$ is a measure for every *DKMO*-entropy Φ . Moreover, this property holds true for every entropy $\Phi \in ENT$ (by (1.21)). De Lellis and Otto [19] characterized this class of vector fields m_0 where the entropy production is a measure for every entropy. Essentially, every limiting configuration m_0 shares some structure properties of maps of bounded variation $BV(\Omega)$; in particular it is possible to give a rigorous definition of the jump set $J(m_0)$ as a \mathcal{H}^1 -rectifiable set so that \mathcal{I}_f makes sense. (A similar result was independently obtained by Ambrosio, Kirchheim, Lecumberry and Rivière [3] using the characterization of m_0 in terms of its phase θ_0 .) The main obstacle is that limiting finite-energy configurations m_0 are not in BV as we already mentioned in Remark 6. However, the situation is better if we focus on either zero-energy configurations (see Remark 4) or dilation invariant configurations (see [30]).

1.4.2 Entropies for S^2 -valued vector fields ⁴

In this section we will introduce a different extension of entropies *ENT* (than the *DKMO*-entropy) that is adapted for solving the second issue in the Γ -convergence program, i.e., to show that \mathcal{I}_f is a lower bound of (1.15). We treat this issue for slightly more general functionals $E_{\varepsilon, \beta}$ defined

⁴All the results appearing in this subsection are part of the article Ignat-Merlet [41]. Therefore, we don't specify in the following this reference for each result.

for S^2 -vector fields $m = (m', m_3) \in H^1(\Omega, S^2)$ (with $m' = (m_1, m_2)$) that are not necessarily divergence-free, but the divergence $\nabla \cdot m = \nabla \cdot m'$ is penalized by the energy $E_{\varepsilon, \beta}$:

$$E_{\varepsilon, \beta}(m) = \int_{\Omega} \left(\varepsilon |\nabla m|^2 + \frac{1}{\varepsilon} g(m_3^2) + \frac{1}{\beta} \left| |\nabla|^{-1} \nabla \cdot m \right|^2 \right) dx,$$

where $\varepsilon > 0$ and $\beta > 0$ are small parameters. We will always assume the following regime

$$\beta = \beta(\varepsilon) \ll \varepsilon \ll 1$$

and that (1.20) holds. (The opposite regime, i.e., $\varepsilon \ll \beta \ll 1$, entails different asymptotic behavior: the energy $E_{\varepsilon, \beta}$ enforces m to take values into S^1 much stronger than satisfying the flux closure condition. This situation is adapted for "cross-tie" walls, see [1, 66, 67].) Notice that $E_{\varepsilon, \beta}$ controls the functional G_ε in (1.15) (for divergence-free configurations): indeed, the second term coincides for both functionals (since $m_{3, \varepsilon}^2 = 1 - |m'_\varepsilon|^2$), while the first term in $E_{\varepsilon, \beta}$ controls the one in G_ε since $|\nabla m_\varepsilon| \geq |\nabla m'_\varepsilon|$. Moreover, the compactness issue discussed in the previous section is still valid for uniformly bounded energy configurations $E_{\varepsilon, \beta}(m_\varepsilon) \leq C$.

In order to obtain sharp lower bounds for $E_{\varepsilon, \beta}$ we introduce a class of *generalized entropies* Φ for which the entropy production is controlled by the energy (with constant 1 comparing to (1.23)) up to a perturbation taking the form of a boundary term. More precisely, we systematically study the particular class of Lipschitz continuous maps $\Phi = (\Phi_1, \Phi_2) \in Lip(S^2, \mathbf{R}^2)$ and $\alpha \in Lip(S^2)$ such that for every smooth $m \in C^\infty(\Omega, S^2)$, the following holds:

$$\nabla \cdot \{\Phi(m)\} + \alpha(m) \nabla \cdot m' \leq \varepsilon |\nabla m|^2 + \frac{1}{\varepsilon} g(m_3^2) + \nabla \cdot \{a_\varepsilon(m) \nabla m\} \quad \text{a.e. in } \Omega, \quad (1.24)$$

where $\varepsilon > 0$ is a small parameter and $a_\varepsilon(x)$ is a linear operator mapping the tangent plane $(T_x S^2)^2$ into \mathbf{R}^2 , for every $x \in S^2$. In the language of differential geometry, $x \mapsto a_\varepsilon(x)$ is a section of the vector bundle

$$\mathcal{B} := \{(x, a) : x \in S^2, a \in \mathcal{L}((T_x S^2)^2, \mathbf{R}^2)\}$$

based on S^2 with fiber $\mathcal{L}(\mathbf{R}^4, \mathbf{R}^2)$. Using the natural differential structure, \mathcal{B} is locally diffeomorphic to $\mathbf{R}^2 \times \mathcal{L}(\mathbf{R}^4, \mathbf{R}^2)$. With the induced topology, we will always assume that the section $x \mapsto a_\varepsilon(x)$ is Lipschitz (in order that (1.24) makes sense). This notion of generalized entropy is inspired by the work of Jin and Kohn [48] on the Aviles-Giga model. The choice of Lipschitz maps is justified below by the study of Bloch walls where the limit line-energies have a quadratic cost in the angle.

Let us first give the connection between generalized entropies for S^2 -valued vector fields and the set of entropies *ENT*. (The assumption (1.20) on g is essential here.)

Proposition 10 *Let $\Phi \in Lip(S^2, \mathbf{R}^2)$, $\alpha \in Lip(S^2)$ and a_ε be a Lipschitz section of \mathcal{B} such that (1.24) holds for every $m \in C^\infty(\Omega, S^2)$. Then (1.5) holds in the sense that*

$$\frac{d}{d\theta} \Phi(z) \cdot z = 0, \quad \text{for almost every } z \in S^1, \quad (1.25)$$

where $\frac{d}{d\theta} \Phi(z)$ denotes the tangential derivative of the restriction $\Phi|_{S^1}$ on the horizontal circle $S^1 := S^1 \times \{0\} \subset S^2$. Conversely, let $\Phi \in C^\infty(S^2, \mathbf{R}^2)$ satisfying (1.5) and $\partial_{m_3} \Phi \equiv 0$ on S^1

(m_3 -symmetric entropies $\Phi(m', m_3) = \Phi(m', -m_3)$ do satisfy this condition). Then there exist a constant $C > 0$ and $\alpha \in C^\infty(S^2)$ such that $C\Phi$ satisfies (1.24) with $a_\varepsilon \equiv 0$ for every $m \in C^\infty(\Omega, S^2)$ and every $\varepsilon > 0$.

The above proposition justifies the name of generalized entropies. The differences with respect to Definition 1 consist in defining our entropies on S^2 (which is the target manifold of our vector fields m in this subsection) and in asking for Φ to be *only* Lipschitz continuous. Observe that the inequality (1.24) implies the following necessary pointwise bounds on generalized entropies (that hold for every potential $g \geq 0$ on \mathbf{R}_+ , so that (1.20) is not necessary here).

Lemma 1 *Let $\varepsilon > 0$, $(\Phi = (\Phi_1, \Phi_2), \alpha) \in Lip(S^2, \mathbf{R}^2) \times Lip(S^2)$ and a_ε be a Lipschitz section of \mathcal{B} such that (1.24) holds for every $m \in C^\infty(\Omega, S^2)$. For every $\tau \in [-\pi, \pi)$, we set*

$$\nu_\tau = (-\sin \tau, \cos \tau, 0) \in S^2 \quad \text{and} \quad \Psi_\tau := \nu_\tau \cdot \Phi = -\sin \tau \Phi_1 + \cos \tau \Phi_2 \in Lip(S^2).$$

Then for almost every point $m \in S^2$, we have

$$|D\Psi_\tau(m) + \alpha(m)\Pi_m\nu_\tau| \leq 2\sqrt{g(m_3^2)}, \quad (1.26)$$

where $D\Psi_\tau(m) \in T_m S^2$ is the gradient of Ψ_τ at m and Π_m denotes the orthogonal projection onto $T_m S^2$.

Let us now explain how the generalized entropies are used for proving lower bound for $E_{\varepsilon, \beta}$ (under the condition (1.20)). Assume that $E_{\varepsilon, \beta}(m_\varepsilon) \leq C$. As explained before, Claim 1 holds, so we may assume that $m_\varepsilon \rightarrow m_0$ in $L^1(\Omega)$ and m_0 satisfies (1.1). Moreover, using the *DKMO*-entropies, we know that all entropy productions of m_0 are measures so that by [19] we can speak about the jump set $J(m_0)$ of m_0 . The question is whether \mathcal{I}_f is a lower bound (in the sense of Γ -convergence) of $E_{\varepsilon, \beta}$ where f and g are related by (1.16). To simplify the presentation, we focus on the following periodic setting corresponding to a zoom around a jump point $x \in J(m_0)$ of wall angle θ . More precisely, we consider the periodic strip

$$\Omega = \mathbf{R} \times \mathbf{R}/\mathbb{Z}$$

and we consider $m \in H_{loc}^1(\Omega, S^2)$ with transitions imposed by the limit condition at infinity

$$\lim_{x_1 \rightarrow \pm\infty} m(x_1, \cdot) = m^\pm = (\cos \theta, \pm \sin \theta, 0) \quad \text{in} \quad L^2(\mathbf{R}/\mathbb{Z}). \quad (1.27)$$

The aim is to obtain the following lower bound: If $\beta = \beta(\varepsilon) \ll \varepsilon \ll 1$, then

$$f(|m^+ - m^-|) \leq \liminf_{\varepsilon \downarrow 0} E_{\varepsilon, \beta}(m_\varepsilon). \quad (1.28)$$

For that, we introduce the following notion of adapted triplet:

Definition 7 *For $\theta \in (0, \pi)$, we will say that a triplet $(\Phi = (\Phi_1, \Phi_2), \alpha) \in Lip(S^2, \mathbf{R}^2) \times Lip(S^2)$ is adapted to the jump (m^-, m^+) if*

$$\Phi_1(m^+) - \Phi_1(m^-) = [\Phi(m^+) - \Phi(m^-)] \cdot \mathbf{e}_1 = f(|m^+ - m^-|) \quad (1.29)$$

and there exists $\varepsilon_0 > 0$ such that for every $0 < \varepsilon \leq \varepsilon_0$ one can construct a Lipschitz section a_ε of \mathcal{B} for which (1.24) holds for every map $m \in C^\infty(\Omega, S^2)$.

The existence of a triplet $(\Phi = (\Phi_1, \Phi_2), \alpha)$ satisfying (1.24) and (1.29) would solve (1.28). Indeed, notice first that

$$\left| \int_{\Omega} \alpha(m) \nabla \cdot m' \right| \leq \|\nabla \cdot m'\|_{\dot{H}^{-1}(\Omega)} \|\nabla[\alpha(m)]\|_{L^2(\Omega)} \leq \|\nabla \alpha\|_{L^\infty} \sqrt{\frac{\beta}{\varepsilon}} E_{\varepsilon, \beta}(m). \quad (1.30)$$

Then integrating (1.24) on Ω and taking into account the boundary conditions (1.29), we would deduce (1.28).

Aviles-Giga model. Let us apply this theory to the case of the quadratic potential $g(t) = t^2$ in the Aviles-Giga model. The following generalized entropy was used by Jin and Kohn [48]. The idea comes from the scalar conservation laws where the entropy production through shocks is asymptotically cubic in the limit of small jumps. Therefore, smooth entropies seem to be adapted for the energy G_ε . For that, let $\Phi : \mathbf{R}^2 \rightarrow \mathbf{R}^2$ be the following smooth extension of the entropy given in Example 1:

$$\Phi(z) = (2z_2(1 - z_1^2) - \frac{2}{3}z_2^3, 2z_1(1 - z_2^2) - \frac{2}{3}z_1^3), \forall z \in \mathbf{R}^2. \quad (1.31)$$

(Notice that Φ is not a *DKMO*-entropy.) Then setting $\alpha(z) = 4z_1z_2$ for $z = (z_1, z_2) \in \mathbf{R}^2$, one checks that (1.24) holds for the triplet (Φ, α) (as maps defined on \mathbf{R}^2) and the section $a_\varepsilon(z)(U, V) = 2\varepsilon z_2(V_1, -U_1)$ with $U = (U_1, U_2) \in \mathbf{R}^2$, $V = (V_1, V_2) \in \mathbf{R}^2$. Moreover, (1.29) is satisfied for $f(t) = t^3/3$. Therefore, one obtains (1.28) for G_ε and also, for $E_{\varepsilon, \beta}$; one can extend it to a general domain Ω so that \mathcal{I}_f is a lower bound of G_ε and $E_{\varepsilon, \beta}$. We recall that the Γ -convergence program is not completely solved for the Aviles-Giga model: The difficulty consists in the upper bound construction for admissible configurations m_0 since the recovery sequences have been constructed *only* for *BV* configurations m_0 (see Conti and De Lellis [16] and Poliakovsky [64]). For general (non *BV*) limiting finite-energy configurations m_0 , the problem is still open.

The model for the Bloch wall. A second application is given by the linear potential $g(t) = t$ and is coming from micromagnetics in the study of Bloch walls. The expected line-energy corresponds to a quadratic cost $f(t) = t^2$. This case is more delicate than the Aviles-Giga model, since smooth entropies are no longer suited to quadratic jumps. This motivates our choice of considering generalized entropies with discontinuous gradients.

First, let us explain why Lipschitz *DKMO*-entropies can detect the quadratic costs over the singular set of limiting configurations. It is due to controlling the entropy production by the energy through an improvement of inequality (1.23) via the control of $|\nabla m_3|^2$ by the energy density of $E_{\varepsilon, \beta}$. If $\beta \ll \varepsilon \ll 1$, Φ is a *DKMO*-entropy and $m_\varepsilon \in H^1(\Omega, S^2)$, by (1.22) and (1.30) one gets

$$\limsup_{\varepsilon \rightarrow 0} \left| \int_{\Omega} \nabla \cdot \{\Phi(m_\varepsilon)\} \zeta \right| \leq \tilde{C}_\Phi \|\zeta\|_\infty \limsup_{\varepsilon \rightarrow 0} E_{\varepsilon, \beta}(m_\varepsilon) \quad \text{for every } \zeta \in C_c^\infty(\Omega),$$

where $\tilde{C}_\Phi = \|\Psi\|_\infty$. The advantage of the above inequality consists in having the RHS only dependent on the L^∞ -norm of Ψ (controlled by the Lipschitz norm of the *DKMO*-entropy Φ) whereas in (1.23) the constant C_Φ depends on the $C^{1,1}$ -norm of Φ . For this reason, if Φ is a Lipschitz continuous map satisfying (1.5) and m_0 is a strong limit of $\{m_\varepsilon\}$ satisfying $\limsup_{\varepsilon \downarrow 0} E_{\varepsilon, \beta}(m_\varepsilon) < \infty$, then $\nabla \cdot \{\Phi(m_0)\}$ is a measure of finite total mass. In [41], we construct a Lipschitz entropy $\Phi = (\Phi_1, \Phi_2)$ that satisfies (1.29) and leads to (1.28) up to a constant. Moreover, we proved that \mathcal{I}_f is a lower bound of $E_{\varepsilon, \beta}$ (up to a constant):

Theorem 11 *Let $\Omega \subset \mathbf{R}^2$ be a bounded domain. Assume that the family $\{m_\varepsilon\}_{\varepsilon \downarrow 0} \subset H^1(\Omega, S^2)$ converges to m_0 in $L^1(\Omega)$ and $\beta = \beta(\varepsilon) \ll \varepsilon \ll 1$. Then*

$$\mathcal{I}_f(m_0) \leq C \liminf_{\varepsilon \downarrow 0} E_{\varepsilon, \beta}(m_\varepsilon),$$

with some $C > 1$ (in fact, one can choose $C = \sqrt{4 + \pi^2}$).

In order to get the desired inequality (1.28) (with $C = 1$), we analyze the existence of adapted triplets. For the 180° Bloch wall (i.e., the biggest possible jump $\theta = \frac{\pi}{2}$), we have a positive answer.

Proposition 11 *There exists a smooth triplet $(\Phi = (\Phi_1, \Phi_2), \alpha)$ adapted to the jump $(-\mathbf{e}_2, \mathbf{e}_2)$. Consequently, (1.28) holds for $\theta = \frac{\pi}{2}$.*

For smaller jumps, we only have a partial result. If m^\pm is the jump of angle $\theta \in (0, \pi/2)$ in (1.27), we define the spherical cap

$$S_\theta := \{m \in S^2 : m_1 \geq \cos \theta\}$$

and the set of vector fields taking values into the cap S_θ and adapted to the jump (m^-, m^+) :

$$\mathcal{C}_\theta := \{m \in H_{loc}^1(\Omega, S^2) : (1.27) \text{ holds and } m(x) \in S_\theta \text{ for a.e. } x \in \Omega\}.$$

Then one can find a triplet $(\Phi = (\Phi_1, \Phi_2), \alpha)$ that is adapted to a jump (m^-, m^+) if we restrict our study to configurations of \mathcal{C}_θ .

Proposition 12 *For every $\theta \in (0, \pi/2)$ and every $\varepsilon > 0$, there exists a smooth triplet $(\Phi_\theta, \alpha_\theta) \in C^\infty(S_\theta, \mathbf{R}^3)$ and a smooth section a_ε of \mathcal{B} such that (1.29) and (1.24) hold for every $m \in C^\infty(\Omega, S_\theta)$. Consequently, if $\{m_\varepsilon\} \subset \mathcal{C}_\theta$, then (1.28) stands true.*

We remark that there is no general recipe for constructing adapted triplets. However, Lemma 1 gives a very useful tool in this context.

Despite Propositions 11 and 12, we prove in [41] that for small jumps, the necessary conditions in Lemma 1 are not compatible with condition (1.29). Consequently, there is no triplet $(\Phi = (\Phi_1, \Phi_2), \alpha)$ adapted to a fixed small jump for general configurations (when the vector fields cover the entire sphere S^2):

Theorem 12 *There exists $\eta > 0$ such that for $0 < \theta < \eta$, there is no triplet $(\Phi = (\Phi_1, \Phi_2), \alpha)$ adapted to the jump (m^-, m^+) .*

However, we strongly believe that (1.28) holds for every angle θ . The conjecture that \mathcal{I}_f is indeed the Γ -limit energy of our 2D model is supported by Theorem 5. It means that there it is not possible to asymptotically decrease the energy by substituting a 1D transition layer by a 2D mesoscopic structure obtained by assembling together 1D transition layers. (This does not rule out the possibility of having 2D microscopic structures at smaller scale than ε inside the transition layers). Moreover, numerical simulations performed in the periodic two-dimensional context indicates that the microscopic transition layers are indeed one-dimensional.

1.4.3 A zigzag pattern ⁵

We analyze here a modified Aviles-Giga model that arises in micromagnetics where the optimal transitions are no longer one-dimensional, but involve two-dimensional microstructure. Even if the limit energy is not of the form \mathcal{I}_f , the method of generalized entropies is also fruitful in this case. The model is the following: we define the functional:

$$F_\varepsilon(m) = \int_\Omega \left(\varepsilon |\nabla m|^2 + \frac{1}{\varepsilon} m_2^2 + \frac{1}{\varepsilon^s} |\nabla|^{-1} \nabla \cdot m|^2 \right) dx,$$

for $\varepsilon > 0$ small, $m \in H^1(\Omega, S^2)$ defined on a domain $\Omega \subset \mathbf{R}^2$ and $s \in (1, 2)$ (this is a technical assumption). Remark that F_ε penalizes the m_2 component comparing to G_ε (or $E_{\varepsilon, \beta}$) penalizing the m_3 component.

Limiting energy. Suppose that we have a family of maps $m_\varepsilon \in H^1(\Omega; S^2)$ with

$$\limsup_{\varepsilon \downarrow 0} F_\varepsilon(m_\varepsilon) < \infty. \quad (1.32)$$

What can we say about the asymptotic behavior of m_ε and the energy $F_\varepsilon(m_\varepsilon)$ as $\varepsilon \downarrow 0$?

As before, it is natural to study this question in the framework of Γ -convergence. To this end, we first need to fix a topology on the space of admissible magnetizations. The strong $L^1(\Omega, \mathbf{R}^3)$ -topology was used for the previous models, but it turns out that F_ε is not coercive enough to deduce compactness from (1.32) in this space. Another possibility is the weak* topology in $L^\infty(\Omega, \mathbf{R}^3)$. Clearly, the limit $m = (m', m_3)$ (as $\varepsilon \downarrow 0$) must have a vanishing second component m_2 and a vanishing distributional divergence $\nabla \cdot m = \nabla \cdot m' = 0$ in Ω . However, we obtain more information about the limit if we first apply a nonlinear transformation to m . In order to do so, we use spherical coordinates (φ, ϑ) so that

$$m = (\cos \varphi \cos \vartheta, \sin \varphi, \cos \varphi \sin \vartheta).$$

The quantity that we need to study is

$$\psi = \sin \vartheta - \vartheta \cos \vartheta,$$

at least if we work in the hemisphere where $|\vartheta| \leq \frac{\pi}{2}$. We will show that as long as ϑ remains sufficiently small, the functional

$$F_0(\psi) = 2 \sup \left\{ \int_\Omega \frac{\partial v}{\partial x_1} \psi dx : v \in C_0^1(\Omega) \text{ with } \sup_\Omega |v| \leq 1 \right\} \quad (1.33)$$

can be identified as the limiting energy. For a sufficiently regular ψ , this is of course

$$F_0(\psi) = 2 \int_\Omega \left| \frac{\partial \psi}{\partial x_1} \right| dx.$$

The lack of a penalization of $\frac{\partial \psi}{\partial x_2}$ means that we can have very rough limiting configurations. On the other hand, almost every restriction to a horizontal line $\Omega \cap (\mathbf{R} \times \{x_2\})$ will be a function of bounded variation. There can be jumps, but these jumps contribute to the energy proportionally

⁵All the results appearing in this subsection are part of the article Ignat-Moser [42]. Therefore, we don't specify in the following this reference for each result.

to the jump height. It is convenient to imagine here that the magnetization depends only on x_1 , and then we can think of a jump as a domain wall. It is worth noting that in general, the wall energy given by F_0 is *not* achieved by a 1-dimensional transition between the two states on either side of the wall (as in the Aviles-Giga model). Instead, in order to obtain the optimal limiting energy given by F_0 , a transition with an additional zigzag structure is required.

Adapted triplet. In order to obtain that F_0 is an optimal lower bound we will use the same strategy based on generalized entropies. More precisely, we study the particular class of Lipschitz continuous maps $\Phi = (\Phi_1, \Phi_2) \in Lip(S^2, \mathbf{R}^2)$ and $\alpha \in Lip(S^2)$ such that for every smooth $m \in C^\infty(\Omega, S^2)$, there holds

$$\nabla \cdot \{\Phi(m)\} + \alpha(m)\nabla \cdot m \leq \varepsilon|\nabla m|^2 + \frac{1}{\varepsilon}m_2^2 \quad \text{a.e. in } \Omega, \quad (1.34)$$

where $\varepsilon > 0$ is a small parameter. In (1.34), we skip the last term in the RHS of (1.24) since it is not important in the sequel. The condition (1.34) yields the corresponding necessary pointwise bounds for an admissible triplet $(\Phi = (\Phi_1, \Phi_2), \alpha)$ as in Lemma 1 where $g(m_3^2)$ is to be replaced by m_2^2 . As explained above, the expected limit energy for a jump of angle $\theta \in (0, \pi/2]$, i.e.,

$$m^\pm = (\cos \theta, 0, \pm \sin \theta) \in S^2 \quad (1.35)$$

is given by

$$F(\theta) = 2\left(\psi(\theta) - \psi(-\theta)\right) = 4\left(\sin \theta - \theta \cos \theta\right).$$

The periodic case. For simplicity, we first focus as before on the periodic situation

$$\Omega = \mathbf{R} \times \mathbf{R}/\mathbb{Z}.$$

For a fixed transition angle $\theta \in (0, \pi/2)$, we set the jump directions m^\pm given by (1.35) and we consider vector fields (periodic in the tangential direction x_2 to the wall) with the desired transition imposed at the boundary:

$$M(\theta) := \left\{ m \in H_{loc}^1(\Omega, S^2) : \lim_{x_1 \rightarrow \pm\infty} m(x_1, \cdot) = m^\pm \text{ in } L^2(\mathbf{R}/\mathbb{Z}) \right\}.$$

Similar to (1.29), we will say that a triplet $(\Phi = (\Phi_1, \Phi_2), \alpha) \in Lip(S^2, \mathbf{R}^3)$ is adapted to the jump (m^-, m^+) if

$$\Phi_1(m^+) - \Phi_1(m^-) = F(\theta) \quad (1.36)$$

and there exists $\varepsilon_0 > 0$ such that for any $0 < \varepsilon \leq \varepsilon_0$, inequality (1.34) holds for every map $m \in C^\infty(\Omega, S^2)$.

We shall see that surprisingly this context is opposite to the Bloch wall model where we could find an adapted triplet for the largest angle, but not for small angles. Here, we prove existence result for walls of small transition angles and non-existence for the biggest angle.

Proposition 13 *There exist an angle $\theta_0 \in (0, \frac{\pi}{2})$ and a Lipschitz triplet $(\Phi = (\Phi_1, \Phi_2), \alpha)$ that is adapted to the jump m^\pm for every $\theta \in (0, \theta_0]$.*

For the biggest jump $\pm \mathbf{e}_3$, we prove a nonexistence result. This result suggests that the zigzag pattern may not be optimal for large angles.

Proposition 14 *There is no smooth triplet $(\Phi = (\Phi_1, \Phi_2), \alpha)$ adapted to the jump m^\pm for $\theta = \pi/2$.*

As we have already seen in Section 1.4.2, existence of adapted triplets are useful for proving the optimal lower bound for F_ε . Indeed, we prove the desired asymptotic minimal value of F_ε on the set $M(\theta)$ for small transition angles θ :

Theorem 13 *There exists an angle $\theta_0 \in (0, \frac{\pi}{2})$ such that the following holds: for every $\theta \in (0, \theta_0]$,*

$$\min_{m_\varepsilon \in M(\theta)} F_\varepsilon(m_\varepsilon) = F(\theta) + o(1) \quad \text{as } \varepsilon \rightarrow 0.$$

The idea of the proof is to match an upper bound coming from the zigzag wall construction with the lower bound based on adapted triplets in Proposition 13. Let us explain the heuristics of

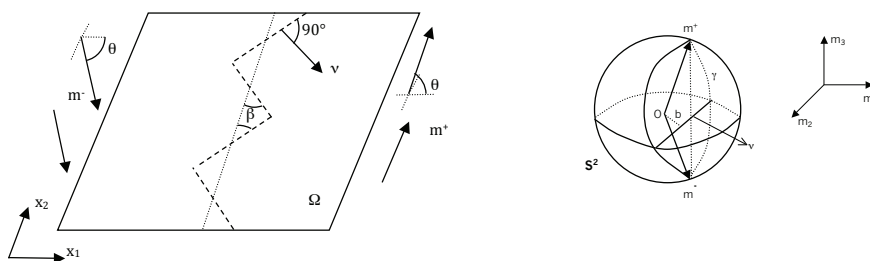


Figure 1.8: The zigzag pattern

deducing the upper bound in Theorem 13. Let $\beta \in [0, \frac{\pi}{2})$ and consider in \mathbf{R}^3 the plane containing the two points $m^\pm \in S^2$ so that $\nu = (\cos \beta, -\sin \beta, 0)$ is the normal vector to the plane (see Figure 1.8). The construction will involve a transition path from m^- to m^+ along the geodesic γ on S^2 within this plane. More precisely, we define

$$b = \cos \theta \cos \beta \quad \text{and} \quad \sigma = \arcsin \frac{\sin \theta}{\sqrt{1-b^2}};$$

the smallest arc γ connecting m^\pm on the circle of radius $\sqrt{1-b^2}$ whose plane is perpendicular to ν is given by

$$\gamma(t) = b\nu + \sqrt{1-b^2}(\sin \beta \cos t, \cos \beta \cos t, \sin t) \quad (1.37)$$

for $-\sigma \leq t \leq \sigma$. For a transition along $\gamma = (\gamma_1, \gamma_2, \gamma_3)$, the expected energy per unit wall length is

$$K(\beta) = 2 \int_{-\sigma}^{\sigma} \gamma_2(t) |\dot{\gamma}(t)| dt.$$

In order to keep the magnetostatic energy small, we will have to use this transition across pieces of a zigzag wall that are tilted with respect to $\{0\} \times (0, 1)$ by the angle β (see Figure 1.8). This increases the length of the wall by the factor $\frac{1}{\cos \beta}$, and in the limit we expect the energy density

$$h(\beta) = \frac{K(\beta)}{\cos \beta}. \quad (1.38)$$

One can check that h is a decreasing function and concludes that

$$\inf_{0 \leq \beta < \frac{\pi}{2}} h(\beta) = \lim_{\beta \rightarrow \frac{\pi}{2}^-} h(\beta) = F(\theta).$$

Observe that the energy cost of a transition of small angle θ is cubic, so that it is asymptotically cheaper than the quadratic energy cost of a Bloch wall transition of the same angle.

Γ -convergence for small transition angles. We now concentrate on families of uniformly bounded energy configurations $\{m_\varepsilon \in H^1(\Omega; S^2)\}$ in a smooth bounded simply-connected domain $\Omega \subset \mathbf{R}^2$, i.e., (1.32) holds. The aim is to establish the structure of limiting configurations of such families and to justify that F_0 is their limit energy (according to the Γ -convergence method). The first issue is to find out the appropriate topology for the desired Γ -convergence result. Obviously, (1.32) entails $m_{\varepsilon,2} \rightarrow 0$ strongly in $L^2(\Omega)$. However, families $\{m_\varepsilon\}$ satisfying (1.32) are in general *not* relatively compact in the strong L^1 topology and the limiting configurations m are not necessarily taking values into S^2 (in general, one only has $|m| \leq 1$ a.e. in Ω). Therefore, one alternative would be to choose the weak* L^∞ -topology for $\{(m_{\varepsilon,1}, m_{\varepsilon,3})\}$. Rather than studying the limiting behavior of $(m_{\varepsilon,1}, m_{\varepsilon,3})$, we focus on the quantity

$$\psi_\varepsilon = f(m_\varepsilon), \tag{1.39}$$

where $f : S^2 \rightarrow \mathbf{R}$ is the function defined by

$$f(m) = \begin{cases} \frac{1}{4}F(\arctan(m_3/m_1)) & \text{if } m_1 > 0, \\ 2 + \frac{1}{4}F(\arctan(m_3/m_1)) & \text{if } m_1 < 0 \text{ and } m_3 \geq 0, \\ -2 + \frac{1}{4}F(\arctan(m_3/m_1)) & \text{if } m_1 < 0 \text{ and } m_3 < 0, \end{cases}$$

extended continuously where $m_1 = 0$ and $m_2 \neq \pm 1$ (here, $\arctan : \mathbf{R} \rightarrow (-\frac{\pi}{2}, \frac{\pi}{2})$). This function has a discontinuity along the semicircle $\{m \in S^2 : m_3 = 0, m_1 \leq 0\}$, and from a geometric point of view, it would be more appropriate to regard f as a function from S^2 into $\mathbf{R}/4\mathbb{Z}$. Since we work mostly in a hemisphere below, we keep \mathbf{R} as the target anyway. The discontinuities at the poles $\pm \mathbf{e}_2$, of course, are unavoidable. Since $|\psi_\varepsilon| \leq 2$ a.e. in Ω , we choose the weak* L^∞ -topology for $\{\psi_\varepsilon\}$ as appropriate for the Γ -convergence result. Extending (1.33) to the limiting functional $F_0 : L^\infty(\Omega) \rightarrow [0, \infty]$, we prove the following Γ -convergence result for small transition angles:

Theorem 14 *There exists an angle $\theta_0 \in (0, \frac{\pi}{2})$ such that the following holds true:*

1) (Compactness and Lower bound) *Let $\{m_\varepsilon\} \subset H^1(\Omega; S^2)$ with (1.32). Consider the family $\{\psi_\varepsilon\}$ associated to $\{m_\varepsilon\}$ via (1.39). Then for subsequences,*

$$\psi_\varepsilon \overset{*}{\rightharpoonup} \psi \text{ in } L^\infty(\Omega) \text{ and } m_{\varepsilon,2} \rightarrow 0 \text{ in } L^2(\Omega). \tag{1.40}$$

If $|\psi_\varepsilon| \leq \frac{1}{4}F(\theta_0)$ a.e. in Ω for every small $\varepsilon > 0$, then

$$F_0(\psi) \leq \liminf_{\varepsilon \downarrow 0} F_\varepsilon(m_\varepsilon).$$

2) (Upper bound) *For every $\psi \in L^\infty(\Omega)$ with $|\psi| \leq \frac{1}{4}F(\theta_0)$ a.e. in Ω , there exists a family $\{m_\varepsilon\} \subset H^1(\Omega; S^2)$ such that (1.40) holds and*

$$F_0(\psi) = \lim_{\varepsilon \downarrow 0} F_\varepsilon(m_\varepsilon).$$

We are aware of only one other situation where the Γ -limit is explicitly known for a problem involving similar microstructures: the problem leading to cross-tie walls in thin ferromagnetic films (see [1, 66, 67]). As shown in Figure 1.5, the cross-tie wall consists in a mixture of vortices and Néel walls (1-dimensional transition layers similar to Bloch walls, but taking values only in S^1). Remarkably, the function $\sin \theta - \theta \cos \theta$ plays an important role in that context as well, although this may be a mere coincidence.

Chapter 2

Singular patterns in thin-film micromagnetics

2.1 Micromagnetics ¹

Ferromagnetic materials are widely used in nowadays as technological tools, especially for magnetic data storage. The modelling of very small ferromagnetic particles is based on the micromagnetic theory. The micromagnetic model states that ferromagnetic materials can be described by a 3D vector-field distribution, called *magnetization*, where the stable configurations correspond to (local) minimizers of the micromagnetic energy. The associated variational problem is nonconvex and nonlocal. Moreover, it is a multi-scale system involving both intrinsic parameters (depending on the nature of the ferromagnetic material) and extrinsic parameters (coming from the geometry of the sample). According to the relative smallness of these parameters, different asymptotic regimes appear and lead to formation of various magnetization patterns.

The qualitative and quantitative analysis of magnetization patterns is an extensively explored topic. Generically, a pattern (stable state) consists in large uniformly magnetized 3D regions (*magnetic domains*) separated by narrow transition layers (*magnetic walls*) where the magnetization varies very rapidly. Depending on the length scales of the system, the experiments predict different type of magnetic walls: 2D wall defects (*Néel walls*, *Bloch walls*, *asymmetric Néel walls*, *asymmetric Bloch walls* etc.), 1D vortex-lines (*Bloch lines*), boundary vortices or different type of microstructures: *cross-tie walls*, *zigzag walls* etc. The main goal is to give a mathematical justification of the physical prediction on the formation and characterization of these defects. Classical methods of functional analysis are often insufficient to detect these phenomena of loss of regularity. New approaches need to be developed in order to implement geometric measure theory contributing to the analysis of partial differential equations and calculus of variations.

2.1.1 The general three-dimensional model

The magnetization of a ferromagnetic sample $\Omega \subset \mathbf{R}^3$ is created by the spontaneous alignment of electron spins and can be described in the non-dimensionalized form by a 3D unit-length vector

¹This section is part of the article of the author [36]

field

$$m : \Omega \rightarrow S^2.$$

Let us assume that the sample is a cylinder, i.e.,

$$\Omega = \Omega' \times (0, t)$$

where Ω' is the cross section of the sample of diameter ℓ and t is the thickness of the cylinder (see Figure 2.1). According to micromagnetics, stable magnetizations in Ω are described by (local)

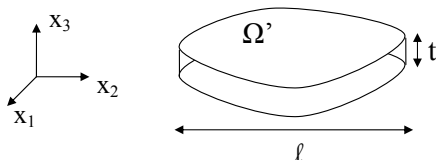


Figure 2.1: A ferromagnetic sample.

minimizers of the energy functional defined as:

$$E^{3D}(m) = d^2 \int_{\Omega} |\nabla m|^2 dx + Q \int_{\Omega} \varphi(m) dx + \int_{\mathbf{R}^3} |\nabla U|^2 dx - 2 \int_{\Omega} H_{\text{ext}} \cdot m dx. \quad (2.1)$$

In the following we explain the four components of the micromagnetic energy E^{3D} .

- The first term, called exchange energy is due to short range interactions of spins and favors parallel alignment of neighboring spins. The constant d is the exchange length and corresponds to an intrinsic parameter of the material of the order of nanometers.
- The second term in (2.1) represents the anisotropy energy that penalizes certain magnetization axes. The anisotropy energy density φ is a nonnegative function with symmetry properties inherited from the crystalline lattice. The preferred directions of magnetization are the zeros of φ . Typically, we have uniaxial or multi-axial anisotropy (e.g., $\varphi(m) = 1 - m_1^2$ that favors the direction $(\pm 1, 0, 0)$) and surface anisotropy (e.g., $\varphi(m) = m_3^4$ where the easy plane is the horizontal one). The quality factor Q is a second intrinsic parameter of the material that measures the strength of the anisotropy energy relative to the stray-field. According to the values of Q , we distinguish two classes of materials: soft materials if $Q < 1$ and hard materials if $Q > 1$.
- The third term of E^{3D} is the stray-field energy and is created by long range interactions between electron spins modelled by the static Maxwell equation. More precisely, the stray-field potential $U : \mathbf{R}^3 \rightarrow \mathbf{R}$ is determined by

$$\begin{aligned} \Delta U &= \nabla \cdot (m 1_{\Omega}) \quad \text{in } \mathbf{R}^3, \\ \text{i.e., } \int_{\mathbf{R}^3} \nabla U \cdot \nabla \zeta dx &= \int_{\Omega} m \cdot \nabla \zeta dx, \quad \forall \zeta \in C_c^{\infty}(\mathbf{R}^3). \end{aligned} \quad (2.2)$$

By the electrostatic analogy, two types of charges generate the potential U : volume charges with density given by the divergence of m in the interior of the sample Ω and surface charges represented by the normal component of the magnetization on the boundary of Ω . Therefore, this nonlocal term favors domain patterns that achieve flux closure.

- The last term in (2.1) denotes the external field energy generated by an applied external field $H_{\text{ext}} : \mathbf{R}^3 \rightarrow \mathbf{R}^3$. It favors alignment of the magnetization with H_{ext} .

More details about the mathematical modelling of micromagnetics can be found in the book of Hubert and Schäfer [32] or in the overview of DeSimone, Kohn, Müller and Otto [26].

We will concentrate on the analysis of *global* minimizers of energy (2.1). In fact, physically accessible *local* minima share the same features as the ground state (see DeSimone, Kohn, Müller, Otto and Schäfer [24]). It is a variational problem relying on the nonconvex constraint $|m| = 1$ and the nonlocality of the stray-field energy due to (2.2). On the other side, four length scales are involved in the system: two intrinsic parameters (d and Q) and two extrinsic scales (t and ℓ). Our approach is based on asymptotic analysis, taking advantage of the presence of small ratios involving these parameters. The combination of nonlocality and nonconvexity with the multiscale nature of the variational problem leads to a rich pattern formation of the magnetization.

2.1.2 A reduced thin-film model

In the following, we are interested in thin ferromagnetic films where we expect the nucleation of several singular patterns of the magnetization (like Néel walls, Bloch lines and boundary vortices). The main issue is to identify the scaling law of the minimum energy and the pattern of the magnetization that achieves this minimum.

Heuristics and scaling. We will heuristically explain in the following the separation of energy scales in the regime of thin films. The balance between the energy terms is responsible for the formation of certain type of walls in function of certain regimes. The ansatz is the following: We assume that the magnetic film $\Omega = \Omega' \times (0, t)$ with $\ell = \text{diam}(\Omega')$ has a small aspect ratio

$$h := \frac{t}{\ell} \ll 1 \quad (2.3)$$

so that the variations of m in the vertical variable x_3 are strongly penalized by the energy. Therefore, we assume that m is invariant in x_3 and depends only on the in-plane variables $x' = (x_1, x_2)$:

$$m = (m', m_3)(x') : \Omega' \rightarrow S^2 \quad \text{and} \quad m \text{ varies on length scales } \gg \frac{t}{\ell}. \quad (2.4)$$

It is also assumed that the external field is in-plane and invariant in x_3 , i.e.,

$$H_{\text{ext}} = (H'_{\text{ext}}(x'), 0).$$

Here and below, the dash ' always indicates a 2D quantity. We always denote $a \ll b$ if $\frac{a}{b} \rightarrow 0$; also, $a \lesssim b$ if $a \leq Cb$ for some universal constant $C > 0$.

Rescaling in the length ℓ of Ω' , i.e., $\tilde{x}' = x'/\ell$, $\tilde{\Omega}' = \Omega'/\ell$, $\tilde{m}(\tilde{x}') = m(x')$ and $\tilde{H}'_{\text{ext}}(\tilde{x}') = H'_{\text{ext}}(x')$, the exchange energy, anisotropy and external field energy can be written as

$$\int_{\Omega} (d^2 |\nabla m|^2 + Q\varphi(m) - 2H_{\text{ext}} \cdot m) dx = td^2 \int_{\tilde{\Omega}'} |\tilde{\nabla}' \tilde{m}|^2 d\tilde{x}' + t\ell^2 \int_{\tilde{\Omega}'} \left(Q\varphi(\tilde{m}) - 2\tilde{H}'_{\text{ext}} \cdot \tilde{m}' \right) d\tilde{x}'. \quad (2.5)$$

What is the appropriate scaling law of the stray-field energy? For configurations (2.4), the static Maxwell equation (2.2) turns into:

$$\Delta U = \nabla' \cdot m' \mathbf{1}_{\Omega} + m \cdot \nu \mathbf{1}_{\partial\Omega} \quad \text{in } \mathbf{R}^3, \quad (2.6)$$

where ν is the unit outer normal vector on $\partial\Omega$. Therefore, the volume charges are given by the in-plane flux $\nabla' \cdot m'$ and the surface charges on the top and the bottom side of the cylinder ($x_3 \in \{0, t\}$) are represented by the out-of-plane component m_3 of the magnetization. Equation (2.6) is a transmission problem that can be solved explicitly using the Fourier transform $\mathcal{F}(\cdot)$ in the horizontal variables (see e.g. [49], [36]) and one computes:

$$\int_{\mathbf{R}^3} |\nabla U|^2 dx = t \int_{\mathbf{R}^2} f\left(\frac{t}{2}|\xi'|\right) \left| \frac{\xi'}{|\xi'|} \cdot \mathcal{F}(m'1_{\Omega'}) \right|^2 d\xi' + t \int_{\mathbf{R}^2} g\left(\frac{t}{2}|\xi'|\right) |\mathcal{F}(m_3 1_{\Omega'})|^2 d\xi',$$

where

$$g(s) = \frac{1 - e^{-2s}}{2s} \quad \text{and} \quad f(s) = 1 - g(s) \quad \text{for every } s \geq 0.$$

Approximating $g(s) \approx 1$ and $f(s) \approx s$ if $s = o(1)$ and as above, rescaling in the length scale ℓ of Ω' , we obtain the following estimate of the stray-field energy:

$$\int_{\mathbf{R}^3} |\nabla U|^2 dx \approx \frac{t^2 \ell}{2} \|(\tilde{\nabla}' \cdot \tilde{m}')_{ac}\|_{\dot{H}^{-1/2}(\mathbf{R}^2)}^2 + \frac{t^2 \ell}{2\pi} \left| \log \frac{\ell}{t} \right| \int_{\partial\tilde{\Omega}'} (\tilde{m}' \cdot \tilde{\nu})^2 d\mathcal{H}^1 + t\ell^2 \int_{\tilde{\Omega}'} \tilde{m}_3^2, \quad (2.7)$$

(see e.g. [22], [49]). This is due to the assumption (2.4), so that indeed the stray-field energy asymptotically decomposes into three terms in the thin-film regime: the first one is penalizing the volume charges

$$(\tilde{\nabla}' \cdot \tilde{m}')_{ac} = \tilde{\nabla}' \cdot \tilde{m}' 1_{\tilde{\Omega}'},$$

as an homogeneous $\dot{H}^{-1/2}$ -seminorm and induces the leading order of the energy of Néel walls, a second term penalizing the lateral charges $\tilde{m}' \cdot \tilde{\nu}$ in the L^2 -norm and responsible for the nucleation of boundary vortices, as well as the third term that counts the surface charges \tilde{m}_3 on the top and bottom of the cylinder and leading to formation of Bloch lines.

Summing up (2.5) and (2.7), we deduce the following reduced 2D thin-film energy:

$$\begin{aligned} \tilde{E}^{2D}(\tilde{m}) &= t d^2 \int_{\tilde{\Omega}'} |\tilde{\nabla}' \tilde{m}|^2 d\tilde{x}' + \frac{t^2 \ell}{2} \int_{\mathbf{R}^2} \left| |\tilde{\nabla}'|^{-\frac{1}{2}} (\tilde{\nabla}' \cdot \tilde{m}')_{ac} \right|^2 d\tilde{x}' + \frac{t^2 \ell}{2\pi} \left| \log \frac{\ell}{t} \right| \int_{\partial\tilde{\Omega}'} (\tilde{m}' \cdot \tilde{\nu})^2 d\mathcal{H}^1 \\ &\quad + t\ell^2 \int_{\tilde{\Omega}'} \left(\tilde{m}_3^2 + Q\varphi(\tilde{m}) - 2\tilde{H}'_{\text{ext}} \cdot \tilde{m}' \right) d\tilde{x}'. \end{aligned} \quad (2.8)$$

We will often refer in the following to the above thin-film energy approximation and *we will drop $\tilde{\cdot}$ in the sequel*.

According to the specific thin-film regime, three types of singular pattern of the magnetization occur: Néel walls, Bloch lines and boundary vortices. In fact, the formation of one of these patterns depends on the scale ordering of the three terms in the RHS of (2.7). Let us now discuss briefly these patterns (and we will present them in more details in the next sections).

Néel walls. The (symmetric) Néel wall is a transition layer describing a one-dimensional in-plane rotation connecting two (opposite) directions of the magnetization. It is generated by the volume charges $(\nabla' \cdot m')_{ac}$ that give the leading order of the energy of a Néel wall. Observe that this term in (2.7) is related at order of $t^2 \ell$ with the limiting stray-field energy generated by the in-plane charges as $h \rightarrow 0$:

$$\Delta u_{ac} = (\nabla' \cdot m')_{ac} \mathcal{H}^2 \llcorner \{x_3 = 0\} \quad \text{in } \mathbf{R}^3.$$

More precisely, the homogeneous $\dot{H}^{-1/2}$ -seminorm of the in-plane divergence of m' is given by the Dirichlet integral of u_{ac} :

$$\int_{\mathbf{R}^3} |\nabla u_{ac}|^2 dx = \frac{1}{2} \int_{\mathbf{R}^2} \left| |\nabla'|^{-\frac{1}{2}} (\nabla' \cdot m')_{ac} \right|^2 dx'. \quad (2.9)$$

Since a Néel wall is a one-dimensional transition layer in the normal direction x_1 to the wall (i.e., $m = m(x_1)$), the RHS in (2.9) becomes the homogeneous $\dot{H}^{1/2}$ -seminorm of the normal component m_1 (on the wall). The Néel wall has two length scales: a core of size

$$\delta := \frac{d^2}{t\ell}$$

and two tails of length scale depending on the confining mechanism. In order that a Néel wall is relevant in a certain regime, one should assume that $\delta \lesssim 1$. The reduced stray-field energy (2.7) per unit length of a Néel wall is of order of

$$E^{2D}(\text{Néel wall}) = O(t^2 \ell / |\log \delta|).$$

A detailed description of the Néel wall is done in Section 2.2.

Bloch line. A Bloch line is a regularization of a vortex at the microscopic level of the magnetization that becomes out-of-plane at the center. The prototype of a Bloch line is given by a vector field

$$m : B^2 \rightarrow S^2$$

defined in a circular cross-section $\Omega' = B^2$ of a thin film and satisfying the flux-closure condition:

$$\nabla' \cdot m' = 0 \quad \text{in } B^2 \quad \text{and} \quad m'(x') = (x')^\perp \quad \text{on } \partial B^2. \quad (2.10)$$

(The magnetization is assumed to be invariant in the thickness direction of the film and the word

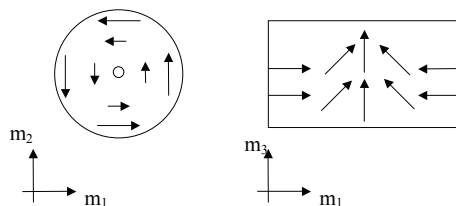


Figure 2.2: Bloch line.

“line” of the Bloch-line pattern refers to the vertical direction.) Since the magnetization turns in-plane at the boundary of the disc B^2 (so, $\deg(m', \partial\Omega) = 1$), a localized region is created, that is the core of the Bloch line of size

$$\eta := d/\ell,$$

where the magnetization becomes perpendicular to the horizontal plane (see Figure 2.2). In order that a Bloch line is relevant in a certain regime, one should assume that $\eta \lesssim 1$. The reduced energy

(2.8) of a configuration (2.10) (in the absence of anisotropy and applied external field) is given by the exchange energy and the surface charges in m_3 :

$$E^{2D}(m) = td^2 \left(\int_{B^2} |\nabla' m|^2 dx' + \frac{1}{\eta^2} \int_{B^2} m_3^2 dx' \right).$$

The Bloch line represents the minimizer of this energy under the constraint (2.10). Due to the similarity to the Ginzburg-Landau type functional, the Bloch line corresponds to the Ginzburg-Landau vortex and the energetic cost of a Bloch line (per unit-length) resides in the exchange energy outside the vortex core:

$$E^{2D}(\text{Bloch line}) = O(td^2 |\log \eta|)$$

with the exact prefactor 2π (see e.g. [36]). We will discuss more precisely this singular pattern in Sections 2.4 and 2.6.

Boundary vortex. Next we address boundary vortices. A boundary vortex corresponds to an in-plane transition of the magnetization along the boundary from ν^\perp to $-\nu^\perp$, see Figure 2.3. The corresponding minimization problem resides in the competition between the exchange energy and the lateral surface charges $m' \cdot \nu$:

$$E^{2D}(m) = td^2 \left(\int_{\Omega'} |\nabla' m|^2 dx' + \frac{|\log h|}{2\pi\delta} \int_{\partial\Omega'} (m' \cdot \nu)^2 d\mathcal{H}^1 \right)$$

within the set of in-plane magnetizations $m : \Omega' \rightarrow S^1$. The minimizer of this energy is an harmonic vector field with values in S^1 driven by a pair of boundary vortices. These have been analyzed in [49, 52, 51, 58, 59]. The transition is regularized on the length scale of the exchange part of the energy, i.e., the core of the boundary vortex has length of size

$$\kappa := \frac{d^2}{t\ell \log \frac{\ell}{\xi}}.$$

In order that a boundary vortex is relevant in a certain regime, one should assume that $\kappa \lesssim 1$. The cost of such a transition has the energy of leading order of

$$E^{2D}(\text{Boundary vortex}) = O(td^2 |\log \kappa|)$$

with exact prefactor π . Even if they generate the same amount of energy, a boundary vortex is different than a "half" vortex (i.e., regularization of $x/|x|$ in the "half" disc B_+^2): the "half" vortex is tangent at the boundary, i.e., $m' \cdot \nu = 0$ on $B_+^2 \cap \{x_2 = 0\}$ (while the boundary vortex isn't), and the boundary vortex is of values into S^1 (while the "half" vortex isn't). We will describe in



Figure 2.3: A micromagnetic boundary vortex

more details boundary vortices in Section 2.5.

Mesoscopic Landau-state in thin films. At the mesoscopic level in a thin-film, we expect that the magnetization satisfies the flux-closure constraint. It consists in assuming that there

are no charges in the sample which would imply that (2.7) vanishes. This type of limit charge-free configurations were predicted in the physics literature (see van den Berg [72]): they are 2D unit-length vector fields of vanishing divergence, i.e.,

$$\begin{cases} m_3 = 0, |m'| = 1 \text{ and } \nabla' \cdot m' = 0 & \text{in } \Omega', \\ m' \cdot \nu = 0 & \text{on } \partial\Omega'. \end{cases} \quad (2.11)$$

This structure reveals the connection with Chapter 1 and explains the formation of line singularities or vortices at the mesoscopic level of the magnetization in thin films (known in physics as the principle of pole avoidance). We already discussed in Chapter 1 that the method of characteristics yields the nonexistence of continuous solutions of (2.11) in bounded simply connected domains. One of the solution of (2.11) (in the sense of distributions) is the “viscosity solution” given via the distance function

$$m = \nabla^\perp \psi, \quad \text{with } \psi(x') = \text{dist}(x', \partial\Omega')$$

that corresponds to the so-called Landau state for the magnetization m' . The line-singularities for solutions m' are an idealization of domain walls at the mesoscopic level. At the microscopic level, they are replaced by smooth transition layers (as Néel walls, Bloch walls etc.) where the magnetization varies very quickly on a small length scale. Note that the normal component of m' does not jump across these discontinuity lines (because of (2.11)); therefore, the normal vector of the mesoscopic wall is determined by the angle between the mesoscopic levels of the magnetization in the adjacent domains (called wall angle).

Regimes. An important step in our analysis consists in identifying reduced models valid in appropriate regimes where the behavior of the singular patterns described above is easier to understand. The choice of the asymptotic regimes will correspond to the energy ordering of the three patterns (Néel walls, Bloch lines and boundary vortices); the choice of the scaling law of the minimal energy determines the constraints of the model (imposed by the patterns of higher energy order) and the singular patterns that are to be neglected (of lower energy order). With these choices, the mathematical approach is based on asymptotic analysis by proving the matching of upper and lower bounds for the energy (in the spirit of Γ -convergence).

Let us now discuss the possible choices of ordering. First of all, we are interested in thin-film regimes (i.e. $h = t/\ell \ll 1$) where all three singular patterns are relevant, meaning that they are contained by the sample:

$$\delta \ll 1, \quad \eta \ll 1, \quad \kappa \ll 1,$$

leading to $t \ll \ell$ and $d \ll \ell$. (In fact, if the Néel wall is relevant, i.e., $\delta \ll 1$, then also the Bloch line and the boundary vortex are contained, i.e., $\eta \ll 1$ and $\kappa \ll 1$.) Second, one can check that

$$\begin{aligned} E^{2D}(\text{Boundary vortex}) &\lesssim E^{2D}(\text{Néel wall}) \\ \text{or } E^{2D}(\text{Boundary vortex}) &\lesssim E^{2D}(\text{Bloch line}), \end{aligned}$$

meaning that a boundary vortex never induces the leading order of the total energy (see [44]). Therefore, one has the following three choices of ordering:

(i)

$$\max \left\{ E^{2D}(\text{Boundary vortex}), E^{2D}(\text{Bloch line}) \right\} \ll E^{2D}(\text{Néel wall}),$$

equivalent with $|\log h| \ll \frac{1}{\delta|\log \delta|}$. A slightly more general regime was treated in [22], where $|\log h| \ll 1/\delta$ and the scaling law of the minimum energy in (2.8) is of order $t^2\ell$. In this case, the 3D stray-field energy (2.7) reduces to (2.9) (at order $t^2\ell$) and the reduced model is rigorously justified via the Γ -convergence method (see [22]): the limiting configurations are invariant in the vertical direction x_3 (justifying the assumption (2.4)), but they are not in-plane since Bloch lines may appear in the reduced model. The regime in [22] is appropriate for permalloy films of diameter of tens of microns and thickness of the order of tens of nanometers. So, it can be achieved experimentally, though not by numerical simulation which is generally restricted to a thickness of the order of sub-microns.

(ii)

$$E^{2D}(\text{Boundary vortex}) \ll E^{2D}(\text{Néel wall}) \ll E^{2D}(\text{Bloch line}),$$

equivalent with

$$\log |\log h| \ll \frac{1}{\delta|\log \delta|} \ll |\log h|. \quad (2.12)$$

It means that the aspect ratio $h = h(\delta)$ is exponentially small with respect to the Néel wall core δ ; in particular, $t \ll d \ll \ell$. This regime is treated in [38] where the choice of the scaling law of the minimal energy is of order of Néel walls, i.e., $t^2\ell/|\log \delta|$. Therefore, due to (2.12), Bloch lines are avoided (since they are too expensive), so that the limiting configurations as $h \rightarrow 0$ are x_3 -invariant and they are in-plane, i.e., $m \in S^1$. The boundary vortices do not contribute to the leading order of minimal energy (since they are lower order). In Section 2.3, we discuss this reduced model: the goal is to prove that the optimal pattern of the magnetization on circular cross-section Ω' is a peculiar vortex structure, driven by a 360° Néel wall accompanied by a pair of boundary vortices at $\partial\Omega'$.

(iii)

$$E^{2D}(\text{Néel wall}) \ll E^{2D}(\text{Boundary vortex}) \ll E^{2D}(\text{Bloch line}), \quad (2.13)$$

equivalent with

$$\frac{1}{\delta|\log \delta|} \ll \log |\log h|.$$

In Section 2.4, we discuss this reduced model. This is part of [44] where the scaling law of the minimal energy is of order of Bloch lines $O(td^2|\log \eta|)$. However, in [44], we did not focus on the level of minimal energy, but rather on metastable configurations where boundary vortices are strongly penalized, so that the limiting configurations as $h \rightarrow 0$ are assumed to be charges-free on the lateral surface, i.e., $m' \cdot \nu = 0$ on $\partial\Omega'$. Indeed, vanishing lateral surface charges would be physical relevant for a global minimizer *only* if boundary vortices were more expensive than both the Néel walls and Bloch line contribution. As explained above, this assumption never happens in the regime $h \ll 1$ and $\delta \ll 1$. Therefore, the stray-field energy (2.7) (in the absence of the middle term in RHS) is not adapted for studying global minimizers in the regime (2.13), but rather for metastable states with vanishing normal component at the lateral surface.

2.2 Néel wall ²

The Néel wall is a dominant transition layer in thin ferromagnetic films (in the regime presented in Subsection 2.1.2). It is characterized by a one-dimensional in-plane rotation connecting two (opposite) directions of the magnetization. It has two length scales: a small core with fast varying rotation and two logarithmically decaying tails. In order for the Néel wall to exist, the tails are to be contained. There are three confining mechanisms for the Néel wall tails: the anisotropy of the material, the steric interaction with the sample edges and the steric interaction with the tails of neighboring Néel walls. In the following, we describe these models that correspond to three nonconvex and nonlocal variational problems depending on a small parameter:

Model 1. Confinement of Néel wall tails by anisotropy. The model is derived from (2.8) as follows (we skip \sim in (2.8)): we assume the quality factor Q to be of order of the aspect ratio h (for simplicity, set $Q = \frac{t}{\ell} \ll 1$), i.e., the material is soft; we also assume that the material anisotropy density is given by $\varphi(m) = m_1^2$ and we impose an applied field $H'_{ext} = \frac{t}{\ell}(\cos \theta, 0)$. Renormalizing the energy (2.8) at order $t^2\ell$, we may assume in the regime $h = \frac{t}{\ell} \ll 1$ that the section $\Omega' = \mathbf{R} \times \mathbf{R}/\mathbb{Z}$ is a periodic strip and the admissible configurations are in-plane magnetizations depending on one variable (normal to the wall) and satisfy the following boundary conditions (that enforce a transition as in (1.27)):

$$m = m(x_1), \quad m_3 = 0, \quad \text{and} \quad m(\pm\infty) = m^\pm := (\cos \theta, \pm \sin \theta, 0), \quad (2.14)$$

where $\theta \in (0, \pi)$ is the wall angle (see Figure 2.4). Therefore, by (2.8), we derive the following functional whose behavior is to be studied asymptotically as $\delta \downarrow 0$:

$$m \mapsto \delta \|m\|_{H^1}^2 + \frac{1}{2} \|m_1\|_{H^{1/2}}^2 + \|m_1 - \cos \theta\|_{L^2}^2, \quad (2.15)$$

where we recall that $\delta = d^2/(t\ell)$ plays the role of the core of the transition.

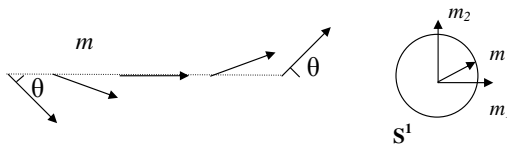


Figure 2.4: Néel wall of angle 2θ .

Observe that the energy (2.15) is invariant under translation. Since configurations m of finite energy are continuous, the boundary conditions in (2.14) enforce a transition (*wall domain*) for the magnetization. One can fix the center of the wall at the origin by setting

$$m(0) = (1, 0).$$

Under these restrictions, a Néel wall corresponds to a minimizer of the energy (2.15).

²All the results appearing in this section are part of the article of the author [35]. Therefore, we don't specify in the following this reference for each result.

The variational problem is nonconvex because of the saturation constraint $|m| = 1$ and nonlocal due to the stray-field interaction. It is a nondegenerate problem since the anisotropy term prevents a Néel wall to spread over the complete domain \mathbf{R} ; therefore, the Néel wall tails are forced to be limited and the energy cannot reach arbitrary small levels. Observe that energy (2.15) only yields a uniform bound of m_1 in $\dot{H}^{1/2}(\mathbf{R})$ that barely fails to control the $L^\infty(\mathbf{R})$ -norm $\|m_1\|_{L^\infty(\mathbf{R})} = 1$. This suggests a logarithmic decay of the energy. Indeed, we prove the following result (see also [20], [38]):

Lemma 2 *Let $I \subset \mathbf{R}$ be a bounded interval and $\delta \ll 1$. For every function $m_1 \in C_c(I)$, the following estimate holds:*

$$\delta \|m_1\|_{\dot{H}^1}^2 + \frac{1}{2} \|m_1\|_{\dot{H}^{1/2}}^2 \geq \frac{\pi + o(1)}{2|\log \delta|} \|m_1\|_{L^\infty}^2 \quad \text{as } \delta \downarrow 0.$$

The idea of this estimate resides in a duality argument combined with a failing Gagliardo-Nirenberg interpolation embedding

$$BV \cap L^\infty(\mathbf{R}^N) \not\subseteq \dot{H}^{1/2}(\mathbf{R}^N).$$

This failing embedding can be corrected by regularizing the homogeneous $\dot{H}^{1/2}$ -seminorm. This perturbation yields a weaker seminorm that is controlled with a logarithmically slow rate having the optimal prefactor $\frac{2}{\pi}$ (see [20]):

For $\delta \ll w$ and for any $\chi : \mathbf{R}^N \rightarrow \mathbf{R}$, we have that

$$\int_{\mathbf{R}^N} \min\left\{\frac{1}{\delta}, |\xi|, w|\xi|^2\right\} |\hat{\chi}|^2 d\xi \lesssim \frac{2}{\pi} \left(\log \frac{w}{\delta}\right) \|\chi\|_{L^\infty} \int_{\mathbf{R}^N} |\nabla \chi|. \quad (2.16)$$

The exact leading order term of the minimal energy in (2.15) was deduced by DeSimone, Kohn, Müller and Otto [21, 23] by matching upper and lower bounds in the case of a 180° Néel wall (i.e., $\theta = \pi/2$):

$$\min_{\theta=\pi/2} \left(\delta \|m\|_{\dot{H}^1}^2 + \frac{1}{2} \|m_1\|_{\dot{H}^{1/2}}^2 + \|m_1\|_{L^2}^2 \right) = \frac{\pi + o(1)}{2|\log \delta|} \quad \text{as } \delta \downarrow 0. \quad (2.17)$$

The analysis of the structure of a minimizer of (2.17) is rather subtle due to the different scaling behavior of the energy terms in (2.15). Remark that omitting the $\dot{H}^{1/2}$ -seminorm, the formulation of (2.17) in terms of $v := m_2$ corresponds to a variational problem associated to the Cahn-Hilliard model (see Cahn and Hilliard [14]):

$$\min_{\substack{v: \mathbf{R} \rightarrow [-1,1] \\ v(0)=0, v(\pm\infty)=\pm 1}} \int_{\mathbf{R}} \left(\frac{\delta}{1-v^2} \left| \frac{dv}{dx_1} \right|^2 + 1 - v^2 \right) dt. \quad (2.18)$$

The minimizer is a transition layer with a single length scale $\sqrt{\delta}$, i.e., $v(x_1) = \tanh(x_1/\sqrt{\delta})$. The first component of the magnetization m_1 would correspond in (2.18) to $\text{sech}(x_1/\sqrt{\delta})$ and the minimal energy is equal to $4\sqrt{\delta}$.

Coming back to our variational problem (2.17), the presence of the nonlocal term as a homogeneous $\dot{H}^{1/2}(\mathbf{R})$ -seminorm in competition with the energy (2.18) creates a second length scale of the transition layer. The Néel wall is divided in two regions: a core ($|x_1| \lesssim w_{core}$) and two

tails ($w_{core} \lesssim |x_1| \lesssim w_{tail}$). This particular structure enables the magnetization to decrease the energy by a logarithmic factor (2.17). Melcher [54, 55] rigorously established the optimal profile of the Néel wall, i.e., the unique minimizer m of (2.17) with $m_1(0) = 1$ exhibits two uniformly logarithmic tails beyond a core region of order δ close to the origin (see Figure 2.5):

$$m_1(t) \sim \frac{|\log |x_1||}{|\log \delta|} \quad \text{for} \quad \delta < |x_1| < 1/e, \text{ i.e. } w_{core} = O(\delta), \quad w_{tail} = O(1).$$

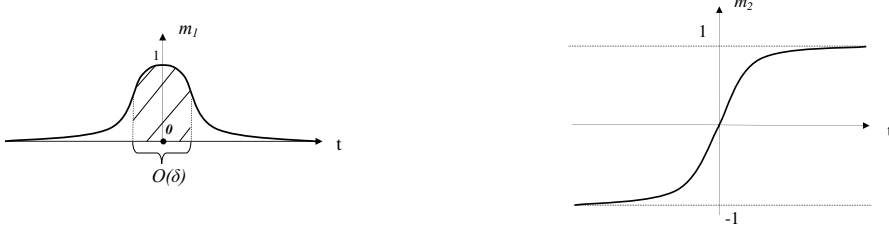


Figure 2.5: First and second component of a 180° Néel wall.

We are interested in the asymptotics of the energy (2.15) as $\delta \downarrow 0$. Due to the logarithmic decay (2.17), we consider a new length scale $\varepsilon > 0$ such that

$$\delta = \varepsilon / |\log \varepsilon|$$

and we renormalize the energy (2.15) by a factor $|\log \varepsilon|$ in order that the minimal energy become of order $O(1)$:

$$E_\varepsilon(m) = \varepsilon \|m\|_{H^1}^2 + |\log \varepsilon| \left(\frac{1}{2} \|m_1\|_{H^{1/2}}^2 + \|m_1 - \cos \theta\|_{L^2}^2 \right). \quad (2.19)$$

Our goal is to study the Γ -convergence of energies $\{E_\varepsilon\}$ as $\varepsilon \downarrow 0$ and to characterize the limiting configurations of the magnetization. We will prove that the limiting configurations are piecewise constant functions of bounded total variation that can take two values $\{m^\pm = (\cos \theta, \pm \sin \theta, 0)\}$, i.e., they belong to

$$\mathcal{A} = \left\{ m_0 : \mathbf{R} \rightarrow \{m^\pm\} : \int_{\mathbf{R}} \left| \frac{dm_0}{dx_1} \right| < \infty \right\}.$$

The Γ -limit energy is proportional to the number of jumps of these configurations and the energetic cost of each jump is $\pi(1 - |\cos \theta|)^2/2$; therefore, we define the following energy for any configuration $m_0 \in \mathcal{A}$:

$$E_0(m_0) = \frac{\pi}{2} (1 - |\cos \theta|)^2 \cdot \left(\text{number of jumps of } m_0 \right). \quad (2.20)$$

Theorem 15 *Let $\theta \in (0, \pi)$. Then*

$$E_\varepsilon \xrightarrow{\Gamma} E_0 \text{ under the } L_{loc}^1(\mathbf{R}, S^1)\text{-topology as } \varepsilon \downarrow 0, \text{ i.e.,}$$

(i) (Compactness and lower bound) *If $\{m_\varepsilon : \mathbf{R} \rightarrow S^1\}_\varepsilon$ satisfies*

$$\limsup_{\varepsilon \downarrow 0} E_\varepsilon(m_\varepsilon) < +\infty,$$

then for subsequences ε , there exists $m_0 \in \mathcal{A}$ such that $m_\varepsilon \rightarrow m_0$ in $L^1_{loc}(\mathbf{R}, S^1)$ as $\varepsilon \downarrow 0$ and

$$\liminf_{\varepsilon \downarrow 0} E_\varepsilon(m_\varepsilon) \geq E_0(m_0);$$

(ii) (Upper bound) For every $m_0 \in \mathcal{A}$, there exists a family of smooth functions $\{m_\varepsilon : \mathbf{R} \rightarrow S^1\}_{\varepsilon \downarrow 0}$ such that $m_\varepsilon - m_0$ has compact support in \mathbf{R} for all ε , $m_\varepsilon - m_0 \xrightarrow{\varepsilon \downarrow 0} 0$ in $L^1(\mathbf{R}, \mathbf{R}^2)$ and

$$\lim_{\varepsilon \downarrow 0} E_\varepsilon(m_\varepsilon) = E_0(m_0).$$

Remark 11 Observe that the energy of a Néel wall of angle 2θ is quartic in θ for small angles θ :

$$\min_{(2.14)} E_\varepsilon \stackrel{\varepsilon \downarrow 0}{=} \frac{\pi}{2} (1 - \cos \theta)^2 \approx \frac{\pi}{8} \theta^4 \quad \text{as } \theta \downarrow 0.$$

We mention that the compactness result fails in general under the strict convergence in BV_{loc} even if the limiting configurations are of bounded variation in \mathbf{R} . In fact, it is constructed in [43] a sequence of magnetizations $\{m_\varepsilon\}$ satisfying (2.14) and of uniformly bounded energies $E_\varepsilon(m_\varepsilon) \leq C$ such that the sequence of total variations $\{ \int | \frac{dm_{1,\varepsilon}}{dx_1} | \}$ blows-up.

Remark 12 One could compare Model 1 with the Aviles-Giga model presented in Subsection 1.4.2. We emphasize that Model 1 is more pertinent to micromagnetics by considering a non-local term $|\log \varepsilon| \|m_1\|_{H^{1/2}}^2$ for the energy $E_\varepsilon(m)$ that penalizes non-vanishing divergence configurations m (which are here 1D). That will infer a delicate multi-scale structure of the transition layer in Model 1 comparing to the one-scale transition layers in the Aviles-Giga model. Since the behavior of E_ε is quartic in the wall angle, the entropy method (used for the Aviles-Giga) doesn't apply here. However, we succeed to show that limiting configurations in Model 1 are BV and to deduce the complete Γ -convergence result for our non-local functionals.

Model 2. Confinement of Néel wall tails by the finite size of the sample. The constraints are given by:

$$m : \mathbf{R} \rightarrow S^1 \text{ and } m(\pm x_1) = m^\pm \text{ for } \pm x_1 \geq 1, \quad (2.21)$$

with $\theta \in (0, \pi)$ (see Figure 2.6), whereas the energy functional is:

$$m \mapsto \delta \|m\|_{H^1}^2 + \frac{1}{2} \|m_1\|_{H^{1/2}}^2 \quad (2.22)$$

with $\delta > 0$ a small parameter. It models a one-dimensional magnetization in a thin-ferromagnetic

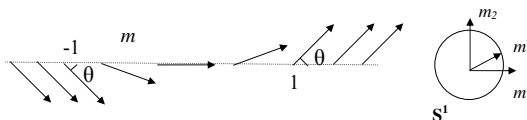


Figure 2.6: Néel wall of angle 2θ confined in $[-1, 1]$.

film of finite width where the effect of crystalline anisotropy and external field is neglected (i.e.,

$Q = 0$ and $H_{ext} = 0$ in (2.8) and the energy rescales as for Model 1). The corresponding variational problem was analyzed in [22], [20], [43]. The main difference with respect to Model 1 consists in the confinement of Néel wall tails by the interaction with the sample edges placed in -1 and 1 in our framework. However, the properties of the transition layer in Model 1 naturally transfer to the structure of the minimizer of (2.22) that satisfies $m(0) = (1, 0)$. It is a two length scale object with a small core of order δ and two logarithmically decaying tails contained in $[-1, 1]$ and it attains the same level of minimal energy $\frac{\pi+o(1)}{2|\log \delta|}$ as $\delta \downarrow 0$. The stability of 180° Néel walls under arbitrary 2D modulation was proved by DeSimone, Knüpfer and Otto [20]. Moreover, we proved in [43] the optimality of the one-dimensional minimizer, i.e., asymptotically, the Néel wall is the unique minimizer of the associated two-dimensional variational problem in the strip Ω' . As before, by rescaling (2.22), the corresponding energy writes:

$$F_\varepsilon(m) = \varepsilon \|m\|_{\dot{H}^1}^2 + \frac{|\log \varepsilon|}{2} \|m_1\|_{\dot{H}^{1/2}}^2 \quad (2.23)$$

for a small parameter $\varepsilon > 0$. We proved in [35] the similar asymptotic of F_ε by the Γ -convergence method as $\varepsilon \downarrow 0$ as in Model 1. The difference will consist in having all the walls confined in the interval $[-1, 1]$.

Model 3. Confinement of Néel wall tails by the neighboring Néel walls. The magnetizations are periodic functions such that:

$$m = e^{i\varphi}, \varphi : \mathbf{R} \rightarrow \mathbf{R} \text{ with } \varphi(x_1 + 2) = \varphi(x_1) \text{ and } \varphi(x_1 + 1) = \varphi(x_1) + \pi \quad (2.24)$$

(see Figure 2.7). The energy is given by:

$$m \mapsto \delta \|m\|_{\dot{H}_{per}^1}^2 + \frac{1}{2} \|m_1\|_{\dot{H}_{per}^{1/2}}^2, \quad (2.25)$$

for a small parameter $\delta > 0$.

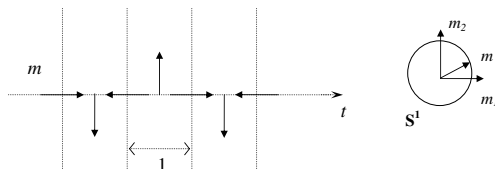


Figure 2.7: Periodic array of winding walls.

This model was investigated by DeSimone, Kohn, Müller and Otto [23] in order to quantify the repulsive interaction of Néel walls. It consists in considering a periodic array of winding walls at a renormalized distance $w = 2$ in the absence of anisotropy and external field. A transition of 180° is enforced in the middle of each period by the constraint (2.24). Therefore, the tails of a Néel wall are limited by the tails of the neighboring walls at a distance $O(1)$ and we expect that this model generates only 180° Néel walls. As before, the following rescaled energy associated to (2.25):

$$G_\varepsilon(m) = \varepsilon \|m\|_{\dot{H}_{per}^1}^2 + \frac{|\log \varepsilon|}{2} \|m_1\|_{\dot{H}_{per}^{1/2}}^2$$

has the same limiting behavior when $\varepsilon \downarrow 0$ as in Model 1.

2.3 360° Néel walls and vortex energy³

360° Néel wall. The aim of the section concerns the special case of 360° Néel walls. For these walls, the magnetization performs a complete rotation across the mesoscopic wall so that it carries a nonzero topological degree. They are characterized by the angle $\alpha \in [0, 2\pi)$ between the mesoscopic direction of the magnetization and the normal direction to the wall (see Figure 2.8). We call these transition layers “360° Néel walls of initial angle α ”. Note that for any mesoscopic Néel wall (with a



Figure 2.8: 360° Néel wall of initial angle α .

wall angle smaller than 360°), the condition to be charge free uniquely determines the initial angle α . For 360° Néel walls, the situation is different: In this case, the condition of being charge-free can be achieved for any initial angle α . Our analysis shows that the initial angle α contributes to the leading order energy of the 360° Néel wall. Another peculiarity of 360° Néel walls (of initial angle $\alpha > 0$) with respect to general Néel walls resides in their internal structure. It consists of two parts with zero magnetic net charge: a first Néel wall of angle $2\pi - 2\alpha$ and a second Néel wall of angle 2α (see Figure 2.8). This means that these two parts only interact by weak dipole–dipole interaction. For this reason the thickness of the 360° Néel wall is much larger than the thickness of the 180° Néel wall. A detailed numerical analysis of the 360° Néel wall, also including the effect of anisotropy and external field, can be found in [61].

The 360° Néel walls we consider in the following are confined by the boundary of the sample (as in Model 2 in Section 2.2). We will assume that the magnetization

$$m = (m_1, m_2) : \mathbf{R} \rightarrow S^1$$

only depends on a single variable $x_1 \in \mathbf{R}$. In this case, the specific one-dimensional energy associated to m in our model reduces to the following expression (see (2.23)):

$$F_\varepsilon(m) = \varepsilon \int_{\mathbf{R}} \frac{1}{1 - m_1^2} \left| \frac{d}{dx_1} m_1 \right|^2 dx_1 + \frac{|\log \varepsilon|}{2} \int_{\mathbf{R}} \left| \frac{d}{dx_1} \right|^{1/2} m_1 \right|^2 dx_1. \quad (2.26)$$

For our analysis of 360° Néel walls, we assume that the initial direction of the magnetization is given by the angle $\alpha \in [0, 2\pi)$ and a complete rotation is imposed by the following condition:

$$m(x_1) = e^{i\alpha} \quad \text{for } |x_1| \geq 1 \quad \text{and} \quad \deg(m) = 1.$$

In other words, using the lifting $m = e^{i\phi}$, the above condition is equivalent to

$$\phi(x_1) = \alpha \quad \text{for } x_1 \leq -1, \quad \phi(x_1) = 2\pi + \alpha \quad \text{for } x_1 \geq 1. \quad (2.27)$$

We finally mention that 360° Néel walls are a commonly observed structure in thin magnetic films, see [32, p. 457]. They typically arise from (global) topological constraints: These can be related

³All the results appearing in this section are part of the article Ignat-Knüpfer [38]. Therefore, we don't specify in the following this reference for each result.

to the geometry of the magnetic sample. As we will show in the second part of this section, the 360° Néel wall is a global minimizing structure for magnetic samples with circular cross-section in a certain regime. Note however that commonly 360° Néel walls occur as metastable states [32].

Our first result concerns the exact leading order energy of a 360° Néel wall with initial angle α .

Theorem 16 *Let $m_\varepsilon : \mathbf{R} \rightarrow S^1$ be a minimizer of (2.26) satisfying (2.27). Then m_ε is a smooth map inside $(-1, 1)$ and its energetic cost is given by*

$$F_\varepsilon(m_\varepsilon) = \pi (1 + \cos^2 \alpha) + o(1) \quad \text{as } \varepsilon \rightarrow 0. \quad (2.28)$$

The result shows that even within the class of 360° Néel walls there is a dependence of the energy with respect to the initial angle α . This result agrees well with a numerical simulation in [61, Fig. 2] where the energetic difference between the two extreme cases $\alpha = 0$ and $\alpha = \pi/2$ by a factor 2 is predicted. Note that we have smoothness in the interior for any critical point of the energy functional (2.26). The main idea for the proof of Theorem 16 is the following: Consider any admissible configuration $m_\varepsilon = (m_{1,\varepsilon}, m_{2,\varepsilon})$ satisfying (2.27) for some given initial angle α . We first prove an optimal lower bound separately for the regions where $m_{1,\varepsilon}$ is larger than $\cos \alpha$ and less than $\cos \alpha$, respectively. These regions correspond to a Néel wall transition of angle $2\pi - 2\alpha$ and 2α , respectively. Then we use the fact that the “interaction” of the nonlocal magnetostatic component of the energy is positive between these two regions.

Vortex induced by 360° Néel wall. Our second goal is to analyze the behavior of a vortex configuration in ultra-thin films of circular cross-section. As we shall explain in the following, a vortex in our model is a very peculiar structure driven by a 360° Néel wall along a radius of a disc, so that the topological degree around the center of the disc is zero. Therefore, it is a completely different configuration than the Bloch line (a structure characteristic of moderately thick ferromagnetic films) or the so called Ginzburg-Landau vortices (characteristic to superconductors) that carry a non-zero topological degree.

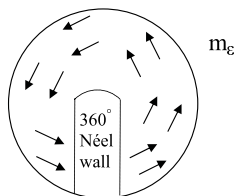


Figure 2.9: Microscopic vortex structure at level ε .

Let us fix the setting: We use the thin-film reduction (2.8) where we will skip \sim . We shall for simplicity ignore the anisotropy and the applied external field (i.e., $Q = 0$ and $H_{ext} = 0$). It is trivial, however, to include a small anisotropy and an appropriately-scaled applied field energy, since Γ -convergence is insensitive to compact perturbations of the functional. We are interested here in ferromagnetic samples of a thin circular film, i.e. $\Omega' = B_\ell$ is the disc of radius ℓ . We use the two dimensionless parameters $\delta = d^2/(t\ell)$ as the size of the core of a Néel wall and $h = t/\ell$ as the aspect ratio of the micromagnetic sample. We focus on the regime of ultra thin-films where $h = h(\delta)$

satisfies (2.12) and the energy scaling is chosen at the level of Néel walls. Rescaling the energy (2.8) by $t^2\ell$, we get the following functional energy over the set of configurations $m : B^2 \rightarrow S^1$:

$$\hat{E}_\delta(m) = \delta \int_{B^2} |\nabla m|^2 dx + \frac{1}{2} \|(\nabla \cdot m)_{ac}\|_{\dot{H}^{-1/2}(\mathbf{R}^2)}^2 + \frac{1}{2\pi} |\log h| \int_{\partial B^2} (m \cdot \nu)^2 d\mathcal{H}^1. \quad (2.29)$$

In this section, we denote the in-plane differential operator by $\nabla = (\partial_{x_1}, \partial_{x_2})$ and since $m \in S^1$, we have $m' \equiv m$ (with $m_3 = 0$). We conjecture that the vortex is asymptotically the minimizer of the above variational problem.

Open Problem 4 *Let $\delta \ll 1$ and let $h = h(\delta)$ satisfying (2.12). If m_δ is a minimizer of (2.29) for $\delta > 0$, then*

$$m_\delta \rightarrow m_0(x) := \frac{x^\perp}{|x|} \quad \text{in } L^2(B^2) \quad \text{and} \quad \lim_{\delta \downarrow 0} |\log \delta| \hat{E}_\delta(m_\delta) = E_0\left(\frac{x^\perp}{|x|}\right),$$

where $E_0\left(\frac{x^\perp}{|x|}\right) = 2\pi$ is the energetic cost (2.28) of a 360° Néel wall with vanishing initial angle $\alpha = 0$.

For the moment, let us simplify the problem by omitting the last term that penalizes the surface charges in (2.29). (We will discuss later the general context of Open Problem 4.) The analysis is based on the following renormalization of two-dimensional micromagnetic energy (already mentioned at Remark 5 in Chapter 1):

$$E_\varepsilon(m) = \varepsilon \int_{B^2} |\nabla m|^2 dx + \frac{|\log \varepsilon|}{2} \int_{\mathbf{R}^2} \left| |\nabla|^{-1/2} (\nabla \cdot m)_{ac} \right|^2 dx, \quad (2.30)$$

where ε is a rescaled small parameter corresponding to the Néel core given by

$$\delta = \varepsilon / |\log \varepsilon| > 0.$$

Our viewpoint is based on the method of Γ -convergence: We enforce the formation of a vortex in the limit $\varepsilon \rightarrow 0$ by considering families $\{m_\varepsilon\}_{\varepsilon > 0}$ of magnetizations that satisfy

$$m_\varepsilon \rightarrow \frac{x^\perp}{|x|} \quad \text{in } L^2(B^2) \quad \text{as } \varepsilon \rightarrow 0 \quad (2.31)$$

and we define the energy of the vortex by the following relaxed problem:

$$E_0\left(\frac{x^\perp}{|x|}\right) = \inf \left\{ \liminf_{\varepsilon \rightarrow 0} E_\varepsilon(m_\varepsilon) : \{m_\varepsilon\} \text{ satisfies (2.31)} \right\}. \quad (2.32)$$

Indeed, the infimum in (2.32) is achieved (and non-trivial). We call a minimizing family, every family $\{m_\varepsilon\}$ that satisfies (2.31) and achieves the minimum (2.32), i.e. $\lim_{\varepsilon \rightarrow 0} E_\varepsilon(m_\varepsilon) = E_0\left(\frac{x^\perp}{|x|}\right)$. The L^2 -compactness of uniformly bounded energy configurations has been proved in [43].

Note that the minimal level of energy E_ε is trivial and all minima are constant since (2.30) does not penalize surface charges $m \cdot \nu \neq 0$ on ∂B^2 (which is the case of (2.29)). In fact, every finite energy configuration $E_\varepsilon(m) < \infty$ does have surface charges on ∂B^2 and zero winding number on each closed curve in B^2 . For this reason, the two constraints of having a degree 1 and the absence of surface charges can only be imposed in the limit $\varepsilon \rightarrow 0$ (as in (2.31)). Our analysis shows that

asymptotically the vortex state represents the minimum energy E_ε under the constraint (2.31). We conjecture that the vortex is still a minimizer if constraint (2.31) is relaxed and convergence is only assumed on the boundary ∂B^2 (i.e., $m_\varepsilon \rightarrow x^\perp$ in $L^2(\partial B^2)$ as $\varepsilon \rightarrow 0$); this is of course a weaker conjecture than Open Problem 4.

The main result characterizes asymptotically the energy of the vortex:

Theorem 17 *Let $\{m_\varepsilon\}$ be a minimizing family in (2.32). Then we have*

$$E_\varepsilon(m_\varepsilon) = 2\pi + o(1) \quad \text{as } \varepsilon \rightarrow 0,$$

so that $E_0(x^\perp/|x|) = 2\pi$.

Note that this result includes the precise leading constant of the minimal energy. Our construction for the upper bound of the energy is based on the inclusion of a 360° Néel wall of initial angle 0 along a radius of the disc (see Figure 2.9). On the other hand, we prove the lower bound of a vortex in a slightly more general context. More precisely, as in [43], we consider localized stray-fields $H : B^3 \rightarrow \mathbf{R}^3$ determined by static Maxwell's equation in the weak sense: For all $\zeta \in C_c^\infty(B^3)$,

$$\int_{B^3} H \cdot \left(\nabla, \frac{\partial}{\partial z} \right) \zeta \, dx dz = \int_{B^2} \nabla \cdot m \, \zeta \, dx, \quad (2.33)$$

where $B^3 \subset \mathbf{R}^3$ is the unit ball in \mathbf{R}^3 and we define the localized micromagnetic energy

$$E_\varepsilon^{loc}(m, H) = \varepsilon \int_{B^2} |\nabla m|^2 \, dx + |\log \varepsilon| \int_{B^3} |H|^2 \, dx dz.$$

Obviously, by (2.9), $E_\varepsilon^{loc}(m, \nabla u_{ac}) \leq E_\varepsilon(m)$ (since E_ε^{loc} counts the stray-field energy only inside the ball B^3). We prove the following estimate for the localized energy:

Theorem 18 *Let $\{m_\varepsilon\}$ be a family satisfying (2.31) and let $H_\varepsilon : B^3 \rightarrow \mathbf{R}^3$ be localized stray-fields associated to m_ε by (2.33). Then we have*

$$E_\varepsilon^{loc}(m_\varepsilon, H_\varepsilon) \geq 2\pi + o(1) \quad \text{as } \varepsilon \rightarrow 0.$$

Crucial for the estimate of the lower bound is the control of the localized stray-field energy. The main idea resides in a dynamical system argument combined with localized interpolation inequalities similar to (2.16). Since the stray-field energy is created by $\nabla \cdot m_\varepsilon$, by Stokes theorem this implies a control for the net flow of m_ε across the boundary of any subdomain of B^2 . The first step of the proof consists in finding such a domain with maximal net flow; as in [20, 43], we consider the flow generated by the vector field m_ε^\perp . Using Stokes theorem, this yields the optimal lower bound for the energy in some particular cases. To get to the general result, a careful analysis is carried out on a partition in small annuli of the domain B^2 by balancing two effects: rotation versus the length of orbits of the flow.

Discussion on Open Problem 4. While we cannot rigorously prove Open Problem 4, we would like to compare the vortex with the typical counter-candidate observed in thin ferromagnetic discs, the so called S -state (see [32]). We show that the vortex has asymptotically lower energy than the

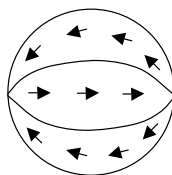


Figure 2.10: S-state.

S -state (see Figure 2.10), thus indicating that the vortex might be indeed global minimizer of the energy. Recall that the vortex corresponds to the viscosity solution of the domain B^2 , i.e.

$$m_0(x) = \nabla^\perp \text{dist}(x, \partial B^2).$$

In our regime, the asymptotic cost of a vortex follows by Theorem 17:

$$E_0(m_0) = 2\pi.$$

The limit configuration of the S -state is represented at the mesoscopic level by

$$S(x) = \begin{cases} \nabla^\perp \text{dist}(x, \partial B_+^2) & \text{if } x \in B_+^2, \\ -\nabla^\perp \text{dist}(x, \partial B_-^2) & \text{if } x \in B_-^2, \end{cases}$$

where $B_\pm^2 = \{x \in B^2 : \pm x_2 \geq 0\}$ are the upper (resp. lower) half-discs (see Figure 2.10). Let γ be the jump set of the S -state, i.e.

$$\gamma = \gamma^+ \cup \gamma^- \quad \text{and} \quad \gamma^\pm(x_1) = (x_1, \pm \frac{1-x_1^2}{2}) \text{ with } x_1 \in (-1, 1).$$

In fact, if we denote by S^\pm the traces of S on γ , one has $S^-(x) = (1, 0)$ and $S^+(x) = \pm \frac{x^\perp}{|x|}$ for $x \in \gamma^\pm$. So, the angle of the jump θ (given by $S^+ = e^{i\theta} S^-$) increases on γ^\pm from 90° to 270° . Furthermore, we denote the corresponding asymptotic energy density of a Néel wall connecting the directions S^+ and S^- by $e(S^+, S^-) = \frac{\pi}{2}(1 - \cos \frac{\theta}{2})^2$. Then

$$E_0(S) = \int_\gamma e(S^+, S^-) d\mathcal{H}^1.$$

Therefore, one computes:

$$\int_\gamma e(S^+, S^-) d\mathcal{H}^1 = 2 \int_{\gamma^+} e(S^+, S^-) d\mathcal{H}^1 = 2\sqrt{2}\pi > E_0(m_0).$$

The above computation shows that the S -state is asymptotically less favorable than the vortex state in the regime (2.12). It is an open question to rigorously prove that the vortex state indeed is the global minimizer over all planar configurations of (2.29).

2.4 Landau state ⁴

In this section, we investigate a common pattern of the magnetization in thin ferromagnetic films (the Landau state), that corresponds to the global minimizer of the micromagnetic energy in the

⁴All the results appearing in this section are part of the article Ignat-Otto [44]. Therefore, we don't specify in the following this reference for each result.

regime (2.13). For that, we focus on a toy problem rather than on the full physical model: We use the thin-film reduction (2.8) and for simplicity, we ignore the anisotropy and the applied external field (i.e., $Q = 0$ and $H_{ext} = 0$). So, let $\Omega \subset \mathbf{R}^2$ be a bounded simply-connected domain with a $C^{1,1}$ boundary corresponding to the horizontal section of a ferromagnetic cylinder of small thickness. We consider magnetizations that are invariant in the out-of-plane variable, i.e.,

$$m = (m_1, m_2, m_3) : \Omega \rightarrow S^2$$

and they are tangent to the boundary $\partial\Omega$, i.e.,

$$m' \cdot \nu = 0 \quad \text{on } \partial\Omega, \quad (2.34)$$

where $m' = (m_1, m_2)$ is the in-plane component of the magnetization and ν is the normal outer unit vector to $\partial\Omega$. The assumption (2.34) is not compatible with our regime (2.13) when analyzing the minimal energy since metastable states of the magnetization under the restriction (2.34) are not minimizers of (2.8). Scaling the energy at order of td^2 , the reduced energy (2.8) can be written as the following functional:

$$E_{\eta,\delta}(m) = \int_{\Omega} |\nabla m|^2 dx + \frac{1}{\eta^2} \int_{\Omega} m_3^2 dx + \frac{1}{2\delta} \int_{\mathbf{R}^2} \|\nabla\|^{-1/2} (\nabla \cdot m')^2 dx,$$

where $\eta = d/\ell$ and $\delta = d^2/(t\ell)$ are two small positive parameters (standing for the size of the Bloch line core and the Néel wall core, respectively). Here, $x = (x_1, x_2)$ are the in-plane variables with the differential operator $\nabla = (\partial_{x_1}, \partial_{x_2})$. In this section, we will always think of

$$m' \equiv m' \mathbf{1}_{\Omega}$$

as being extended by 0 outside Ω . Observe that the boundary condition (2.34) is necessary so that the homogeneous $\dot{H}^{-1/2}$ -seminorm of $\nabla \cdot m'$ is finite since

$$\nabla \cdot m' = (\nabla \cdot m') \mathbf{1}_{\Omega} + (m' \cdot \nu) \mathbf{1}_{\partial\Omega} \quad \text{in } \mathbf{R}^2.$$

We are interested in the asymptotic behavior of minimizers of the energy $E_{\eta,\delta}$ in the regime

$$\eta \ll 1 \quad \text{and} \quad \delta \ll 1.$$

The characteristic singular patterns expected in this context are the Néel walls together with topological defects (due to (2.34)) standing for interior vortices (the Bloch lines) or "half" Bloch lines at the boundary. Recall that the energy $E_{\eta,\delta}$ per unit length of a Néel wall of angle 2θ (with $\theta \in (0, \frac{\pi}{2}]$) is given by:

$$\frac{\pi(1 - \cos \theta)^2 + o(1)}{2\delta |\log \delta|} \quad \text{as } \delta \rightarrow 0, \quad (2.35)$$

(see (2.20)). The formation of interior or boundary vortices is explained by the competition between the exchange energy and the penalization of the m_3 -component for configurations tangent at the boundary. Indeed, there is no S^1 -configuration that is of finite exchange energy and satisfies (2.34). There are only two possible situations:

- If m' does not vanish on $\partial\Omega$, then (2.34) implies that m' carries a nonzero topological degree, $\deg(m', \partial\Omega) = \pm 1$. In this case, we expect the nucleation of an interior vortex of core-scale η (i.e.,

Bloch line in the micromagnetic jargon). The scaling of the vortex energy is related to the minimal Ginzburg-Landau (GL) energy (see Bethuel, Brezis & Helein [7]):

$$\min_{\substack{m' \in H^1(\Omega, \mathbf{R}^2) \\ m' = \nu^\perp \text{ on } \partial\Omega}} \int_{\Omega} g_\eta(m') \, dx = (2\pi + o(1)) |\log \eta| \quad \text{as } \eta \rightarrow 0, \quad (2.36)$$

where the GL density energy is given in the following:

$$g_\eta(m') = |\nabla m'|^2 + \frac{1}{\eta^2} (1 - |m'|^2)^2. \quad (2.37)$$

- The second situation consists in having zeros of m' on the boundary. Therefore, we expect that GL boundary vortices do appear. Roughly speaking, they correspond to "half" of an interior vortex where the vector field m' is tangent at the boundary and vanishes at the core; therefore they are different from the micromagnetic boundary vortices that take values into S^1 , so they never vanish. Remark the importance of the regularity of $\partial\Omega$ in estimate (2.36). In fact, if $\partial\Omega$ has a corner and the boundary condition $m' = \nu^\perp$ on $\partial\Omega$ in (2.36) is relaxed to (2.34), then estimate (2.36) does not hold anymore, it depends on the angle of the corner. Therefore, at the microscopic level, topological point defects do appear in the Landau state pattern and are induced by (2.34).

The aim of the section is to show compactness of magnetizations energetically $E_{\eta,\delta}$ close to the Landau state in order to rigorously justify the limit behavior (2.11): the delicate issue consists in having the constraint $|m| = 1$ conserved in the limit. For that, we have to evaluate the energetic cost of the Landau state. We expect that the leading order energy of a Landau state is given by the topological point defects and Néel walls. The Landau state configuration consists in several Néel walls and either one interior Bloch line or two "half" Bloch lines placed at the boundary of the sample Ω . Therefore, by (2.35) and (2.36), we expect that the energy of the Landau state has the following order:

$$2\pi |\log \eta| + \frac{A}{\delta |\log \delta|}, \quad (2.38)$$

for some positive $A > 0$ depending on the length and angle of Néel walls.

Main results. First of all, we want to rigorously prove the upper bound (2.38) for the Landau state. Our result gives the exact leading order energy of the Landau state in the case of a stadium domain Ω (see Figure 1.6). Note that the Landau state of a stadium consists in a single Néel wall of 180° around the jump set of the viscosity solution (in our example, the length of the wall is equal to $2L$, so that by (2.35), $A = \pi L$ in (2.38)).

Theorem 19 *Let Ω be a stadium domain (as in Figure 1.6). In the regime $\eta \ll \delta \ll 1$, there exists a C^1 vector field $m_{\eta,\delta} : \Omega \rightarrow S^2$ that satisfies (2.34) and*

$$E_{\eta,\delta}(m_{\eta,\delta}) \leq 2\pi |\log \eta| + \frac{\pi L + o(1)}{\delta |\log \delta|} \quad \text{as } \delta \downarrow 0. \quad (2.39)$$

Observe that the vortex energy in the above estimate is relevant only if its energy costs at least as much as a Néel wall, i.e., $\frac{1}{\delta |\log \delta|} \lesssim |\log \eta|$ (otherwise, the vortex energy would be absorbed by the term $o(\frac{1}{\delta |\log \delta|})$). This regime leads to a size η of the vortex core exponentially smaller than the size δ of the Néel wall core (see Remark 13).

Now we state our main result on the compactness of the S^2 -valued magnetizations that have energies near the Landau state. The issue consists in rigorously justifying that the constraint $|m| = 1$ is conserved by the limit configurations as $\eta, \delta \rightarrow 0$. The regime where we prove our result corresponds to the case where a topological defect is energetically more expensive than the Néel wall:

Theorem 20 *Let $\alpha \in (0, \frac{1}{2})$ be an arbitrary constant. We consider the following regime between the small parameters $\eta, \delta \ll 1$:*

$$\eta^{1/2} \lesssim \delta, \quad (2.40)$$

$$\log |\log \eta| \lesssim \frac{1}{\delta |\log \delta|}. \quad (2.41)$$

For each η and δ , we consider C^1 vector fields $m_{\eta, \delta} : \Omega \rightarrow S^2$ that satisfy (2.34) and

$$E_{\eta, \delta}(m_{\eta, \delta}) - 2\pi |\log \eta| \quad \left\{ \begin{array}{l} \leq 2\pi\alpha |\log \eta| \\ \lesssim \frac{1}{\delta |\log \delta|} \end{array} \right. \quad (2.42)$$

$$\lesssim \frac{1}{\delta |\log \delta|} \quad (2.43)$$

Then the family $\{m_{\eta, \delta}\}_{\eta, \delta \downarrow 0}$ is relatively compact in $L^2(\Omega, S^2)$ and any accumulation point $m : \Omega \rightarrow S^2$ satisfies

$$m_3 = 0, \quad |m'| = 1 \text{ a.e. in } \Omega \quad \text{and} \quad \nabla \cdot m' = 0 \text{ distributionally in } \mathbf{R}^2. \quad (2.44)$$

The proof of compactness is based on an argument of approximating S^2 -valued vector fields by S^1 -valued vector fields away from a small defect region. This small region consists in either one interior vortex or two boundary vortices. The detection of this region is done in Theorem 21 below and uses some topological methods due to Jerrard [47] and Sandier [68] for the concentration of the Ginzburg-Landau energy around vortices (see also Lin [53], Sandier & Serfaty [70]). Away from this small region, the energy level *only* allows for line singularities. Therefore, the compactness result for S^1 -valued vector fields in [43] applies.

Let us discuss the assumptions (2.40), (2.41), (2.42) & (2.43). Inequality (2.43) assures that cutting out the topological defect (one vortex or two boundary vortices), the remaining energy rescaled at the energetic level of Néel walls is uniformly bounded. Inequality (2.42) together with the choice of $\alpha < \frac{1}{2}$ mean that the energy cannot support three "half" vortices and is precisely explained in Theorem 21 below. Inequality (2.41) is imposed due to our method to detect a boundary vortex: it leads to a loss of energy of order $O(\log |\log \eta|)$ with respect to the expected half energy $\pi |\log \eta|$ of an interior vortex (see Theorem 21 and Proposition 15). This amount of energy could leave room for configurations of Néel walls that may destroy the compactness of $|m'| = 1$. Therefore, to avoid this scenario, (2.41) is imposed. The regime (2.40) is rather technical: it is needed in the approximation argument of S^2 -valued vector fields by S^1 -valued vector fields away from the vortex balls. In fact, starting from the values of m' on a square grid of size η^β , the S^1 -approximation argument requires zero degree of m' on each cell, leading to the condition $\beta < 1 - \alpha$; furthermore, the condition $\eta^\beta \lesssim \delta$ is needed in order that the approximating S^1 -valued vector fields induce a stray-field energy of the same order of m' . Therefore, (2.40) can be improved to a larger regime

$$\eta^\beta \lesssim \delta \quad \text{for any} \quad \beta < 1 - \alpha$$

(Theorem 20 is stated for the value $\beta = 1/2$ which is the universal choice for every $\alpha < 1/2$). However, this slightly improved condition is weaker than the complete regime implied by (2.42) as explained in the following remark.

Remark 13 Any limit configuration m' satisfies (2.44). If Ω is a bounded simply-connected domain different than discs, m' has at least one ridge (line-singularity) that corresponds to a Néel wall. Therefore, the minimal energy verifies $\min_{(2.34)} E_{\eta,\delta} - 2\pi|\log \eta| \gtrsim \frac{1}{\delta|\log \delta|}$. Combining with (2.42), it follows that

$$\frac{1}{\delta|\log \delta|} \lesssim |\log \eta|;$$

in particular, $\eta \lesssim e^{-\frac{1}{\delta|\log \delta|}}$, i.e., the core of the vortex is exponentially smaller than the core of the Néel wall. However, in the proof of Theorem 20, this much stronger constraint with respect to (2.40) is not needed.

We prove the following result of the concentration of Ginzburg-Landau energy around one interior vortex or two boundary vortices for vector fields tangent at the boundary:

Theorem 21 *Let $\alpha \in (0, \frac{1}{2})$ and $\Omega \subset \mathbf{R}^2$ be a bounded simply-connected domain with a $C^{1,1}$ boundary. Then there exists $\eta_0 = \eta_0(\alpha, \partial\Omega) > 0$ such that for every $0 < \eta < \eta_0$, if $m' : \Omega \rightarrow \overline{B^2}$ is a C^1 vector field that satisfies (2.34) and*

$$\int_{\Omega} g_{\eta}(m') dx \leq 2\pi(1 + \alpha)|\log \eta|, \quad (2.45)$$

then there exists either a ball $B(x_1^, r^*) \subset \Omega$ (called vortex ball) with $r^* = \frac{1}{|\log \eta|^3}$ and*

$$\int_{B(x_1^*, r^*)} g_{\eta}(m') dx \geq 2\pi \left| \log \frac{r^*}{\eta} \right| - C, \quad (2.46)$$

or two balls $B(x_2^, r^*)$ and $B(x_3^*, r^*)$ (called boundary vortex balls) with $x_2^*, x_3^* \in \partial\Omega$ and*

$$\int_{(B(x_2^*, r^*) \cup B(x_3^*, r^*)) \cap \Omega} g_{\eta}(m') dx \geq 2\pi \left| \log \frac{r^*}{\eta} \right| - C, \quad (2.47)$$

where $C = C(\alpha, \partial\Omega) > 0$ is a constant depending only on α and on the geometry of $\partial\Omega$.

The condition $\alpha < 1/2$ is essential in our proof. In fact, if no topological defect exists in the interior (in which case, condition (2.34) induces boundary vortices), we perform a mirror-reflection extension of m' outside the domain. Roughly speaking, the GL energy in the extended domain doubles, i.e., it is of order $2\pi(2 + 2\alpha)|\log \eta|$ and the topological degree at the new boundary is equal to two; in order to avoid the formation of three interior vortices in the extended region, we should impose $2 + 2\alpha < 3$, i.e., $\alpha < 1/2$.

Observe that the Ginzburg-Landau energy concentration for a boundary vortex in (2.47) has a cost of order $\pi|\log \eta| - C \log |\log \eta|$ provided that the boundary has regularity $C^{1,1}$. We conjecture that the same energetic cost for a boundary vortex holds true if the boundary has regularity $C^{1,\beta}$, $\beta \in (0, 1)$. However, if the boundary regularity is only C^1 , then the energetic cost of a boundary vortex may decrease to $(\pi - \frac{C}{\log |\log \eta|})|\log \eta|$ where $C > 0$ is a universal constant. This indicates that the loss of energy of order $\log |\log \eta|$ in (2.47) could occur for boundary vortices in $C^{1,\beta}$ -domains and the order of this energy loss increases to $\frac{|\log \eta|}{\log |\log \eta|}$ for C^1 boundaries as $\beta \rightarrow 0$. This claim is supported by the following example for a C^1 boundary domain:

Proposition 15 *We consider in polar coordinates the following C^1 domain $\Omega = \{(r, \theta) : r \in (0, \frac{1}{20}), |\theta| < \gamma(r) = \frac{\pi}{2} - \frac{1}{\log \log \frac{1}{r}}\}$. For every $0 < \eta < 1$, there exists a C^1 -function $m'_\eta : \Omega \cap B_{1/200} \rightarrow \mathbf{R}^2$ that satisfies (2.34) on $\partial\Omega \cap B_{1/200}$ and*

$$\int_{\Omega \cap B_{1/200}} g_\eta(m'_\eta) dx \leq (\pi - \frac{C}{\log |\log \eta|}) |\log \eta|,$$

where $C > 0$ is some universal positive constant (independent of η).

2.5 Boundary vortices ⁵

In this section, we analyze a special thin-film regime where boundary vortices appear. We will assume small aspect ratio, i.e. $h = t/\ell \ll 1$ and that the Néel walls have a large core $\delta = d^2/(t\ell)$, i.e.,

$$\delta \gg 1 \quad \text{or} \quad \delta = O(1),$$

which is the opposite context with respect to the ordering presented in Subsection 2.1.2.

a) The regime of very small films, characterized by

$$\delta \gg |\log h|$$

was considered by Kohn-Slastikov [49] with the scaling law of minimal energy chosen at the order of $t^2\ell |\log h|$. (In this regime, Néel walls and boundary vortices are not contained by the sample). Then the exchange term in the energy dominates completely (since rescaling by $t^2\ell |\log h|$, its coefficient in (2.8) is equal to $\delta/|\log h| \gg 1$) and the magnetization becomes an in-plane constant vector field. The corresponding reduced energy (in the sense of Γ -convergence) was derived in [49] and is related to earlier work of Carbou [15]. Their result shows that the nonlocal stray-field energy (2.7) reduces to a local contribution of the boundary $\int_{\partial\Omega'} (m' \cdot \nu)^2 d\mathcal{H}^1$.

b) Slightly larger films, where

$$\delta = \alpha |\log h|$$

with $0 < \alpha < \infty$ and the minimal energy scales as $t^2\ell |\log h|$ were also studied by Kohn-Slastikov [49]. In this context, Néel walls are not contained by the sample, while boundary vortices have a core size of order $O(1)$. Since in this regime Bloch lines have higher cost than boundary vortices, the limiting magnetizations are still required to be in-plane

$$m' : \Omega' \subset \mathbf{R}^2 \rightarrow S^1,$$

but no longer need to be constant. Instead, the exchange energy and the boundary contribution compete, and the rescaled energy E^{3D} (at the order of $t^2\ell |\log h|$) Γ -converges to

$$E^{2D}(m') = \alpha \int_{\Omega'} |\nabla m'|^2 dx + \frac{1}{2\pi} \int_{\partial\Omega'} (m' \cdot \nu)^2 d\mathcal{H}^1.$$

A second limit, describing the behavior of $\frac{1}{\alpha} E^{2D}$ when $\alpha \rightarrow 0$, was examined by Kurzke [52, 51]. As there is no $m' \in H^1(\Omega', S^1)$ that satisfies $m' \cdot \nu = 0$ on $\partial\Omega'$ for simply-connected bounded

⁵All the results appearing in this section are part of the article Ignat-Kurzke [39]. Therefore, we don't specify in the following this reference for each result.

domains Ω' , the limit is characterized by *boundary vortices*, whose interaction is governed by a (local) renormalized energy.

c) The case where $\delta = O(1)$ was studied by Moser [58, 59] when the minimal energy scaling is at order of $\log |\log h|$. Here, all three patterns (Néel walls, boundary vortices, Bloch lines) are contained by the sample and the ordering is given by

$$E^{2D}(\text{Néel wall}) \ll E^{2D}(\text{Boundary vortex}) \ll E^{2D}(\text{Bloch line}),$$

as in regime (iii) in Subsection 2.1.2. Due to the scaling law of the energy of $O(\log |\log h|)$, both the stray-field (represented by the lateral surface charges) and exchange terms survive in the limit. The balance between these terms produces boundary vortices. The corresponding vortex interaction is nonlocal here, in contrast to the local renormalized energy in [51].

Model. The aim of this section is to show the existence of a boundary vortex regime with purely exchange-driven and local vortex interaction. To do so, we show that the double limit in [49] and [51] can be replaced by a direct approach. The context is the following: our regime is given by

$$1 \ll \delta \ll |\log h|.$$

Here, the Néel wall is not contained by the sample, but boundary vortices and Bloch lines may nucleate knowing that a boundary vortex energetically costs less than a Bloch line. The scaling law of the minimal energy is chosen at the level of a boundary vortex, i.e., $O(d^2 t |\log \kappa|)$ where we recall that $\kappa = d^2/(t\ell \log(\ell/t))$. Therefore, our regime is equivalent with the assumption $h \ll 1$ and $\frac{1}{|\log h|} \ll \kappa = \kappa(h) \ll 1$. The full energy E^{3D} (in the absence of anisotropy and external field) will be rescaled as

$$E_h(m_h) = \frac{1}{h|\log \kappa|} \int_{\Omega_h} |\nabla m_h|^2 dx + \frac{1}{\eta^2 h |\log \kappa|} \int_{\mathbf{R}^3} |\nabla U_h|^2 dx, \quad (2.48)$$

where

$$\Omega_h = \Omega' \times (0, h)$$

is the rescaled sample and $\Omega' \subset \mathbf{R}^2$ is a $C^{1,\alpha}$ domain with $\text{diam } \Omega' = 1$. (Here, the core of the Bloch line η can be written in function of the aspect ratio h and the boundary vortex core κ as $\eta^2 = \kappa h |\log h|$.) We highlight the fact that here we consider the full model, i.e., we don't assume invariance of magnetization in the vertical direction x_3 . The rescaled configurations $m_h(x) = m(\ell x)$ and the stray-field potential $U_h(x) = \frac{1}{\ell} U(\ell x)$ satisfy

$$m_h : \Omega_h \rightarrow S^2, \quad \Delta U_h = \nabla \cdot (m_h \mathbf{1}_{\Omega_h}) \quad \text{in } \mathbf{R}^3. \quad (2.49)$$

Our goal is to derive the reduced model as $h \rightarrow 0$ (in the sense of Γ -convergence). Let us first discuss the compactness issue for uniformly bounded energy configurations m_h that yields the correct topology of Γ -convergence. It consists in regarding for averaged magnetization (in x_3 -component):

$$\bar{m}_h(x') = \frac{1}{h} \int_0^h m_h(x', x_3) dx_3, \quad x' = (x_1, x_2) \in \Omega'.$$

Then $\bar{m}_h \in H^1(\Omega', \bar{B}^3)$ and the trace of \bar{m}_h on $\partial\Omega'$ belongs to $H^{1/2}(\Omega', \bar{B}^3)$. We will prove relative compactness of $\{\bar{m}_h\}_h$ at the boundary $\partial\Omega'$ in $L^2(\partial\Omega')$ where the limiting configurations m_0 belong

to $BV(\partial\Omega', S^1)$. Moreover, the boundary Jacobians associated to the in-plane vector field \bar{m}'_h on the boundary $\partial\Omega'$ are uniformly bounded measures.

Boundary Jacobian. This notion is defined as follows: for every $\bar{m}'_h \in H^1(\Omega', \mathbf{R}^2)$, we denote the (usual) jacobian of \bar{m}'_h by

$$\text{jac}(\bar{m}'_h) = \frac{1}{2} \nabla \times (\bar{m}'_h \wedge \nabla \bar{m}'_h) = \partial_{x_1} \bar{m}'_h \wedge \partial_{x_2} \bar{m}'_h \in L^1(\Omega').$$

We call *boundary jacobian*, the operator $D : H^1(\Omega', \mathbf{R}^2) \rightarrow (C^{0,1})^*(\bar{\Omega}')$ defined as

$$\int_{\Omega'} D(\bar{m}'_h) \zeta \, dx' := \int_{\Omega'} \left(2 \text{jac}(\bar{m}'_h) \zeta + \bar{m}'_h \wedge \nabla \bar{m}'_h \cdot \nabla^\perp \zeta \right) dx', \quad \text{for every } \zeta \in C^{0,1}(\bar{\Omega}').$$

It is a continuous operator and

$$\int_{\Omega'} D(\bar{m}'_h) \zeta \, dx' = \int_{\partial\Omega'} \bar{m}'_h \wedge \partial_\tau \bar{m}'_h \zeta \, d\mathcal{H}^1 \quad \text{if } \bar{m}'_h \in C^1(\bar{\Omega}', \mathbf{R}^2). \quad (2.50)$$

Note that $D(\bar{m}'_h)$ acts only on the boundary $\partial\Omega'$ (which has a natural meaning whenever $\bar{m}'_h \in C^1(\bar{\Omega}')$). Indeed, by density of $C^1(\bar{\Omega}')$ in $H^1(\Omega', \mathbf{R}^2)$ and the continuity of the operator D over $H^1(\Omega', \mathbf{R}^2)$, it means that D can be seen as an operator on the boundary acting on $H^{1/2}(\partial\Omega', \mathbf{R}^2)$ which gives a meaning of the RHS of (2.50) if $\bar{m}'_h \in H^{1/2}(\partial\Omega', \mathbf{R}^2)$.

Vorticity and renormalized energy. We expect that the limiting measure of $\{D(\bar{m}'_h)\}_{h \downarrow 0}$ is the vorticity measure

$$J_0 = \pi \sum_{j=1}^N d_j \delta_{a_j}, \quad (2.51)$$

carried by the boundary vortices $a_j \in \partial\Omega'$ of "degree" $d_j \in \mathbb{Z}$ satisfying $\sum_{j=1}^N d_j = 2$. A boundary vortex a_j of "degree" $d_j \in \mathbb{Z}$ corresponds to a jump of size $d_j \pi$ in the lifting of the limit magnetization m_0 . More precisely, we introduce a lifting $\psi : \partial\Omega' \rightarrow \mathbf{R}$ of the tangent vector $\tau = e^{i\psi}$ on $\partial\Omega'$ such that ψ is continuous on $\partial\Omega'$ except on a jump point with the size of the jump equal to 2π (after a complete turn on $\partial\Omega'$). This explains the above constraint $\sum_j d_j = 2$. The limit magnetization $m_0 = e^{i\varphi_0}$ belongs to $BV(\partial\Omega', S^1)$ and has the property that $\psi - \varphi_0$ is a piecewise constant function with values into $\pi\mathbb{Z}$, so that the total variation of $\psi - \varphi_0$ coincides with the mass of the vorticity measure:

$$J_0 = \partial_\tau(\psi - \varphi_0) \text{ on } \partial\Omega' \quad \text{and} \quad \|J_0\|_{\mathcal{M}(\partial\Omega')} = \int_{\partial\Omega'} |\partial_\tau(\psi - \varphi_0)| = \pi \sum_{j=1}^N |d_j|.$$

This result is very similar to the Ginzburg-Landau type functionals, the difference here residing in the concentration of the jacobian on the boundary rather than at the interior of the domain. Similar to [7], we define the solution V of the inhomogeneous Neumann problem:

$$\begin{cases} \Delta V = 0 & \text{in } \Omega', \\ \frac{\partial V}{\partial \nu} = \partial_\tau \psi - J_0 & \text{on } \partial\Omega', \end{cases}$$

and let $R \in C(\bar{\Omega}')$ be the continuous harmonic function in Ω' given by

$$R(x') := V(x') - \sum_{j=1}^N d_j \log|x' - a_j|, \quad x' \in \Omega'.$$

The renormalized energy corresponding to $\{(a_j, d_j)\}$ is defined as follows:

$$W\left(\{(a_j, d_j)\}\right) = -\pi \sum_{1 \leq i < j \leq N} d_i d_j \log |a_i - a_j| + \frac{1}{2} \int_{\partial\Omega'} V \partial_\tau \psi - \frac{\pi}{2} \sum_{j=1}^N d_j R(a_j).$$

Main result. We prove the following Γ -convergence result:

Theorem 22 *Assume that $h \ll 1$ and let $\kappa = \kappa(h)$ be such that $\frac{1}{|\log h|} \ll \kappa \ll 1$.*

1) (Compactness and lower bound) *If $m_h : \Omega_h \rightarrow S^2$ is a sequence of magnetizations such that*

$$\limsup_{h \rightarrow 0} E_h(m_h) < \infty,$$

then for a subsequence, the x_3 -averaged magnetizations $\bar{m}_h \rightarrow m_0 = e^{i\varphi_0}$ in $L^2(\partial\Omega')$ where $\psi - \varphi_0 \in BV(\partial\Omega', \pi\mathbb{Z})$ and averaged boundary Jacobians $\{D(\bar{m}'_h)\}_{h \downarrow 0}$ converge to a vorticity measure $J_0 = \partial_\tau(\psi - \varphi_0)$ of the form (2.51). The energy satisfies the following lower bound:

$$\liminf_{h \rightarrow 0} E_h(m_h) \geq \|J_0\|_{\mathcal{M}(\partial\Omega')}.$$

Furthermore, if the "degrees" d_j belong to $\{\pm 1\}$ for every $1 \leq j \leq N$, then we have the following optimal lower bound at the second order of the energy:

$$\liminf_{h \rightarrow 0} |\log \kappa| (E_h(m_h) - \|J_0\|_{\mathcal{M}(\partial\Omega')}) \geq W(\{a_j, d_j\}) + \gamma_0 \|J_0\|_{\mathcal{M}(\partial\Omega')},$$

where $\gamma_0 = 1 - \log 2$ and W is the renormalized energy defined above.

2) (Upper bound) *Given a configuration of disjoint boundary points $a_j \in \partial\Omega'$ and $d_j \in \mathbb{Z}$ with $\sum_{j=1}^N d_j = 2$, there exists a family of magnetizations $m_h : \Omega_h \rightarrow S^2$ such that the averaged magnetizations $\bar{m}_h \rightarrow m_0 = e^{i\varphi_0}$ in $L^2(\partial\Omega')$ where $\partial_\tau \varphi_0 = \partial_\tau \psi - J_0$ and the boundary Jacobians $\{D(\bar{m}'_h)\}_{h \downarrow 0}$ converge to the vorticity measure J_0 and*

$$\lim_{h \rightarrow 0} E_h(m_h) = \pi \sum_{j=1}^N |d_j|.$$

Furthermore, if $|d_j| = 1$ for all $j = 1, \dots, N$, then m_h can be chosen such that

$$\lim_{h \rightarrow 0} |\log \kappa| (E_h(m_h) - \pi N) = W(\{a_i, d_i\}) + \pi N \gamma_0.$$

Our strategy in proving this theorem is as follows. First, we reduce the energy $E_h(m_h)$ to a simplified functional defined for averaged magnetizations \bar{m}_h :

$$\bar{E}_h(\bar{m}_h) = \frac{1}{|\log \kappa|} \left(\int_{\Omega'} |\nabla' \bar{m}_h|^2 dx' + \frac{1}{\eta^2} \int_{\Omega'} (1 - |\bar{m}'_h|^2) dx' + \frac{1}{2\pi\kappa} \int_{\partial\Omega'} (\bar{m}_h \cdot \nu)^2 d\mathcal{H}^1 \right).$$

In fact, the energy $\bar{E}_h(\bar{m}_h)$ is close to $E_h(m_h)$ up to $o(\frac{1}{|\log \kappa|})$ (note that $o(1)$ would suffice for the first leading order of the Γ -limit development). This is done by a careful series of estimates that improve in a more quantitative way results of Carbou [15] and Kohn-Slastikov [49]. Then we show that the averaged magnetizations \bar{m}'_h can be approximated by S^1 -vector fields with small energy error, using an argument related to the one explained in Section 2.4. This allows us to show compactness of the boundary Jacobians based on a new argument that avoids rearrangement inequalities used initially in [52]. Finally, we show the Γ -convergence result. Essentially, the idea here is to reduce to the pure boundary vortex regime using η -compactness type estimates.

2.6 Bloch line⁶

We consider the full micromagnetic model (2.1) in a spherical magnetic domain $\Omega = B_\ell \subset \mathbf{R}^3$ where the effect of anisotropy and an applied external field generates a Bloch line inside the sample Ω . The mechanism is the following: the material has an uniaxial anisotropy $Q\varphi(m)$ with $\varphi(m) = m_3^2$ that favors the vertical axis x_3 . Moreover, the external field turns around the axis \mathbf{e}_3 , i.e.,

$$H_{ext} = \lambda H_0, \quad \text{with} \quad H_0(x) = \frac{(-x_2, x_1, 0)}{\sqrt{x_1^2 + x_2^2}}, \quad x \in \mathbf{R}^3$$

with an intensity λ . It is expected that a Bloch line is generated along the vertical axis for strong anisotropy (i.e., the quality factor $Q \gtrsim 1$ is not small) and strong external field intensity λ .

We first adimensionalize the model: we introduce two nondimensionalized parameters

$$\epsilon = \frac{d}{\ell\sqrt{Q}} \quad \text{and} \quad \eta = \frac{d}{\ell}.$$

Rescaling in the length scale ℓ , i.e., $\tilde{x} = x/\ell$, $\tilde{m}(\tilde{x}) = m(x)$, $\tilde{U}(\tilde{x}) = \frac{1}{\ell}U(x)$ and choosing $\lambda = \lambda_0\eta^2|\log \epsilon|/2$ with λ_0 a tuning parameter, the rescaled energy at order ℓd^2 can be written as (for simplicity of notation, we skip $\tilde{\cdot}$ in the sequel):

$$E^{3D}(m) = \int_{B^3} |\nabla m|^2 dx + \frac{1}{\epsilon^2} \int_{B^3} m_3^2 dx + \frac{1}{\eta^2} \int_{\mathbb{R}^3} |\nabla U|^2 dx - \lambda_0 |\log \epsilon| \int_{B^3} H_0 \cdot m dx$$

where $m : B^3 \rightarrow S^2$ and $\Delta U = \nabla \cdot (m \mathbf{1}_{B^3})$ in \mathbf{R}^3 . We denote the energy density of $E^{3D}(m)$ by $e^{3D}(m)$. We are interested in the regime $\epsilon, \eta = \eta(\epsilon) \ll 1$ with

$$\epsilon^2 \ll \eta^2 |\log \epsilon| \ll 1,$$

i.e., $d \ll \ell$ and $Q \gtrsim 1$. This problem is very similar to the 3D Ginzburg-Landau type problems for superconductors where line vortices nucleate inside, typically, by imposing a fixed Dirichlet boundary condition with topological defects (see e.g. [11], [69]). The difference with respect to the above model resides in the free-boundary feature of the problem (even if the anisotropy and external field impose a boundary condition in the limit $\epsilon \rightarrow 0$).

The aim is to study the asymptotic behavior of the minimal energy E^{3D} as well as the singular pattern appearing for minimizers m_ϵ as $\epsilon \rightarrow 0$. A Bloch line is asymptotically created between the two poles $P_\pm = (0, 0, \pm 1)$ with a core of order ϵ . The expected result is given below:

Open Problem 5 1) Let $m_\epsilon : B^3 \rightarrow S^2$. Then as $\epsilon \rightarrow 0$,

$$\liminf_{\epsilon \rightarrow 0} \frac{E^{3D}(m_\epsilon)}{|\log \epsilon|} \geq 2\pi |P_- P_+| - \lambda_0 |B^3|.$$

2) Moreover, if

$$\lim_{\epsilon \rightarrow 0} \frac{E^{3D}(m_\epsilon)}{|\log \epsilon|} = 2\pi |P_- P_+| - \lambda_0 |B^3|,$$

then $m_\epsilon \rightarrow \frac{(x')^\perp}{|x'|}$ in $W^{1,1}(B^3)$ and the following measures converge as $\epsilon \rightarrow 0$,

$$\mu_\epsilon = \frac{e^{3D}(m_\epsilon)}{|\log \epsilon|} \mathcal{H}^3 \llcorner \mathbf{R}^3 \rightarrow 2\pi \mathcal{H}^1 \llcorner \{P_- P_+\} - \lambda_0 \mathcal{H}^3 \llcorner B^3.$$

⁶This subject is part of the PhD thesis of my student Pierre Bochart [10].

2.7 Cross-over from symmetric to asymmetric walls ⁷

We have already presented the (symmetric) Néel wall in Section 2.2 as an x_3 -invariant transition layer that is predominant in thin films. For thicker films, we expect that asymmetric walls (i.e., varying in the x_3 -direction) become favorable as stray-field free transition layers. In this section, we are interested in the critical regime of the cross-over from symmetric to asymmetric walls in soft ferromagnetic films.

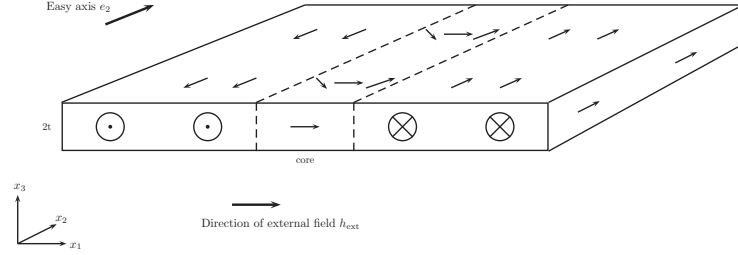


Figure 2.11: A 180° domain wall perpendicular to x_1 -direction.

Model. We consider a magnetic material $\Omega \subset \mathbf{R}^3$ with the easy axis $e_2 = \begin{pmatrix} 0 \\ 1 \\ 0 \end{pmatrix}$ driven by an anisotropy density $Q\varphi(m)$ with $\varphi(m) = m_1^2 + m_3^2$. The domain wall is set to be parallel to the x_2x_3 -plane as in Figure 2.11. In order to deal with arbitrary wall angles $\theta \in [0, \frac{\pi}{2}]$ between the directions

$$m^\pm = (\cos \theta, \pm \sin \theta, 0),$$

we apply an external field $H_{\text{ext}} = Q(\cos(\theta), 0, 0)$ in the normal direction to the wall plane. The aim consists in studying the specific energy of a domain wall per unit length in x_2 -direction and to understand the behavior of the transition layer that achieves the minimal energy. Hence, the admissible magnetizations are considered to be x_2 -invariant and connect the two mesoscopic directions m^\pm inside the x_1x_3 -plane:

$$m = m(x_1, x_3) \in S^2, \quad (x_1, x_3) \in \omega := \mathbf{R} \times (-t, t), \quad m(\pm\infty, \cdot) = m^\pm. \quad (2.52)$$

Rescaling in the thickness variable t , i.e., $\tilde{x} = x/t$, $\tilde{\omega} = \omega/t$, $\tilde{m}(\tilde{x}) = m(x)$, $\tilde{U}(\tilde{x}) = U(x)/t$, the specific energy (per unit length in x_2) is given by

$$\tilde{E}_{2D}(\tilde{m}) = d^2 \int_{\tilde{\omega}} |\tilde{\nabla} \tilde{m}|^2 d\tilde{x} + t^2 \int_{\mathbf{R}^2} |\tilde{\nabla} \tilde{U}|^2 d\tilde{x} + Qt^2 \int_{\tilde{\omega}} \left((\tilde{m}_1 - \cos(\theta))^2 + \tilde{m}_3^2 \right) d\tilde{x}, \quad (2.53)$$

where the differential operator $\tilde{\nabla}$ refers to the variables $\tilde{x} = (\tilde{x}_1, \tilde{x}_3)$ and $\tilde{U} : \mathbf{R}^2 \rightarrow \mathbf{R}$ is the 2D stray-field potential given by

$$\tilde{\Delta} \tilde{U} = \tilde{\nabla} \cdot (\tilde{m} 1_{\tilde{\omega}}) \quad \text{in } \mathbf{R}^2.$$

Observe that the scaling of the stray-field energy is the same as for the Bloch wall, i.e.,

$$\int_{\mathbf{R}^2} |\tilde{\nabla} \tilde{U}|^2 d\tilde{x} = \|\tilde{\nabla} \cdot (\tilde{m} 1_{\tilde{\omega}})\|_{H^{-1}(\mathbf{R}^2)}^2.$$

⁷All the results appearing in this section are part of the articles Döring-Ignat-Otto [28], [27]. Therefore, we don't specify in the following these references for each result.

Throughout the section, we skip \sim .

Symmetric walls. As we explained in Section 2.2, in the regime of thin films (corresponding to small thickness t), the (symmetric) Néel wall m is the favorable transition layer: $\frac{\partial m}{\partial x_3} = 0$ in ω (i.e., $m = m(x_1)$ is invariant in x_3) and $m_3 = 0$ in ω (i.e., $m \in S^1$). It is a two-length scale object with a core of size $w_{core} = O(d^2/t)$ and two logarithmically decaying tails $w_{core} \lesssim |x_1| \lesssim w_{tail} = O(t/Q)$. Even if it doesn't satisfy the flux-closure constraint, it is invariant with respect to the group of symmetries generated by the charges $\nabla \cdot m$ in ω and $m_3 = 0$ on $\partial\omega$:

- 1) $x_1 \rightarrow -x_1, x_3 \rightarrow -x_3, m_2 \rightarrow -m_2$;
- 2) $x_1 \rightarrow -x_1, m_3 \rightarrow -m_3, m_2 \rightarrow -m_2$;
- 3) $x_3 \rightarrow -x_3, m_3 \rightarrow -m_3$;
- 4) *Id.*

The specific energy of a Néel wall is given by

$$E_{2D}(\text{symmetric Néel wall}) = O\left(t^2 \frac{1}{\log \frac{w_{tail}}{w_{core}}}\right) = O\left(t^2 \frac{1}{\log \frac{t^2}{d^2 Q}}\right)$$

(see e.g. [63], [26]).

Asymmetric walls. The main feature of an asymmetric wall resides in the flux-closure, i.e., it is a smooth transition layer m that satisfies (2.52) and

$$m : \omega \rightarrow S^2, \nabla \cdot m = 0 \quad \text{in } \omega \quad \text{and} \quad m_3 = 0 \quad \text{on } \partial\omega. \quad (2.54)$$

Observe that $m' = (m_1, m_2) : \partial\omega \rightarrow S^1$ since m_3 vanishes on $\partial\omega$, so that one can define a topological degree for m' on $\partial\omega$ (where $\partial\omega$ is the closed "infinite" curve $(\mathbf{R} \times \{\pm 1\}) \cup (\{\pm\infty\} \times [-1, 1])$). The physical experiments predict two type of asymmetric walls related to the breaking of symmetries and the degree of m' on $\partial\omega$:

1. For small angles θ , the system prefers the so-called asymmetric Néel wall. The main features reside in the conservation of symmetry 1) and 4) and in having a vanishing degree of m' on $\partial\omega$ (see Figure 2.12). Due to symmetry 1), the asymmetric Néel wall has the m_2 component vanishing on a curve symmetric with respect to the center of the wall (by $x \rightarrow -x$). Moreover, m_2 is not monotone at the surface $|x_3| = 1$.
2. For large angles θ , the system prefers the so-called asymmetric Bloch wall. In fact, as the angle θ grows, there is a breaking of symmetry with respect to the asymmetric Néel wall, so that the asymmetric Bloch wall conserves only the trivial symmetry 4). Another difference resides in the nonvanishing topological degree on $\partial\omega$ carried by asymmetric Bloch wall (i.e., $\deg(m', \partial\omega) = 1$). Therefore, a vortex is nucleated at the center of the wall, and the curve of zeros of m_2 is no longer symmetric with respect the center of the wall (see Figure 2.12). Moreover, the m_2 -component is expected to be monotone at the surface $|x_3| = 1$.

The asymmetric wall has a single length scale $w_{core} \sim t$ and the specific energy resides in the exchange energy of order (see e.g. [63], [26])

$$E_{2D}(\text{asymmetric wall}) = O(d^2).$$

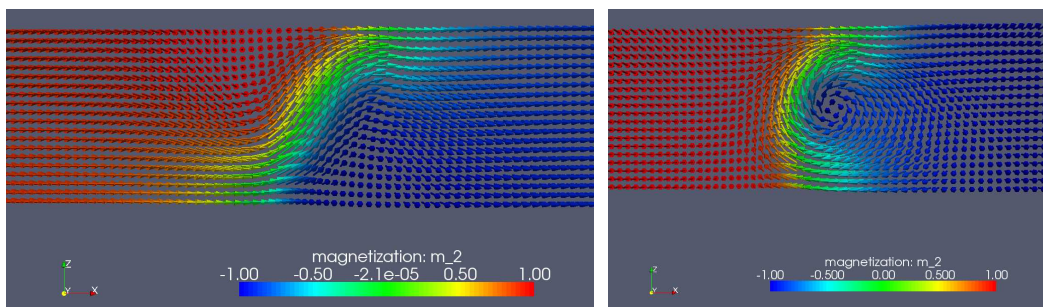


Figure 2.12: Asymmetric Néel wall (on the left) and asymmetric Bloch wall (on the right). Numerics (made by L. Döring).

Regime. We focus on the challenging regime of soft materials and thickness t close to the exchange length d where we expect the cross-over in the scaling energy of symmetric walls (Néel wall) and asymmetric walls:

$$Q \ll 1 \quad \text{and} \quad |\log Q| \sim \left(\frac{t}{d}\right)^2.$$

Rescaling the energy (2.53) by d^2 and setting

$$\rho := Q \frac{t^2}{d^2} \ll 1 \quad \text{and} \quad \lambda := \frac{t^2}{d^2 |\log \rho|} > 0,$$

then $\lambda = O(1)$ is a tuning parameter in the system and the rescaled energy, which is to be minimized, can be written as:

$$E_\rho(m) = \int_\omega |\nabla m|^2 dx + \lambda |\log \rho| \int_{\mathbf{R}^2} |\nabla U|^2 dx + \rho \int_\omega \left((m_1 - \cos(\theta))^2 + m_3^2 \right) dx$$

under the constraint

$$m : \omega = \mathbf{R} \times [-1, 1] \rightarrow S^2, \quad m(\pm\infty, \cdot) = m^\pm, \quad U : \mathbf{R}^2 \rightarrow \mathbf{R}, \quad \Delta U = \nabla \cdot (m \mathbf{1}_\omega) \text{ in } \mathbf{R}^2.$$

To fix the center of the transition we set

$$\bar{m}_2(0) := \int_{-1}^1 m_2(0, x_3) dx_3 = 0.$$

Main result. We are interested in understanding the dependance in the wall angle θ of the asymptotic behavior of the minimal energy E_ρ and to describe the qualitative properties of minimizing transition layers as $\rho \rightarrow 0$.

We expect the following scenario (for $\rho \ll 1$): for small angles $0 \leq \theta \leq \theta^* = \theta^*(\lambda)$, the transition layer is symmetric, i.e., driven by the (symmetric) Néel wall, so that the minimal energy resides in the logarithmic decaying tails of the Néel wall. In fact, if λ is very small, then the system will always prefer the symmetric transition layer. However, for larger λ , there exists a critical angle θ^* where a bifurcation occurs: an asymmetric wall becomes favorable to nucleate into the core of the transition. In fact, for large wall angles $\theta > \theta^*$, the optimal transition layer has a core

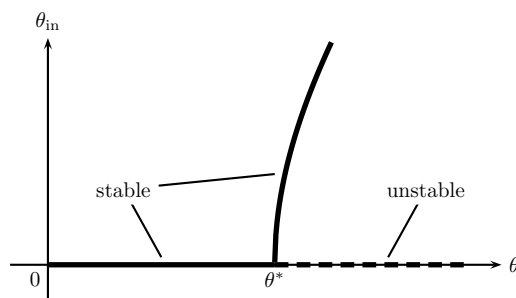


Figure 2.13: Bifurcation diagram for the angle θ_{in} of the asymmetric core part, depending on the global wall angle θ .

driven by the exchange energy where the transition layer is charge-free, while outside the core, it preserves the tails of the symmetric wall (driven by the stray-field energy). The splitting into the core and the tails is determined by an angle θ_{in} of the asymmetric part of the wall. In fact, the angle θ_{in} optimizes the balance between the energy of asymmetric part of the transition in the core (turning from $-\theta_{in}$ to θ_{in}) and the energy of the symmetric part of the wall inside the tails (where the transition completes the rotation by an angle $\theta_{out} = \theta - \theta_{in}$).

This separation of the minimal energy is justified by the following Γ -convergence result at the level of minimizers:

Theorem 23 *Let $\theta \in (0, \frac{\pi}{2}]$. As $\rho \rightarrow 0$ we have the following splitting of the minimal energy:*

$$\min_{(2.52)} E_\rho \rightarrow \min \left\{ E_{asym}(\theta_{in}) + \lambda E_{sym}(\theta - \theta_{in}) : \theta_{in} \in [0, \pi/2] \right\} \quad (2.55)$$

where the asymmetric wall energy is given by

$$E_{asym}(\theta_{in}) := \min_{(2.54)} \left\{ \int_\omega |\nabla m|^2 dx \mid \bar{m}_2(0) = 0, m(\pm\infty, \cdot) = (\cos(\theta_{in}), \pm \sin(\theta_{in}), 0) \right\} \quad (2.56)$$

while the symmetric wall energy can be written for $\theta_{out} = \theta - \theta_{in}$ as:

$$E_{sym}(\theta_{out}) := 2\pi (\cos(\theta_{in}) - \cos(\theta))^2.$$

Observe now that the symmetric part of the energy is quartic for small angles θ (as the Néel wall), i.e., $E_{sym} \lesssim \theta^4$. Therefore, in order to understand the bifurcation at the critical angle θ^* (when both symmetric and asymmetric walls are favorable), by (2.55) we need to compute the asymptotic expansion of the asymmetric energy at order θ^4 as $\theta \rightarrow 0$. For that, we will prove

$$E_{asym}(\theta) = E_0 \theta^2 + E_1 \theta^4 + o(\theta^4),$$

with some positive constants $E_0 > 0$ and $E_1 > 0$ that we compute explicitly. This allows us to heuristically determine a critical angle θ^* , at which the symmetric Néel wall loses stability and an asymmetric core is generated. Moreover, a new path of stable critical points with increasing inner wall angle θ_{in} branches off of $\theta_{in} = 0$ (see Figure 2.13).

Leading order of E_{asym} : We will determine the first leading order term $E_0\theta^2$ of the asymmetric wall energy when the transition angle $\theta \rightarrow 0$. Moreover, we prove the asymptotic behavior of an asymmetric transition layer m_θ :

$$m_\theta = (\cos \theta, (\sin \theta)m_2^*, 0) + O(\theta^2), \quad \text{as } \theta \rightarrow 0,$$

where m_2^* is a minimizing transition layer of the following problem

$$E_0 = \min \left\{ \int_\omega |\nabla f|^2 dx \mid f: \omega \rightarrow \mathbf{R}, f(\pm\infty, \cdot) = \pm 1, \int_{-1}^1 f^2(\cdot, x_3) dx_3 = 1, \bar{f}(0) = 0 \right\}. \quad (2.57)$$

The asymptotic analysis is done by matching upper and lower bound in the spirit of the Γ -convergence at the level of minimizers:

Theorem 24 *The leading order coefficient of E_{asym} is given by:*

$$E_0 = \lim_{\theta \rightarrow 0} \frac{E_{asym}(\theta)}{\theta^2}$$

where E_0 is the minimal energy value (2.57). There are only two minimizers of E_0 corresponding to $\sigma \in \{\pm 1\}$ that we explicitly determine:

$$m_2^*(x) = \tanh\left(\frac{\pi}{2}x_1\right) + \sigma\sqrt{2}\sin\left(\frac{\pi}{2}x_3\right)\sqrt{1 - \tanh^2\left(\frac{\pi}{2}x_1\right)}, \quad x = (x_1, x_3) \in \omega.$$

Moreover, one computes $E_0 = 4\pi$.

The above theorem already justifies the physical prediction on the asymmetric Néel wall: First of all, observe that m_2^* is a non-monotone function on the surface $\{|x_3| = 1\}$, so that the same behavior is conserved by the second component of the asymmetric Néel wall. Second, observe that the curve where m_2^* vanishes is symmetric with respect to the origin, so that the zeros of the second component of an asymmetric Néel wall conserves the same symmetry (as predicted by numerical simulations in Figure 2.12).

Second leading order of E_{asym} : We will now determine the second leading order term $E_1\theta^4$ of the asymmetric wall energy in the asymptotic of the transition angle $\theta \rightarrow 0$. Moreover, the behavior of the asymmetric transition layer m_θ is expected to have the following second order expansion in θ :

$$m_\theta = (\cos \theta, (\sin \theta)m_2^*, 0) + (\sin^2 \theta) \hat{m} + O(\theta^3), \quad \text{as } \theta \rightarrow 0, \quad (2.58)$$

where m_2^* is a minimizing transition layer of E_0 (given by Theorem 24) and \hat{m} has the following components:

$$\hat{m}_1 = \frac{1 - (m_2^*)^2}{2}, \quad \hat{m}_2 = 0 \quad \text{and} \quad \partial_{x_3} \hat{m}_3 = \partial_{x_1} \frac{(m_2^*)^2}{2} \quad \text{in } \omega$$

where \hat{m}_3 is uniquely determined by the boundary condition $\hat{m}_3 = 0$ on $\partial\omega$. Using this heuristic expansion (2.58), one computes that

$$\int_\omega |\nabla m_\theta|^2 dx = \theta^2 E_0 + \theta^4 E_1 + o(\theta^4)$$

with some exact constant

$$E_1 = \frac{304}{105}\pi.$$

The following result rigorously proves the above second order term of E_{asym} by matching upper and lower bound:

Theorem 25 *We have the following second-leading order coefficient*

$$E_1 = \lim_{\theta \rightarrow 0} \frac{(E_{\text{asym}}(\theta) - \theta^2 E_0)}{\theta^4}.$$

Now we can rigorously justify the supercritical bifurcation in the wall angle from symmetric to asymmetric optimal profile (as shown in Figure 2.13). By Theorem 25, we have that

$$E_{\text{asym}}(\theta) = 4\pi\theta^2 + \frac{304}{105}\pi\theta^4 + o(\theta^4). \quad (2.59)$$

If θ is the transition wall angle, it means by Theorem 23 that:

$$\min_{(2.52)} E_\rho = \min_{\theta_{\text{in}} \in [0, \pi/2]} \left(E_{\text{asym}}(\theta_{\text{in}}) + 2\pi\lambda (\cos(\theta_{\text{in}}) - \cos(\theta))^2 \right) + o(1) \quad \text{as } \rho \rightarrow 0, \quad (2.60)$$

where θ_{in} is the angle of the inner asymmetric core part. For small θ , combining with (2.59), the RHS of (2.60) as function of $\theta_{\text{in}} \in [0, \theta]$ has the unique critical point $\theta_{\text{in}} = 0$ if $\theta \leq \theta^*$ where the bifurcation angle θ^* is given by

$$\theta^* = \arccos \left(1 - \frac{E_0}{2\pi\lambda} \right) + o(1), \quad \text{as } \theta \rightarrow 0.$$

(Observe that θ^* is well defined provided that $\lambda \geq E_0/(4\pi)$; therefore, the bifurcation appears only if λ is large enough.) For $\theta > \theta^*$, the optimal splitting angle θ_{in} becomes positive and the symmetric wall becomes unstable under symmetry-breaking perturbations; hence, the asymmetric wall becomes favored by the system. Moreover, the second variation of the RHS of (2.60) at θ^* is positive so that the bifurcation from symmetric to asymmetric wall is supercritical.

Bibliography

- [1] F. ALOUGES, T. RIVIÈRE, AND S. SERFATY, *Néel and cross-tie wall energies for planar micromagnetic configurations*, ESAIM Control Optim. Calc. Var., 8 (2002), pp. 31–68 (electronic). A tribute to J. L. Lions.
- [2] L. AMBROSIO, C. DE LELLIS, AND C. MANTEGAZZA, *Line energies for gradient vector fields in the plane*, Calc. Var. Partial Differential Equations, 9 (1999), pp. 327–255.
- [3] L. AMBROSIO, B. KIRCHHEIM, M. LECUMBERRY, AND T. RIVIÈRE, *On the rectifiability of defect measures arising in a micromagnetics model*, in Nonlinear problems in mathematical physics and related topics, II, vol. 2 of Int. Math. Ser. (N. Y.), Kluwer/Plenum, New York, 2002, pp. 29–60.
- [4] P. AVILES AND Y. GIGA, *A mathematical problem related to the physical theory of liquid crystal configurations*, in Miniconference on geometry and partial differential equations, 2 (Canberra, 1986), vol. 12 of Proc. Centre Math. Anal. Austral. Nat. Univ., Austral. Nat. Univ., Canberra, 1987, pp. 1–16.
- [5] ———, *The distance function and defect energy*, Proc. Roy. Soc. Edinburgh Sect. A, 126 (1996), pp. 923–938.
- [6] ———, *On lower semicontinuity of a defect energy obtained by a singular limit of the Ginzburg-Landau type energy for gradient fields*, Proc. Roy. Soc. Edinburgh Sect. A, 129 (1999), pp. 1–17.
- [7] F. BÉTHUEL, H. BREZIS, AND F. HÉLEIN, *Ginzburg-Landau vortices*, Progress in Nonlinear Differential Equations and their Applications, 13, Birkhäuser Boston Inc., Boston, MA, 1994.
- [8] F. BETHUEL AND X. M. ZHENG, *Density of smooth functions between two manifolds in Sobolev spaces*, J. Funct. Anal., 80 (1988), pp. 60–75.
- [9] S. BIANCHINI, C. DE LELLIS, AND R. ROBYR, *SBV regularity for Hamilton-Jacobi equations in \mathbb{R}^n* , Arch. Ration. Mech. Anal., 200 (2011), pp. 1003–1021.
- [10] P. BOCHARD, *Bloch line in micromagnetics*, in preparation.
- [11] J. BOURGAIN, H. BREZIS, AND P. MIRONESCU, *$H^{1/2}$ maps with values into the circle: minimal connections, lifting, and the Ginzburg-Landau equation*, Publ. Math. Inst. Hautes Études Sci., (2004), pp. 1–115.

- [12] H. BREZIS, P. MIRONESCU, AND A. C. PONCE, $W^{1,1}$ -maps with values into S^1 , in Geometric analysis of PDE and several complex variables, vol. 368 of Contemp. Math., Amer. Math. Soc., Providence, RI, 2005, pp. 69–100.
- [13] W. BROWN, *Micromagnetics*, Wiley Interscience Publishers, New York, 1963.
- [14] J. CAHN AND J. HILLIARD, *Free energy of a nonuniform system I. interfacial energy*, J. Chem. Phys., 28 (1958), pp. 258–267.
- [15] G. CARBOU, *Thin layers in micromagnetism*, Math. Models Methods Appl. Sci., 11 (2001), pp. 1529–1546.
- [16] S. CONTI AND C. DE LELLIS, *Sharp upper bounds for a variational problem with singular perturbation*, Math. Ann., 338 (2007), pp. 119–146.
- [17] J. DÁVILA AND R. IGNAT, *Lifting of BV functions with values in S^1* , C. R. Math. Acad. Sci. Paris, 337 (2003), pp. 159–164.
- [18] C. DE LELLIS, *An example in the gradient theory of phase transitions*, ESAIM Control Optim. Calc. Var., 7 (2002), pp. 285–289 (electronic).
- [19] C. DE LELLIS AND F. OTTO, *Structure of entropy solutions to the eikonal equation*, J. Eur. Math. Soc. (JEMS), 5 (2003), pp. 107–145.
- [20] A. DESIMONE, H. KNÜPFER, AND F. OTTO, *2-d stability of the Néel wall*, Calc. Var. Partial Differential Equations, 27 (2006), pp. 233–253.
- [21] A. DESIMONE, R. V. KOHN, S. MÜLLER, AND F. OTTO, *Magnetic microstructures—a paradigm of multiscale problems*, in ICIAM 99 (Edinburgh), Oxford Univ. Press, Oxford, 2000, pp. 175–190.
- [22] A. DESIMONE, R. V. KOHN, S. MÜLLER, AND F. OTTO, *A reduced theory for thin-film micromagnetics*, Comm. Pure Appl. Math., 55 (2002), pp. 1408–1460.
- [23] ———, *Repulsive interaction of Néel walls, and the internal length scale of the cross-tie wall*, Multiscale Model. Simul., 1 (2003), pp. 57–104.
- [24] A. DESIMONE, R. V. KOHN, S. MÜLLER, F. OTTO, AND R. SCHÄFER, *Two-dimensional modelling of soft ferromagnetic films*, R. Soc. Lond. Proc. Ser. A Math. Phys. Eng. Sci., 457 (2001), pp. 2983–2991.
- [25] A. DESIMONE, S. MÜLLER, R. V. KOHN, AND F. OTTO, *A compactness result in the gradient theory of phase transitions*, Proc. Roy. Soc. Edinburgh Sect. A, 131 (2001), pp. 833–844.
- [26] ———, *Recent analytical developments in micromagnetics*, in The Science of Hysteresis , Vol. 2, Elsevier Academic Press, 2005, pp. 269–381.
- [27] L. DÖRING, R. IGNAT, AND F. OTTO, *Asymmetric domain walls of small angle in micromagnetics*, preprint.
- [28] ———, *Cross-over from symmetric to asymmetric transition layers in micromagnetics*, preprint.

- [29] M. GIAQUINTA, G. MODICA, AND J. SOUČEK, *Cartesian currents in the calculus of variations. II*, vol. 38 of *Ergebnisse der Mathematik und ihrer Grenzgebiete. 3. Folge. A Series of Modern Surveys in Mathematics [Results in Mathematics and Related Areas. 3rd Series. A Series of Modern Surveys in Mathematics]*, Springer-Verlag, Berlin, 1998. Variational integrals.
- [30] Y. GIGA, M. KUBO, AND Y. TONEGAWA, *Magnetic clusters and fold energies*, *Proc. Roy. Soc. Edinburgh Sect. A*, 137 (2007), pp. 23–40.
- [31] F. GOLSE, P.-L. LIONS, B. PERTHAME, AND R. SENTIS, *Regularity of the moments of the solution of a transport equation*, *J. Funct. Anal.*, 76 (1988), pp. 110–125.
- [32] A. HUBERT AND R. SCHÄFER, *Magnetic Domains : The Analysis of Magnetic Microstructures*, Springer-Verlag, Berlin, 1998.
- [33] R. IGNAT, *Two-dimensional unit-length vector fields of vanishing divergence*, preprint.
- [34] ———, *The space $BV(S^2, S^1)$: minimal connection and optimal lifting*, *Ann. Inst. H. Poincaré Anal. Non Linéaire*, 22 (2005), pp. 283–302.
- [35] ———, *A Γ -convergence result for Néel walls in micromagnetics*, *Calc. Var. Partial Differential Equations*, 36 (2009), pp. 285–316.
- [36] ———, *A survey of some new results in ferromagnetic thin films*, in *Séminaire: Équations aux Dérivées Partielles. 2007–2008, Sémin. Équ. Dériv. Partielles, École Polytech., Palaiseau, 2009*, pp. Exp. No. VI, 21.
- [37] ———, *Gradient vector fields with values into S^1* , *C. R. Math. Acad. Sci. Paris*, 349 (2011), pp. 883–887.
- [38] R. IGNAT AND H. KNÜPFER, *Vortex energy and 360° néel walls in thin-film micromagnetics*, *Comm. Pure Appl. Math.*, 63 (2010), pp. 1677–1724.
- [39] R. IGNAT AND M. KURZKE, *An effective model for boundary vortices in thin-film micromagnetics*, in preparation.
- [40] R. IGNAT AND B. MERLET, *Entropy method for line energies*, *Calc. Var. Partial Differential Equations*, accepted.
- [41] R. IGNAT AND B. MERLET, *Lower bound for the energy of Bloch walls in micromagnetics*, *Arch. Ration. Mech. Anal.*, 199 (2011), pp. 369–406.
- [42] R. IGNAT AND R. MOSER, *A zigzag pattern in micromagnetics*, *J. Math. Pures Appl.*, accepted.
- [43] R. IGNAT AND F. OTTO, *A compactness result in thin-film micromagnetics and the optimality of the Néel wall*, *J. Eur. Math. Soc. (JEMS)*, 10 (2008), pp. 909–956.
- [44] ———, *A compactness result of Landau state in thin-film micromagnetics*, *Ann. Inst. H. Poincaré Anal. Non Linéaire*, 28 (2011), pp. 247–282.

- [45] P.-E. JABIN, F. OTTO, AND B. PERTHAME, *Line-energy Ginzburg-Landau models: zero-energy states*, Ann. Sc. Norm. Super. Pisa Cl. Sci. (5), 1 (2002), pp. 187–202.
- [46] P.-E. JABIN AND B. PERTHAME, *Compactness in Ginzburg-Landau energy by kinetic averaging*, Comm. Pure Appl. Math., 54 (2001), pp. 1096–1109.
- [47] R. L. JERRARD, *Lower bounds for generalized Ginzburg-Landau functionals*, SIAM J. Math. Anal., 30 (1999), pp. 721–746 (electronic).
- [48] W. JIN AND R. V. KOHN, *Singular perturbation and the energy of folds*, J. Nonlinear Sci., 10 (2000), pp. 355–390.
- [49] R. V. KOHN AND V. V. SLASTIKOV, *Another thin-film limit of micromagnetics*, Arch. Ration. Mech. Anal., 178 (2005), pp. 227–245.
- [50] S. N. KRUŽKOV, *First order quasilinear equations with several independent variables.*, Mat. Sb. (N.S.), 81 (123) (1970), pp. 228–255.
- [51] M. KURZKE, *Boundary vortices in thin magnetic films*, Calc. Var. Partial Differential Equations, 26 (2006), pp. 1–28.
- [52] ———, *A nonlocal singular perturbation problem with periodic well potential*, ESAIM Control Optim. Calc. Var., 12 (2006), pp. 52–63 (electronic).
- [53] F. H. LIN, *Vortex dynamics for the nonlinear wave equation*, Comm. Pure Appl. Math., 52 (1999), pp. 737–761.
- [54] C. MELCHER, *The logarithmic tail of Néel walls*, Arch. Ration. Mech. Anal., 168 (2003), pp. 83–113.
- [55] ———, *Logarithmic lower bounds for Néel walls*, Calc. Var. Partial Differential Equations, 21 (2004), pp. 209–219.
- [56] P. MIRONESCU, *Lifting of S^1 -valued maps in sums of Sobolev spaces*, preprint.
- [57] ———, *S^1 -valued Sobolev maps*, preprint.
- [58] R. MOSER, *Ginzburg-Landau vortices for thin ferromagnetic films*, AMRX Appl. Math. Res. Express, 1 (2003), pp. 1–32.
- [59] ———, *Boundary vortices for thin ferromagnetic films*, Arch. Ration. Mech. Anal., 174 (2004), pp. 267–300.
- [60] F. MURAT, *Compacité par compensation: condition nécessaire et suffisante de continuité faible sous une hypothèse de rang constant*, Ann. Scuola Norm. Sup. Pisa Cl. Sci. (4), 8 (1981), pp. 69–102.
- [61] C. B. MURATOV AND V. V. OSIPOV, *Theory of 360° domain walls in thin ferromagnetic films*, Journal of Applied Physics, 104 (2008), p. 053908.
- [62] M. ORTIZ AND G. GIOIA, *The morphology and folding patterns of buckling-driven thin-film blisters*, J. Mech. Phys. Solids, 42 (1994), pp. 531–559.

- [63] F. OTTO, *Cross-over in scaling laws: a simple example from micromagnetics*, in Proceedings of the International Congress of Mathematicians, Vol. III (Beijing, 2002), Beijing, 2002, Higher Ed. Press, pp. 829–838.
- [64] A. POLIAKOVSKY, *Upper bounds for singular perturbation problems involving gradient fields*, J. Eur. Math. Soc. (JEMS), 9 (2007), pp. 1–43.
- [65] T. RIVIÈRE, *Dense subsets of $H^{1/2}(S^2, S^1)$* , Ann. Global Anal. Geom., 18 (2000), pp. 517–528.
- [66] T. RIVIÈRE AND S. SERFATY, *Limiting domain wall energy for a problem related to micromagnetics*, Comm. Pure Appl. Math., 54 (2001), pp. 294–338.
- [67] ———, *Compactness, kinetic formulation, and entropies for a problem related to micromagnetics*, Comm. Partial Differential Equations, 28 (2003), pp. 249–269.
- [68] E. SANDIER, *Lower bounds for the energy of unit vector fields and applications*, J. Funct. Anal., 152 (1998), pp. 379–403.
- [69] ———, *Ginzburg-Landau minimizers from \mathbb{R}^{n+1} to \mathbb{R}^n and minimal connections*, Indiana Univ. Math. J., 50 (2001), pp. 1807–1844.
- [70] E. SANDIER AND S. SERFATY, *Vortices in the magnetic Ginzburg-Landau model*, Progress in Nonlinear Differential Equations and their Applications, 70, Birkhäuser Boston Inc., Boston, MA, 2007.
- [71] L. TARTAR, *Compensated compactness and applications to partial differential equations*, in Nonlinear analysis and mechanics: Heriot-Watt Symposium, Vol. IV, vol. 39 of Res. Notes in Math., Pitman, Boston, Mass., 1979, pp. 136–212.
- [72] H. VAN DEN BERG, *Self-consistent domain theory in soft-ferromagnetic media. II, basic domain structures in thin film objects*, J. Appl. Phys., 60 (1986), pp. 1104–1113.